Calixarene and coordination complex hosts for anions.

A thesis submitted for the fulfilment of the requirements for the degree of

Doctor of Philosophy

In the faculty of Science of Durham University

by

Naseem-ul-Ghani Qureshi

Department of Chemistry

Durham University

South Road

Durham

Abstract

My Ph.D research is mainly based on 'calixarene and coordination complex hosts for anion'. The research is to make synthetic chloride ion channels for possible treatment of cystic fibrosis. Our approach is based on derivatives of larger calix[n]arenes. Calixarenes are chalice-shaped molecules that form readily under base catalyzed-condensation of tert-butyl phenol with formaldehyde. We have synthesized calixarenes which were tuned at the lower rim with bromo alkyl nitrile and reduced followed by reaction with a series of different isocyanates bearing fluorescent functional groups capable of binding and sensing chloride and nitrate.

We are also interested how the host ligand binds with metal anions in solution and solid state chemistry. We synthesised simple pyridyl urea ligands and isomorphs. Their anion binding studies are discussed in terms of solid state and solution chemistry. Solid state structures based on silver and copper metal forming contact ion pairs with series of anions like nitrate, chloride, bromide, trifluoroacetate and boron tetrafluoride. Their solution based anion binding studies were performed and control titration results show that these hosts bind anions in a one to one fashion which was confirmed with solid state structures. An interesting aspect is that 2-ureidopyridine ligand exists in four different anhydrous crystal forms (I – IV^0), which can be crystallized by several techniques. It was found that forms I and II only crystallize without another polymorph from methanol solution or in presence of inorganic salts. Thermoanalysis shows that all the modifications melt without previous transition and applying the heat of fusion rule proves this system to be completely monotropic. The crystal structures show that the molecule forms one intramolecular and two intermolecular hydrogen bonds to give S(6) and dimeric $R_2^2(8)$ graph synthons in all four structures. However packing arrangements differ strikingly and since the hydrogen-bonding arrangement is the same for all the four forms, the differences in energy measured by thermoanalytical methods can only be caused by the different packing arrangements involving combinations of the weaker interactions, with the CH$^{\cdots}$S contacts being among the obvious differences. Thus, this system is a clear example in which the presence of robust, reproducible hydrogen bonded synthons does not lead to any control or predictability of polymorphic form.

To my father Prof. Abdul Ghani Qureshi

Acknowledgement

First and foremost I would like to thank Prof. Jonathan W. Steed for stimulating and challenging projects, and the knowledge that he has shared with me over the course of my studies. I would like to thank Prof. Judith A. K. Howard(ex- head of the department of chemistry), Durham University, Higher Education Commission Pakistan, Charles Walles Trust Pakistan and Dr. Wali Mohammad Trust for partial funding. Beside this our deepest thanks to all the members, trustees and Project Managers who had helped me by awarding partial fellowships. In these members I am grateful to Mr. Jehanzeb Khan (Project Manager HEC Pakistan), Dr. Tim Butchard (Trustee Charles Walles Trust Pakistan), Mr. Wajid Shamsul Hassan (Ambassador of Pakistan, UK), Mr. Talha Saeed(Education officer), Mr. Syed Fazal Hassan (Senior Officer Education Section) and Mrs. Elizabeth Wood (Chemistry Store Officer) and David Hodgson (second supervisor).

In the group and department of Chemistry, I would like to thank Dimitri S. K.Yufit, Gareth O. Lloyd and Katharina Fucke for all the help and crystal structure determination. All the support staff have helped me hugely, in particular Alan Kenwright and Ian in NMR, as well Jaroslava Dostal for elemental analyses and Mike Jones and Lara Turner for mass spectrometry. Thanks go to Doug Carswell for DSC.

On a personal front, I am thankful to Anil Suri, Hazrat Hussain, Naveed A. Zaidi, Sajid Jahangir, Aijaz Soomro, Akhtar Rind, Peter Byrne, Adam Todd, Adam Swinburne, Jonathan Foster, Joseph T. Lenthal, Mark, Maria, Charllote and anyone I forgot.

Finally, my chemistry will not have produced any result without the patience and moral support of my wife Farzana Qureshi who had helped me lot to finish my Doctoral research training here in Durham University, United Kingdom.

Table of Contents

List of Figures

List of Tables

List of Schemes

Abbreviations

acac	acetylacetonate anion
$AgCF_3SO_3$	silver trifluromethanesulphonate
br (NMR, IR)	broad
d (NMR)	doublet
dd (NMR)	doublet of doublet
DMSO	dimethyl sulphoxide
DNA	deoxyribose nucleic acid
DSC	differential scanning calorimetry
DTFA	deuterated trifluroacetic acid
ESI-MS	electro-spray ionisation-mass spectrometry
h	hour
Hz	hertz
J	coupling constant
K_{11}	1:1 host:guest binding constant
Ka	association constant
m (NMR)	multiplet
MEOH	methanol
MeCN	acetonitrile
MS	mass spectrometry
NMR	nuclear magnetic resonance
PEG	polyethylene glycol
ppm	parts per million
RT	room temperature
$R_2^2(8)$	8 membered ring having 2 donor and 2 acceptor
s (NMR)	singlet
t (NMR)	triplet
TCE	tetrachloroethane
TBAOAC	tetrabutyl ammonium acetate
TBABr	tetrabutyl ammonium bromide
TBACl	tetrabutyl ammonium chloride
$TBANO_3$	tetrabutyl ammonium nitrate

Chapter 1: Introduction

1.1 Anion Binding

1.1.1 The history of anion binding

The beginning of modern supramolecular chemistry is generally traced to the work of Pedersen,[1, 2] who reported series of cyclic polyethers, synthesized from aromatic vicinal diols, reacted with dihaloalkanes in presence of two equivalent of sodium hydroxide base as shown in Scheme **1.1**.[1, 2] The series of substituted crown ethers for example; 12-crown-4 ethers **1.1,** benzo-12-crown-4 **1.2**, benzo-18-crown-6 **1.3**, benzo-cyclohexyl-18-crown-6 **1.4** and dibenzo-18-crown-6 **1.5** and their metal complexing properties were reported in 1967.[2] Affinity of the crown ethers for alkali metal salts, which can be monitored in the case of benzo-18-crown-6 **1.5** by the intensity of the 275 nm absorption band, which increases with increase in cation size. In the same year Shriver and Biallas reported the chelation of bidendate Lewis acids $X_2B(CH_2)_2BX_2$ (X = F, Cl) stabilized by four equivalents of methanol solvent to form a dimethyl ether-1,2-bis(difluoroboryl)ethane.[3] They used a series of alkoxide ions derived from triphenylmethanol, for example, to form a series of ethers substituted with alkyl or aryl groups.[2] In this work, boron acts as a Lewis acid by accepting a lone pair of electron from oxygen of the alcohol to form a bidendate ligand. In 1968, Park and Simmons showed encapsulation of halide ions by 1, 11–diazabicyclo [9.9.9] nonacosane **1.6** in presence of deuterated trifluoroacetic acid (DTFA). This binding process resulted in an equilibrium mixture being established between the two types of isomers on leaving the mixture for a longer time.[4, 5] They noticed that the equilibrium was not disturbed at room temperature, but sudden sharp changes in the NMR spectrum were observed on heating the mixture at 65 ^{0}C as shown in Figure **1.2.**.

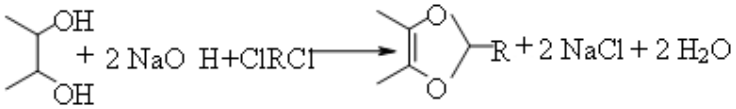

Scheme 1.1 General mechanism of base induced diol reaction (R = cyclic or alkyl group etc.).

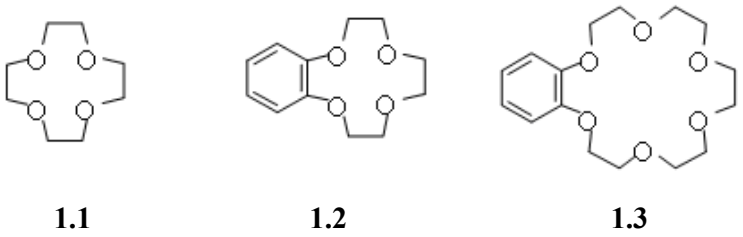

1.1 **1.2** **1.3**

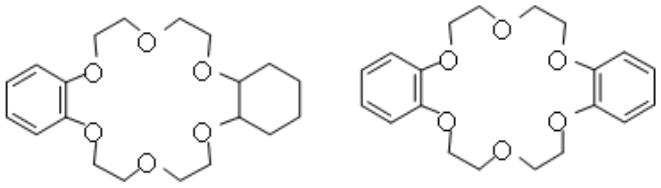

1.4 **1.5**

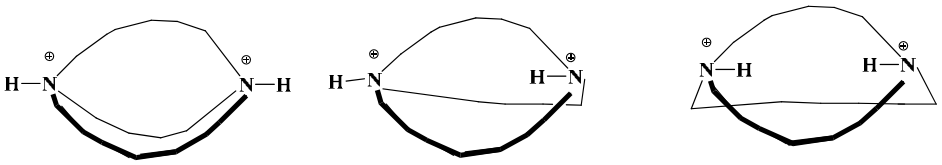

out – out out – in in – in

Scheme 1.2 Isomerism in protonated diazabicyclononacosane 1.6 [23, 24]

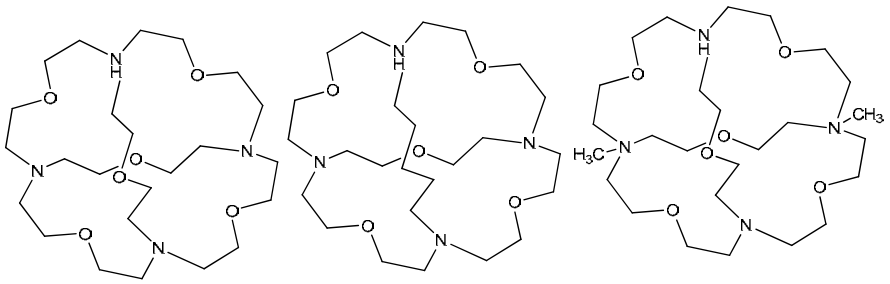

1.7 **1.8** **1.9**

Lehn and coworkers also reported the ellipsoidal hexaprotonated macrobicyclic receptor **1.10** which they found to be selective for the linear anions, particularly azide N_3^- (log K = 4.3 in aqueous solution) that are complementary to the shape of the cavity.[8]

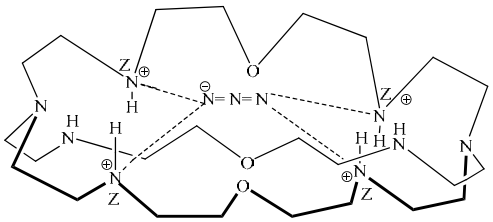

Figure 1.1 Protonated receptor 1.10 as the N_3^- complex.[8]

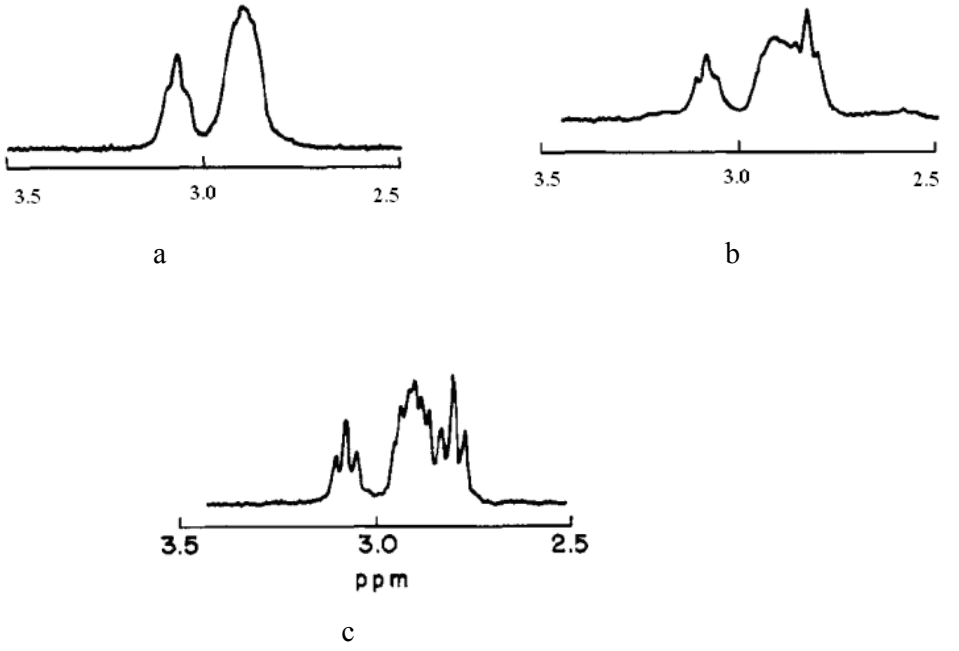

Figure 1.2 ^{1}H-NMR spectra of CH_2 resonances of 1.10 in 50% DTFA.[4, 5]
1 equivalent of NaCl has been added; (a) t = 1 min, 23 ^{0}C; (b) t = 21 days, 23 ^{0}C.
(c) t = 21 days, 65 ^{0}C

Sessler and coworkers have reported the anion binding ability of calixpyrrole **1.11** (meso-octaalkyl porphyrinogen) macrocycle receptor, first synthesized in the nineteenth century by Baeyer.[9] They showed that this receptor forms complexes with fluoride, chloride and dihydrogen phosphate with stability constants of 17200, 350, and 100 M^{-1} respectively in CD_2Cl_2.[10, 11] The conformation of the macrocycle in the solid state changes dramatically upon anion complexation.

The free calixpyrrole adopts a 1,3-alternate conformation where in adjacent rings are oriented in opposite directions. However, the crystal structure of chloride complex

1.11·Cl^- (Figure **1.4**) reveals that the macrocycle adopts a cone conformation with four pyrrole NH groups forming hydrogen bonds to the bound chloride. Sessler and coworkers have also reported a calixpyrrole based solid support gel for the separation of anions by high performance liquid chromatography (HPLC).[10] This potentially industrially useful application of solid supported receptors allows the separation of small oligonucleotides (with 12 -18 membered chains in length). Other uses of this solid supported type of receptor include the incorporation of electrochemically active molecular hosts designed to sense anionic guests into ion-selective electrodes, and the preparation of solid supported optical sensors for anions.[10] Sessler, Vogtle and coworkers have reported the synthesis of a bipyrrole catenane based receptor that forms extremely stable complexes with anions.[11] NMR spectroscopic titration techniques revealed that the catenane binds anions with very high stability constants (up to 10^7 M^{-1} with $H_2PO_4^-$ in deuterated tetrachloethane).[13, 14]

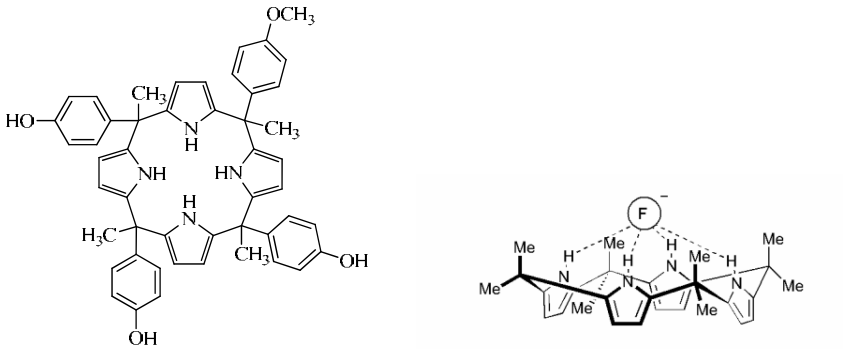

(a) (b)

Figure 1.3 (a) Pyrrole receptor 1.11 and (b) Molecular structure of 1.11 with bound fluoride anion.[31]

This high stability is attributed to the formation of a tetrahedral cavity between the rings, which provides ideal coordination geometry for the tetrahedral anion coordination. Lehn and Hosseini have reported protonated ammonium macrocycles **1.13** and **1.14** that can discriminate between dicarboxylate ions based on their size. Receptor **1.13** binds with shorter chain carboxylates (m = 2, 3) more strongly, while **1.14** preferentially binds longer alkyl chains (m = 5, 6).[15]

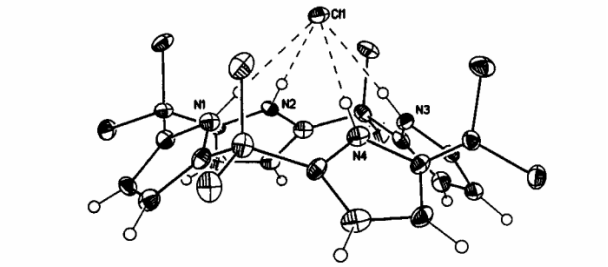

Figure 1.4 X-ray crystal structure of 1.12 with bound chloride ion.

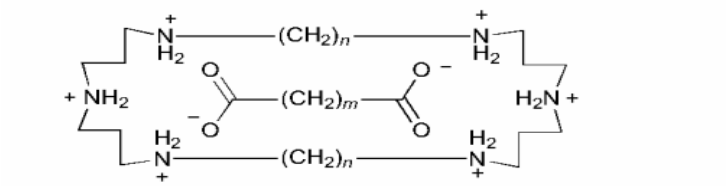

1.13: $n = 7$ $m = 2,3,5,6$

1.14: $n = 10$

1.1.2 Recent work in anion binding

Anion recognition is a growing field of research and there are good introductory texts and reviews available on the subject.[16 - 18] Considerable attention has been given to anion recognition particularly because anions are ubiquitous throughout biological systems. They carry genetic information (DNA is a polyanion) and the majority of enzyme substrates and co-factors are anionic.[16] A well-known example is carboxypeptidase A, an enzyme that coordinates to the C-terminal carbooxylate group of polypeptides by the formation of an arginine-asparate salt bridge, and catalyses the hydrolysis of this residue. The salt bridge binding motif is also observed in zinc / DNA complexes and RNA stem loop protein interactions.[19] Anions also play roles in the areas of medicine and catalysis, whilst pollutant anions have been linked to the eutrophication of the rivers (from the over use of phosphate-containing fertilizers) and carcinogenesis (metabolites of nitrate).[18] The production of pertechnetatate during the reprocessing of nuclear fuel (and its subsequent discharge into the seas and oceans) is also a matter of environmental concern.[37] Adding hydrogen bond donor groups to organic hosts has been a key tool in providing recognition for specific anion geometries.[20, 21] The design of anion receptors is particularly challenging and there are number of reasons for this.[18] Anions are larger than isoelectronic cations and therefore have lower charge to radius ratio. For example: $F^- > Na^+$; $Cl^- > K^+$ in ionic radi. Anion charge depends on pH; with a change in pH, anions can become protonated and lose their negative charge. Therefore, it is important that anion receptors should work within the pH range in which the anion is non-protonated. Anion binding is also influenced by the hydrophobicity of the molecule.[18] Hydrophobic anions such as Br^-, I^- and ClO_4^- are generally bound more strongly in a hydrophobic binding sites. The geometry of the molecule is also one of the important factors for selective anion recognition. Anions have been classified on the basis of their geometry and charge. Anion guests need a particular host back bone to selectively bind depending on the geometry, hydrogen bonding, solvent and a particular pH range of host.

1.1.3 Urea based anion hosts

Anions play very important part in daily life and specific ion effects are ubiquitous in chemistry and biology.[22] An example is the reoccurring trend called the Hofmeister series loosely based on hydrophobicity, which is generally more pronounced for anions than for cations.[23] The typical ordering of the anion series and some of its related properties are shown in Figure **1.5**.

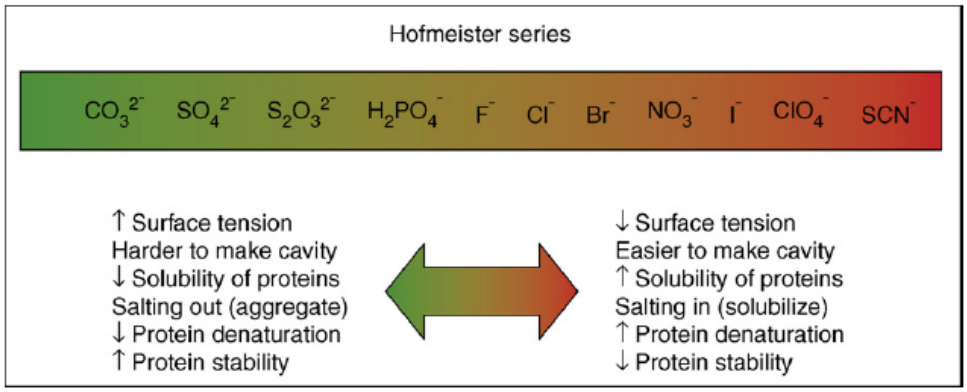

Figure 1.5 The Hofmeister series[42]

The species to the left of Cl^- are referred to as kosmotropes, while those to its right are called chaotropes. These terms originally are referred an ion's ability to alter the hydrogen bonding network of water (Figure **1.5**). The kosmotropes, which are believed to be 'water structure makers', are strongly hydrated and have stabilizing and salting-out effects on protein and macromolecules. On the other hand, chaotropes ('water structure breakers') are known to be destabilizing folded proteins and give rise to salting in behaviour.

Hydrogen bonding is directional and hence is a very useful property in designing receptors with specific shape, complementary to the different anion geometries.[21] In urea related compounds two hydrogen bonds from the urea NH groups, can form a bidentate interaction to anions imparting particular geometric constrain.[24] Urea and thiourea are particularly good hydrogen bond donors and are excellent receptors for Y-shaped anions such as carboxylate, through the formation of two hydrogen bonds, and for spherical anions such as chloride, bromide and iodide.[25]

Even simple urea based receptors form very stable complexes with more highly charged and more basic bidentate anions. Umezawa and co-workers have synthesized some urea, bis(urea) and bis(thiourea) receptors such as **1.15** and **1.16**, which exhibit selective hydrogen bonding with dihydrogen phosphate over the other anions such as acetate, dicarboxylates, chloride, nitrate and perchlorate.[24] They reported that the highest binding constant was observed for dihydrogen phosphate for urea receptor **1.17** and acetate for **1.18**. The receptors' binding mode was shown to be different in each case.[24] Gale and co-workers have reported the synthesis of macrocyclic amidoureas such as **1.19**. The stability constant of **1.19** with a variety of putative anionic guests was elucidated using ^{1}H NMR spectroscopic titration. This data showed that chloride is more strongly bound than bromide in DMSO-d_6 / 0.5% water mixture.[45]

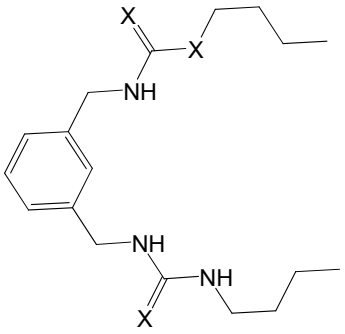

1.15 X = O
1.16 X = S

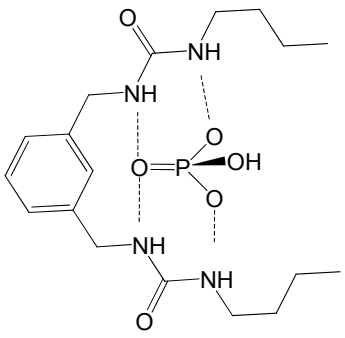

1.17

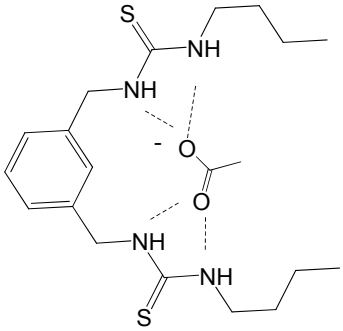

1.18

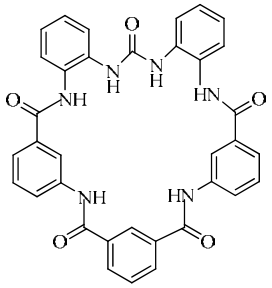

1.19

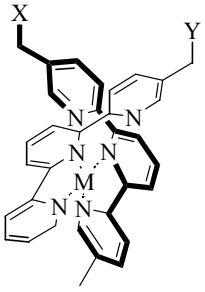

1.20 M = Ru
1.21 M = Fe

Hamilton has used a metal template receptor binding strategy with ruthenium and iron terpyridine derivatives. Metalloreceptor **1.20** was synthesized by using a Gabriel amine synthesis followed by final treatment with butyl isocyanate to form a terpyridyl ligand. The ruthenium complex **1.20** was obtained by heating this terpyridyl derivative ligand with 0.5 equivalent of $[RuCl_2(DMSO)_4]$ in ethylene glycol, and the iron complex **1.21** by mixing the aqueous solution of the receptors and $(NH_4)_2Fe(SO_4)_2$. Both complexes were isolated as their PF_6^- salts. Displacement of the terpyridine ligand occurred on addition of dicarboxylates to the iron containing receptor **1.21**. However, in the case of the inert ruthenium receptor **1.20** displacements did not occur, instead the carboxylate anions bound to the thiourea groups. Association constants were obtained for a variety of dicarboxylate guests (glutarate $K_a = 8.3 \times 10^3\ M^{-1}$, adipate $K_a = 2.9 \times 10^3\ M^{-1}$ and pimelate $K_a = 6.0 \times 10^3\ M^{-1}$) and suggest a degree of flexibility in the anion binding site.[27]

In a recent communication, Hamilton has extended the terpyridine binding metal with variety of substrate binding domains based on hydrophobic, polar, or charged groups. They have flexibility to form complexes with the variety of anions. Ruthenium based receptor **1.20** forms stable complexes with dicarboxylate anion in a 2:2 fashion as shown in **1.22**.[28]

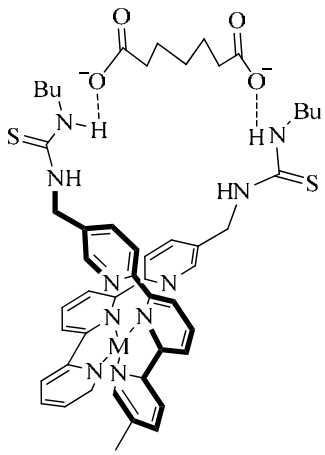

1.22

Smith and coworkers have reported urea-boronate compounds **1**.**23** and **1**.**24**, which form zwitterions when treated with methanol solvent. The boronate urea was prepared from 2-aminophenyl boronic acid, which was further treated with appropriate isocyanate to give

heterocycles **1**.**23** and **1**.**24**. Condensation of these heterocycles in benzene resulted in the formation of a zwitterionic compound.

When heterocycles **1**.**23** and **1**.**24** are treated with KHF_2 in methanol solvent this gives difluoro analogues **1.25** and **1.25**. Binding studies were undertaken with the pinacol boronate hosts **1**.**23** and **1**.**24** with tertiary butylammonium acetate in DMSO-d_6 solvent. The titration isotherm nicely matches a 1:1 binding model and reveals that the *ortho*-substituted derivatives bind acetate about 20 times better than *meta* substituted controls. Even more impressive is the difluroboronates **1.25** and **1**.**26**, which binds acetate 150 times better than their control compound **1**.**27**. The 1:1 binding stochiometry was verified by a Job plot analysis.[29, 30]

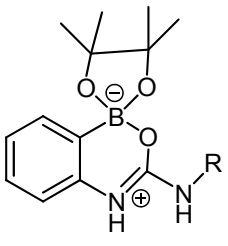

1.**23** R = CH_3

1.**24** R = C_8H_{17}

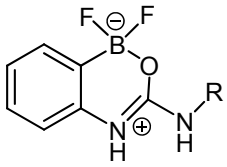

1.25 R = CH_3

1.26 R = C_8H_{17}

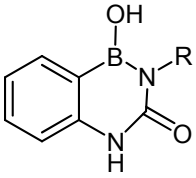

1.**27**

Davis has reported steroid based urea / thiourea receptors **1**.**28** and **1**.**29**. The new receptors are synthesized from cholic acid via Boc protected aminosteroids, which can be converted to urea and thiourea groups. These urea and thiourea moieties do not show any intermolecular hydrogen bonding owing to the backbone preorganisation. The steroidal unit also increases the solubility in non-polar media. Additional features of the hosts include increased in hydrogen bonding affinity for anions by the use of electron withdrawing substituents to raise the donor power and appended aliphatic substituents resulting in increased in lipophilicity and solubility in organic solvents.[31]

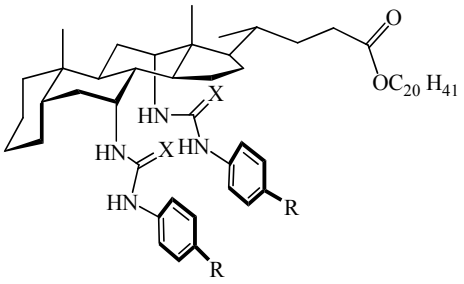

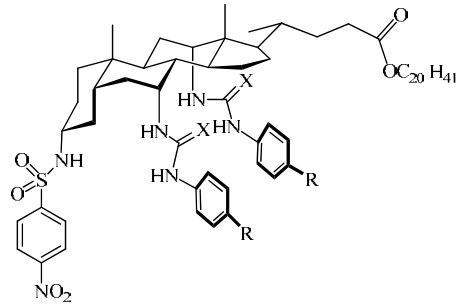

1.**28** R= H, X = O

1.**29** R = CF_3, X = O

1.30 R = H, X = O

1.31 R = H, X = S

1.32 R = CF_3, X = S

1.1.4 Electrostatic interactions

In early work, Schmidchen produced a series of macrotricyclic quarternary ammonium receptors (**1**.**33 – 1.36**) prepared by the methylation of parent tertiary amine.[32, 33]

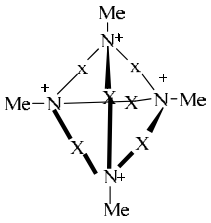

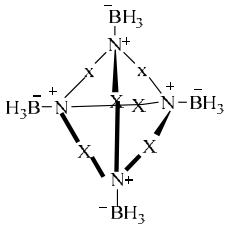

1.33 X = -$(CH_2)_6$-

1.34 X = -$(CH_2)_{10}$-

1.**35** X = -$(CH_2)_6$-

1.**36** X = -$(CH_2)_{10}$-

This type of receptor binds a variety of anionic guests in water, as it is positively charged, for example forming a strong complex with iodide characterized by X-ray crystallography (Figure **1.6**).[32, 33] Steed has reported molecular pedants based on hexasubstituted core coupled with arms and hydrogen bonding groups such as amines as the primary binding site along with a cationic pyridinium electrostatic binding site. These hexasubstituted cores impart a cone conformation stabilized by hydrogen bonding. The cationic pyridinium moiety possesses relatively acidic CH protons ortho to the pyridinium nitrogen atom which can also interact with anions.[34]

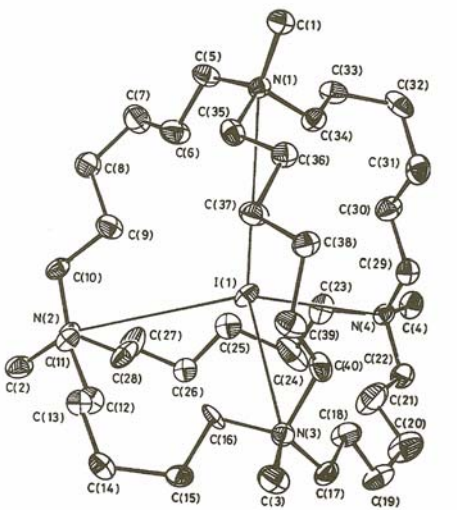

Figure 1.6 X-Ray structure of the iodide ion complex with receptor [14].[33]

1.2 Calixarenes

1.2.1 Calixarenes and their history

The calixarenes are a major class of supramolecular host compounds, along with the cyclodextrins and cyclophanes.[97], [100] The first calixarene was reported by Bayer almost a century ago[9] and their chemistry was further developed by Zinke and Ziegler.[35] They reported that a hard, stiff polymeric material was formed by the simple reaction of aldehydes and a *para*-substituted phenol, resulting in the formation of a macromolecule. During the 1980's, the calixarenes were popularized by Gutsche and co-workers who gave them the calixarene name.[103] Originally, calixarenes were used as enzyme mimics because of their hydrophobic cavity. The word calixarenes refers to basket shaped molecules (calix = bowl like; arenes = aromatic rings).[96] Because of their ready availability, calixarene derivatives have been used in a range of molecular and supramolecular systems, for example in metal complexation studies,[36, 37] anion binding,[17] host-guest chemistry, and they exhibit interesting inclusion phenomena. [17] These days calixarenes are ubiquitous in supramolecular chemistry including anion and cation binding, transport and sensing. [17] The range of available calixarenes has expanded so much that perhaps the calixarene name as originally envisaged by Gutsche is not justified. There is no doubt that the cyclic tetrameric hydroxyl terminated systems form calix (bowl-like) structures, but alkylation at the lower rim of calixarene can often lead to the formation of different conformers, while the higher calix[*n*]arenes where $n > 5$ do not have bowl-shaped structures.[38]

1.2.2 Conformation and symmetry of the calixarenes

Shinkai and others had proposed that the name of calixarene is only justified if the molecule is underivatised at the lower or upper rim. As soon as it is substituted the vase-like calix conformation is often disrupted to give a variety of other possible conformers.[38] For example, O-alkyl substituents frequently bring about not only the well-known cone conformation but also the partial–cone, 1,2-alternate and 1,3-altenate forms with the partial cone conformation being the most stable.[106, 39] Computational studies predict that even tetra O-alkylated cone calix[4]arene does not adopt regular C_{4v} symmetry, but distorts to a C_{2v} form with a pinched cone conformation.[106, 40] These different conformations of calixarenes (shown in Figures **1.7** and **1.8**) are an interesting feature of their chemistry. It has also been suggested that reaction conditions have significant effects on calixarene stereochemistry, particularly when the product is stereochemically relatively rigid, as is the case with bulky substituent groups. The amount of base and the identity of the alkali metal cation (for example the choice of potassium carbonate or cesium carbonate) has a significant effect on the conformation of the calixarene product. Potassium carbonate is a weaker base than cesium carbonate, and the Cs^+ cation can also engage in $Cs^+\cdots\pi$ interactions with the calixarene ring, stabilizing the cone conformer.[41] The stereochemistry also depends on the reaction condition, solvent and temperature. Regen and others have reported the interconversion of upper rim modified tetracarboxylic acid calix[4]arene as shown in Figure **1.8** in which the C_{2v} (pinched cone) isomer is the most stable and more thermodynamically favourable conformer.[40] The fact that the pinched cone conformers have not been detected in solution has been rationalized in terms of a rapid interconversion between the two equivalent C_{2v} forms.[38] The ^{1}H-NMR spectrum in DMSO-d_6 at 23 ^{0}C is consistent with a cone (and also a rapidly equilibrating pinched cone) structure; i.e. a well defined pair of doublets was observed for the bridging methylene groups at the 4.32 and 3.37 ppm (J_{AB} = 3.0 Hz). Broadening of the spectrum was observed in TCE (at 23 ^{0}C), which sharpened on reducing the temperature. Spectral data, coalescence temperature (Tc) and Gibbs free energy calculations confirm that the pinched cone conformers are in dynamic equilibrium.[42] These workers also concluded that internal hydrogen bonding also plays a vital role in stabilizing the pinched cone conformer.[21]

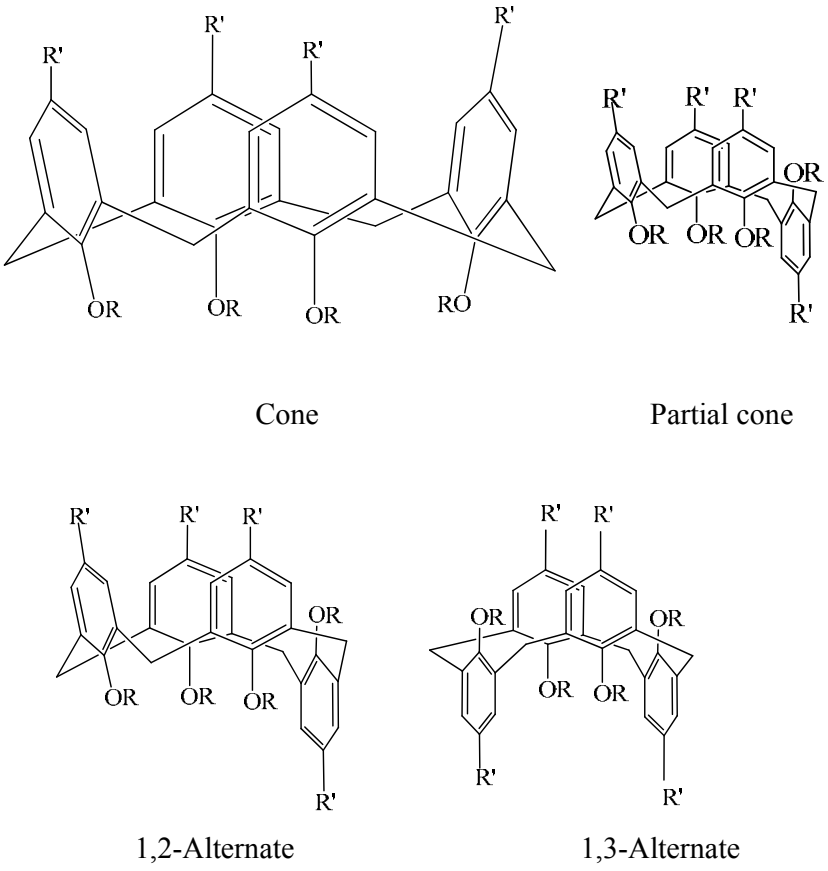

Figure 1.7 Different conformations of calix[4]arenes

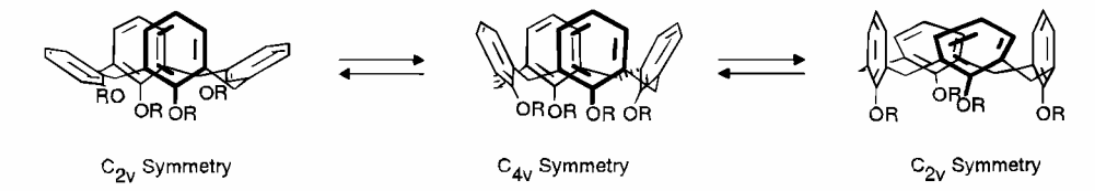

Figure 1.8 Symmetry of cone calix[4]arenes

Arudini and others have reported that a calix[4]arene substituted with two carboxylic acid groups at the upper rim that forms hydrogen-bonded dimers in solution in which the calix[4]arene can adopt the pinched cone conformation. The ^{1}H-NMR spectrum of that material is dependent on the solvent. In the polar CD_3OD the compound is conformationally mobile, while from the data in $CDCl_3$ it appears that the flattened cone conformation is imposed by intramolecular hydrogen bonding.[39, 43]

Shinkai has reported that the pinched cone conformation of calixarenes can be stabilized by the addition Ag^+, which interacts with the aromatic rings.[38] Reinhoudt has reported molecular modelling calculations on various conformers of debutylated calix[4]arene, which suggest that the 1,3-alternate conformation has a lower energy, but there is not much difference between the methyl calixarene and tert-butyl calixarenes, in which electrostatic interactions favours the cone conformation. Solvent also has also some effects.[44]

Reinhoudt and coworkers have reported significant effects of solvents in molecular modelling studies because water molecules are able to compensate for the loss of OH···OH hydrogen bonds upon conformational transition, and the process is concerted.[21, 45]

1.2.3 Phenol derived calixarenes

Calixarenes can be divided into different classes, according to the starting materials from which they are derived. For example, phenol and resorcinol derived systems, oxa- and azacalixarenes. We will restrict our discussion to the common phenol and resorcinol derived calixarenes that are most relevant to this project. Phenol derived calix[*n*]arenes (where *n* = 4, 6, 8; **1.37** – **1.39**) have been studied by a number of groups including those of Gutsche, Prama, Atwood and Shinkai.[96] Such macrocyclic molecules are synthesized by the simple mixing of formaldehyde, para tertiary butyl phenol in presence of base to form tetrameric, hexameric or octameric products depending upon the concentration of base and yields can be highly variable. The mechanism of base induced cyclization is based on the abstraction of proton from the one of the para-substituted phenolic alcohols to form a nucleophile, which is further stabilized at the position ortho to the substituted phenolic OH group. Nucleophilic attack takes place at the electrophilic centre of formaldehyde (as shown in Scheme **1.3**.[15] These reaction sequences depend on thermodynamic parameters, like effective heat control and base concentration.

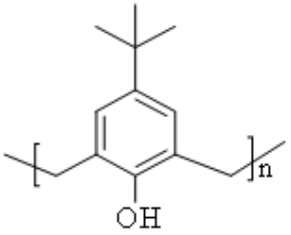

1.37 *n* = 4

1.38 *n* = 6

1.39 *n* = 8

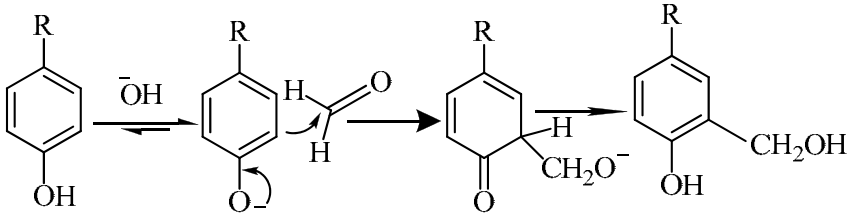

Scheme 1.3 Mechanism for the initial steps in base-induced calixarene synthesis.

1.2.4 Resorcinol derived calixarenes

The product derived from the acid-catalyzed reaction of resorcinol and formaldehyde has been assigned a linear dimeric structure, although it may actually be a polymer.[46] Resorcinol and formaldehyde are known to react under acid and base- induced conditions to form polymers that have long commercial use adhesives. Use of an aldehyde other than formaldehyde can give calixarene-like cyclic oligomers terms calix[*n*]resorcarenes or just simple [*n*]resorcarenes. Hogberg reported a one step synthesis of C-methyl calix[4]resorcinarene.[47] Hogberg has reported a series of diasteroisomers and suggested that the system is in dynamic equilibrium causing the diasteroisomer distribution to be a function of time. At different time intervals, different isomers have been formed and the isomer distribution depends in part on whether the reaction is under kinetic or thermodynamic control.[47] Resorcinarenes have been prepared from acetaldehyde, propionaldehyde, isobutyraldehyde, isovalderaldehyde, heptaaldehyde, dodecylaldehyde, benzaldehyde, p-bromo benzaldehyde and ferrocene carboxy aldehydes giving rise to a wide variety of readily prepared analogues.[48]

1.2.5 Calixarene based anion receptors

The incorporation of hydrogen bonding substituent groups at the upper or lower rim of calixarenes give receptors suitable for anion binding.[49] A number of researchers have tried to tune the calixarene by functionalizing the receptors in this way. In nature phosphate and sulphate, binding proteins are excellent receptors for anion transport. A very high selectivity in binding is observed for prokaryotic, periplasmic phosphate and sulphate binding proteins, which demonstrate $>10^5$ selectivity for binding phosphate over sulphate and vice versa.[18] These kinds of anion binding protein rely exclusively on multiple hydrogen bonding interactions to interact with the anion guest. Functionalization of a calixarene with upper rim sulphonamide substituents leads to a three-dimensional cavity which complexes tetrahedral HSO_4^- better than spherical Cl^- or planar NO_3^-. Association constant measurements confirm that Y-shaped anions have highest association constant in these sulphonamide based systems. Substitution of benzamide with a dichloro moiety at one end further enhances the association constant. Amide and bis(amide) groups display excellent affinity for Y-shaped anions compared to tetrahedral anions.[106] Lothak and Sessler had attached tetraphenyl porphrin units to the calixarene skeleton via the ureido function to give a novel series of calixarene – porphyrin conjugate anion receptors **1.40** – **1.42.**[10, 14]

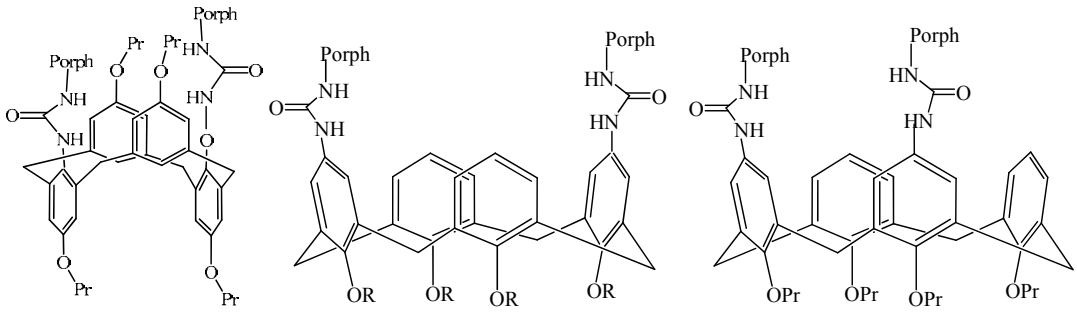

1.40 **1.41** R = propyl **1.42**

Binding constants were determined using UV–vis spectroscopic titration based on the strong absorption of the appended porphyrin moieties and these compounds can serve as receptors for anion and cation binding. The complexation of selected anions (Cl^- , Br^- , I^-, and NO_3^-) was studied by UV-visible titration in CH_2Cl_2. Addition of anions as the NBu_4^+ salts resulted in a tiny red shift (0.5 nm), a hypochromicity of the Soret maximum, a small broadening at about 440 nm, and welldefined isobestic points. The deliberate

modification of structural motif significantly affects the anion binding by the calix[4]arene–porphyrin units, but in general the receptors exhibit affinity for small spherical anions such as Cl^- and Br^-. The binding constant decreases with increasing anion diameter, however even the tetra propyl substituted 1,3-alternate calixarene does not hinder anion complexation. This means that the linkers attached to the calix[4]arene lower rim are flexible enough to accommodate series of anions, although larger anions such as I^- and NO_3^- are bound more weakly.[10, 50]

Titration experiments were performed for **1.43** in ($CHCl_3$: CH_3CN = 4:1 v/v) using a constant calixarene concentration (0.5-2.0 mM) and increasing concentration of the appropriate anion to obtain a different host / guest ratios. Strong binding of Cl^- was observed because of hydrogen bonding as shown in Figure **1.9**. Job's plot analysis suggested 1:1 binding not 1:2 despite the apparently ditopic nature of the hosts. The two pairs of ureido moieties are separated by more than 11 Å and hence inter-anion repulsive interaction are unlikely to be responsible. The lack of anion affinity at the second binding site in fact arises from the geometry of the molecule. Upon binding the first anion the two propoxy groups on the opposite site of the 1,3–alternate receptor become closer to each other resulting in steric hindrance at the second possible binding site.[51]

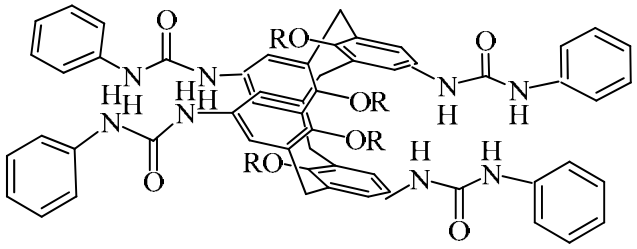

1.43 R = Pr

This work by the group of Lothak was aimed at the incorporation of bridging spacer groups to give rigidity (preorganisation) in double calixarene systems.[50] Such preorganisation was accomplished by introducing bis(calixarene) based complexes **1.44** and **1.45**. Associations constant studies in $CHCl_3$ / DMSO-d_6 (4:1 v/v) confirmed that **1.44** have a higher binding constant for spherical anions like Cl^-. The addition of benzoate showed the highest association constants (almost 20 times higher than other anions), making the much better preorganisation of bis calixarene receptor **1.45** confirming the cooperative effect between the two ureido groups. On the other hand a

similar derivative to **1.44** with two amido substitutents did not exhibit any complexation ability towards halides and benzoate.[51]

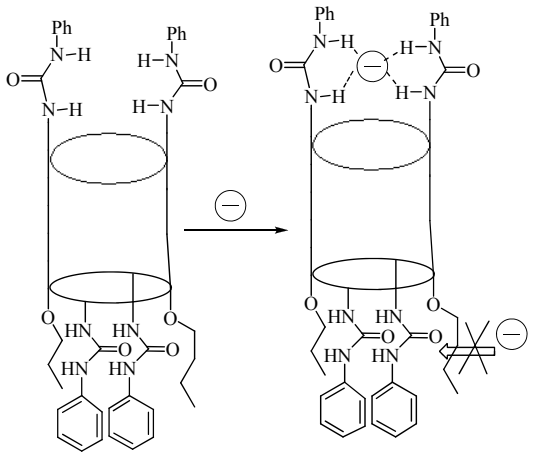

Figure 1.9 Schematic diagrams showing that binding to a second anion in 1.43 is not possible

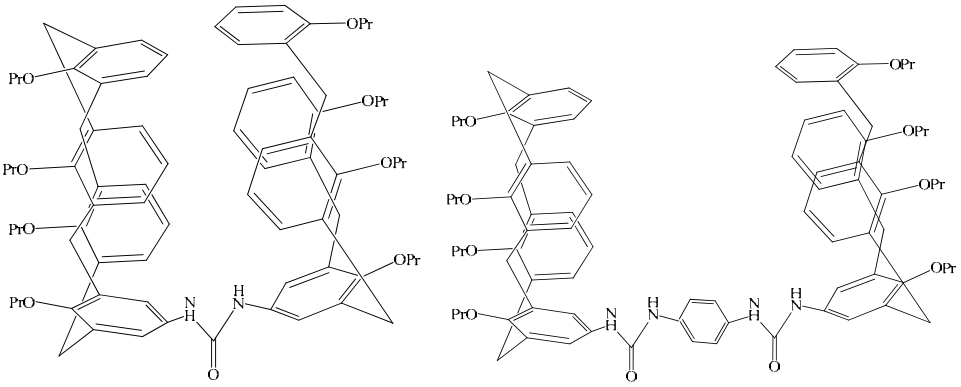

1.44 **1.45**

Tutlani has reported functionalized calix[4]crown urea **1.47** and unsubstituted crown calixarene urea **1.46**. Results indicated that both the compound **1.46** and **1.47** bind Cl^-, Br^-, NO_3^- and $H_2PO_4^-$ albeit to a different extent. Compound **1.47** forms more stable complexes with $H_2PO_4^-$ than compound **1.46** does. The presence of crown bridging group in compound **1.47** increases the binding ability toward Cl^- and Br^- slightly and decreases the ability towards the $H_2PO_4^-$.

Ion pair recognition has also attracted the attention of supramolecular chemists. Beer and coworkers have discovered that the presence of a suitable cation increases the binding ability of anion receptors containing cation-binding units. Compound **1.47** includes a 15-crown-5 unit, which is well known to form stable complexes with Na^+. On addition of Na^+ in presence of DMSO-d_6, solution of the receptor **1.47** resulted in the binding of the metal cation within the crown ether units while the counter anion is bound by the urea functionalities.

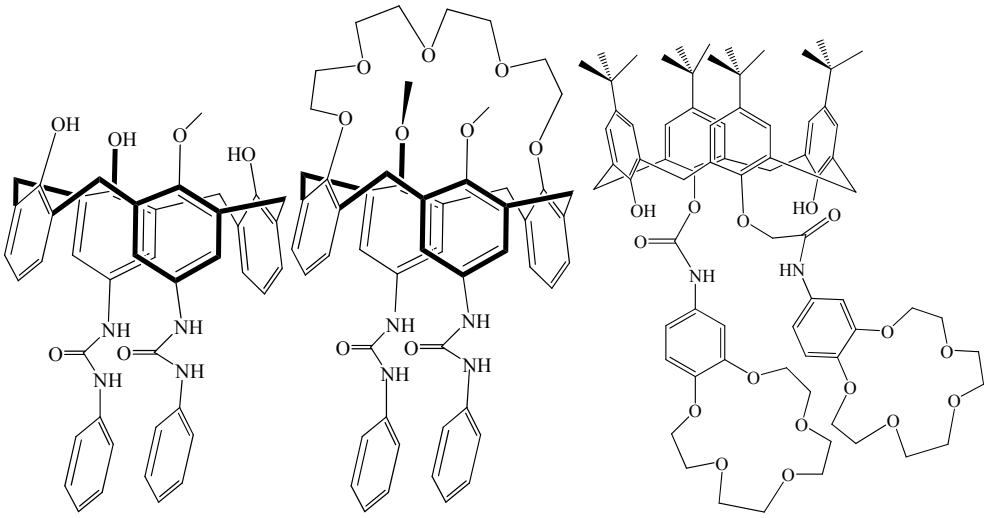

1.46 **1.47** **1.48**

The design of ligands for the simultaneous complexation of cationic and anionic guest species is an emerging and topical field of coordination chemistry.[52] These multisite ligands can be tailored to exhibit novel cooperative and allosteric behaviour whereby the binding of one guest can influence, through the electrostatic and conformational effects, the subsequent coordination of the counter ion. Such systems have potential as new selective extraction and transportation reagent for metal salt ion pair species of environmental importance. Beer and coworkers have introduced the benzocrown **1.48** based on a lower rim substituted calixarene. The ^{1}H-NMR studies in the presence of Na^+ and K^+ cations in deuterated acetonitrile solvent demonstrated the formation of **1.48**·M^+ (M = Na, K) in which the metal is bound in between the crown ether units while the anion is bound by the amide functional groups. Calixarenes substituted with two crown ethers form complexes with K^+, Ba^{2+}, NH_4^+ exclusively at the crown ether binding sites in a 1:1 intramolecular sandwich like fashion. Compound **1.48** and **1.49** form anion complexes

with Cl^-, NO_3^-, $H_2PO_4^-$ and HSO_4^-. The heteroditopic (cation and anion binding) receptors **1.50** and **1.51** based on rhenium bipyridyl (**1.50**) and ferrocene-derived units (**1.51**) have been prepared, which selectively bind alkali metal cations at the lower rim. ^{1}H-NMR spectroscopic titration studies revealed that the strength and selectivity of anion binding is dependent upon the presence of the calix[4]arene moieties and the nature of the bridging group, with the preorganized receptors **1.50** and **1.51** forming strong complexes in deuterated DMSO solutions. Co-bound lithium, sodium and potassium cations were found to significantly enhance the strength of iodide binding in acetonitrile solutions with the largest positive cooperative binding effect was observed with **1.50** and sodium cations. Cyclic voltametric investigation revealed that **1.51** can electrochemically recognize carboxylate and halide anions. In the presence of lithium cation the electrochemical response of bromide anion was significantly amplified.[53]

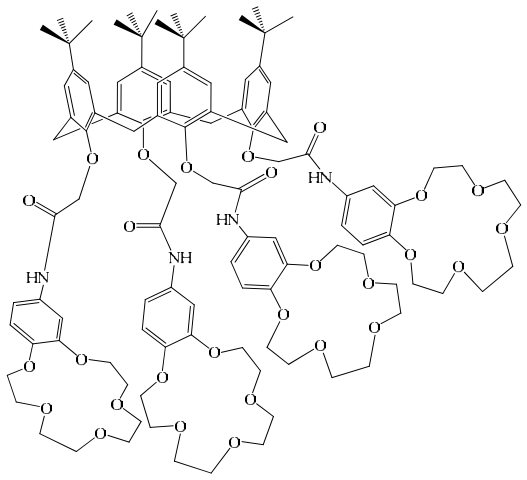

1.49

Reinhoudt and coworkers has reported transport of hydrophilic salts by the mixture of anion and cation receptors. Anion transfer to the membrane phase affects the extraction efficiency of salt transport by cation carriers **1.52** and **1.53**. They concluded that the ditopic receptor **1.54** and **1.55** CsCl or KCl much faster than the monotopic cation receptor **1.52** or **1.53**. The faster transport is due to a higher extraction constant K_{ex} despite lower diffusion constant of the ditopic receptor.[54] Lhotak and co-workers have reported a calix[4]arene based ion pair receptor based on thio-amide **1.56**, which selectively binds tetrahedral anions such as a tetraphenyl phosphinate in preference to Y-shaped anions such as acetate. Selective anion binding was achieved with acetate forming

a 1:1 complex, but in presence of Na^+ there was no change in the binding. The binding constant was increased by a factor of up to 400 times with biphenyl phosphate anion and Na^+.[51]

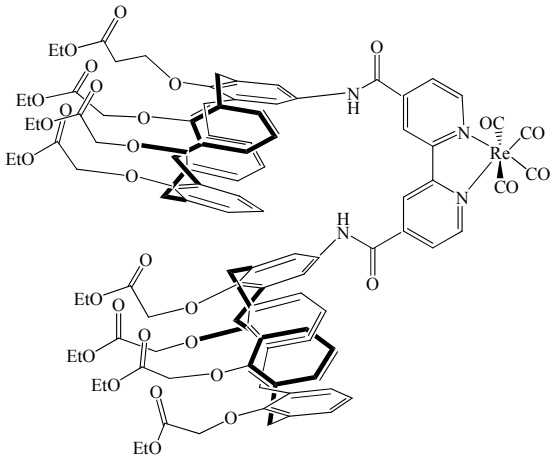

1.50

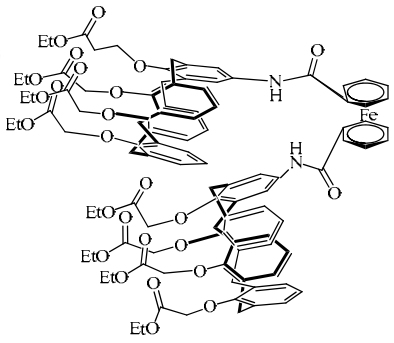

1.51

Biphenyl phosphate is bound significantly less strongly. This is in contrast to results from Umezawa and from Tobe based on hydrogen bonding who reported that the simple receptors featuring a *m*-xylyl bis(thiourea) motif bound phosphates significantly more strongly than acetate.[24] Liu has reported the binding and synthesis of calix[4]arene urea based host **1.57** a ditopic receptor for carboxylate anion. Their binding constant measurements suggest that **1.57** bind a series of dicarboxylate guests more strongly than monocarboxylates. The highest association constant (K_a = 1100 M^{-1}) was reported for the tertiary butyl meta dicarboxylate anion, almost 22 times higher than the monocarboxylate guest. The researchers suggested that the different binding affinity imply that the *p*-xylylene spacer plays a crucial role in the dicarboxylate recognition **1.57**.[55] In the case of hydrogen bonding interaction between the carboxylate anion and urea group, two linear hydrogen-bonding donors is more stable than the bent hydrogen-bonding group as shown in Figure **1.10**.

This molecular modelling calculation suggested that electronic effects have more importance than hydrogen bonding effects. The host molecule is not large enough to accommodate the guest into the cavity, but it tries to accommodate the benzene ring outside the cavity as shown in Figure **1.10**, other effects like van der waals forces, π - π

interactions, CH- π interactions do not imply any valuable contribution in host guest chemistry in this case.[62]

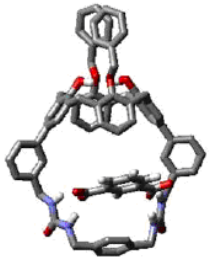

Figure 1.10 Structure showing that linear hydrogen bond is preferred over bent hydrogen bond group.

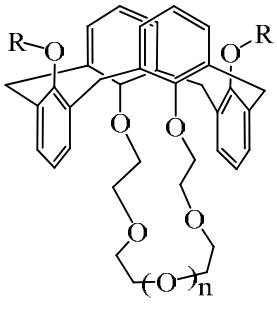

1.52

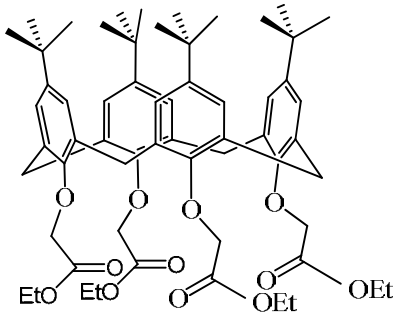

1.53

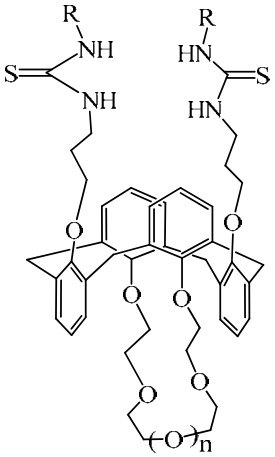

1.54 *n* =1; R = 2-ethyl hexyl

1. 55 *n* = 2; R = 2-ethyl hexyl

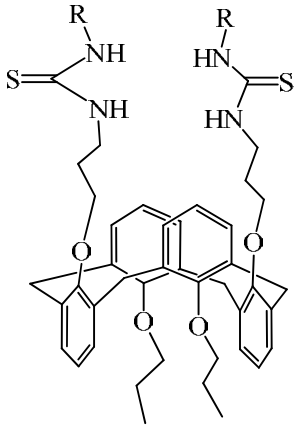

1.56

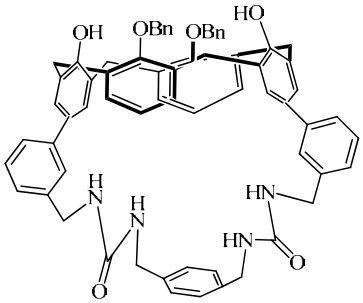

1.57

Reinhoudt's group have produced a series of papers relating to the synthesis of calixarene based urea and thiourea moiety suitable for membrane transport and ion sensing based on chemically modified field effect transistor CHEMFETS. Functionalization of the lower rim of p-tert-butyl-calix[4]arene with two urea or thiourea groups to give **1.59** and **1.60**, results in a class of receptor selective for spherical anions that are bound exclusively through hydrogen bonding.[106] The ^{1}H-NMR spectroscopic determinations of binding constants in $CDCl_3$ reveals selectivity for Cl^- over Br^- and I^-. The stochiometry is 1:1 in all cases as was confirmed by Job plot analysis. The association constants are strongly dependent on the nature of the substituent at the urea moiety. The bidendate phenyl urea derivative **1.60** shows the strongest complexation (Ka for $Cl^- = 7.1 \times 10^3$ M^{-1}) and is the most selective Cl^-. Another paper reports the complexation of halide and tricarboxylate anions by neutral urea-derivatized *p*-tert-butylcalix[6]arene **1.61**, symmetrically functionalized with three thiourea groups at the 1,3,5-phenolic positions linked by a

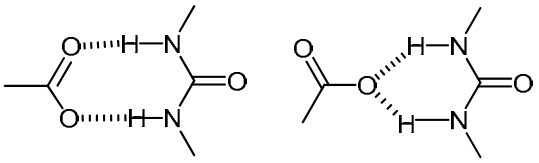

1.58

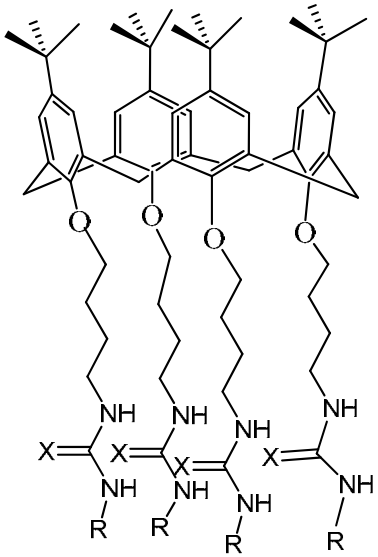

1.59 X = O

1.60 X = S

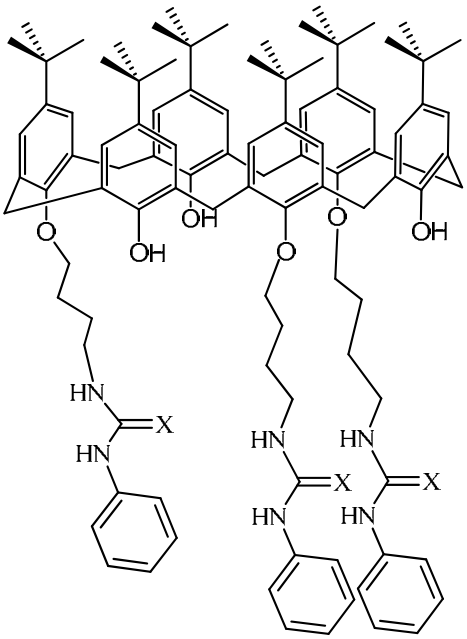

1.61 X = O

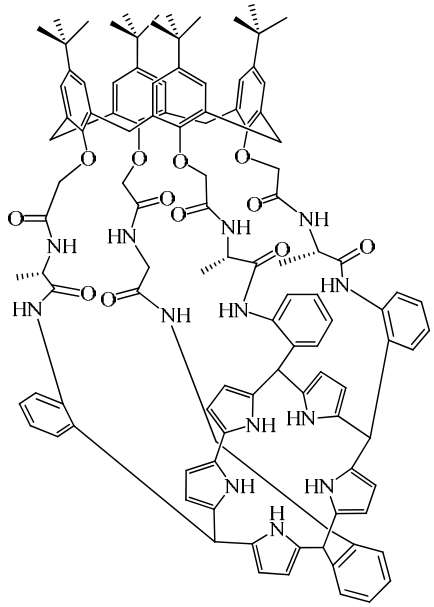

1.62

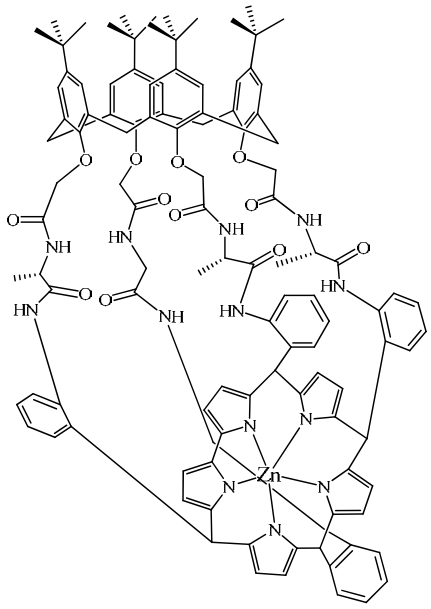

1.62·Zn

The catalytic activity was measured for the series of dinucleotides, namely, GpG, UpU, CpC, ApG and ApA. For ApA, the activity slightly increases with increase in concentration, and the small slope (k_2 = 10^{-3} M^{-1} s^{-1}) suggests that a relatively low concentration has been formed. It was also confirmed that GpG cleaves 8.5 times faster

than UpU and 160 times faster than ApA. These studies demonstrated that the higher activity of GpG than UpU or ApA is due to enhanced binding to Zn(II) and also due to the higher rate of conversion. As most reactive nucleotides like GpG and UpU have an acidic amide NH group that can be deprotonated by Zn(II) bound hydroxide group and resulting anionic form a stable complex with zinc(II).[57] The majority of biological processes take place in an aqueous environment. Artificial receptors soluble in water can mimic natural processes such as specific recognition of bioactive molecule (antigens, microbial /viral pathogens, and nucleotides) or enzymatic transformations of the substrates, helping to reveal mechanistic detail.[58] Ungaro and coworkers have reported water-soluble upper rim calixarenes that can bind to plasmid DNA. The *p*-guanidium calix[n]arenes (**1.65** – **1.70**) have been studied for their DNA binding ability. Water solubility and cytotoxicity were analyzed before the DNA work. It was confirmed that these receptors are not cytotoxic and exhibit high water solubility (confirmed with the help of UV-visible spectroscopy). It was also observed that *p*-guanidium calixarenes substituted with octyl chains form the nanoscopic gels even at lower concentrations. DNA binding studies were reported for **1.65**, **1.67** and **1.68** using bp plasmid pEGFP-Cl and monitored by agarose gel electrophoresis mobility shift assay (EMSA).

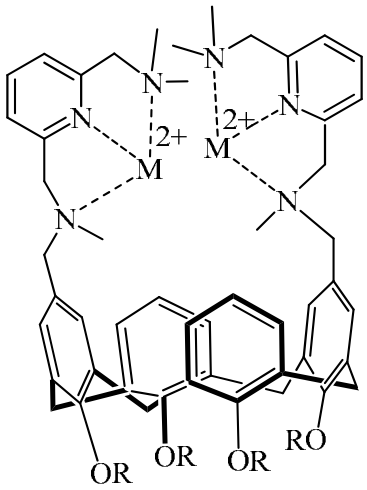

1. 63 R = CH_2CH_2OEt, M = Zn, R' = H

1.64 R = CH_2CH_2OEt, M = Zn, R' = H

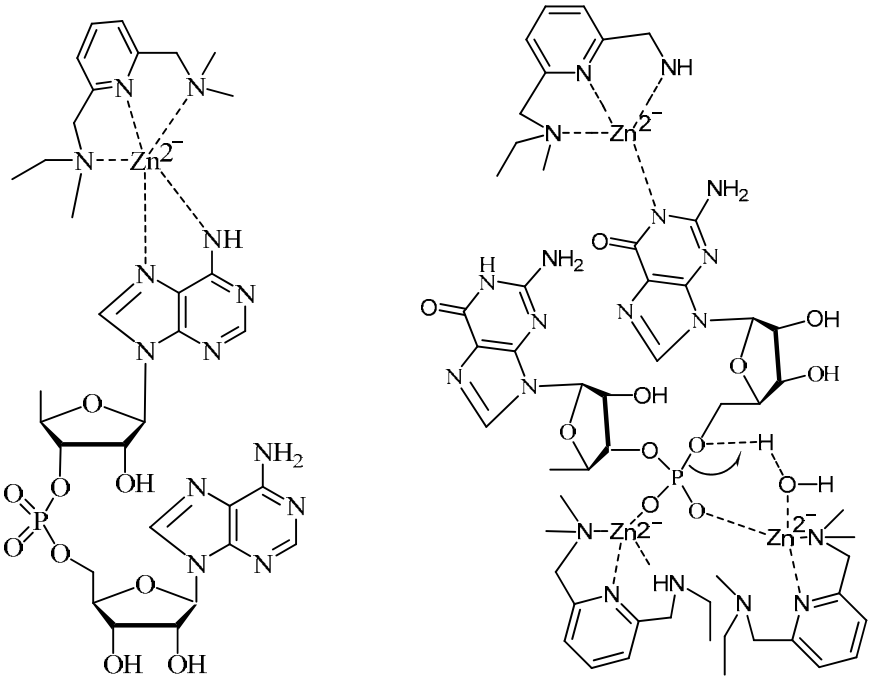

Figure 1.11 Schematic diagram showing the binding of dinucleotide with Zinc anion.

The best linear shift was observed for receptor **1.65**, which starts to bind plasmid at 12.5 mM. AFM investigations allowed the interaction between the different macrocycles and DNA to be directly visualized and the structure of the complexes to be correlated with the transfection properties of the ligands.[59]

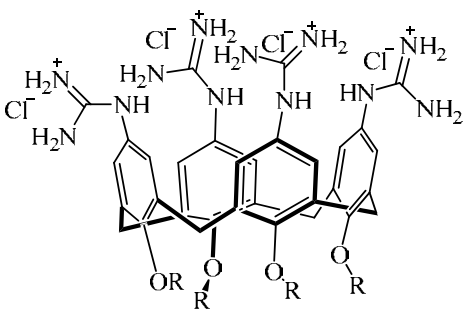

1.65 R = C_3H_7: 4G4Pr –cone

1.66 R = C_6H_{13}: 4G4Hex –cone

1.67 R = C_8H_{17}: 4G4Oct –cone

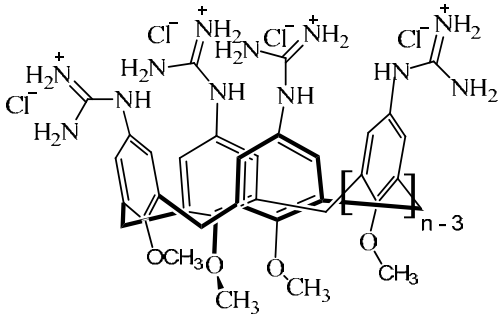

1.68 *n* = 4: 4G4Me – mobile

1.69 *n* = 6: 6G6Me – mobile

1.70 *n* = 8: 8G8Me – mobile

In fact images collected with this technique show that the calix[4]arenes substituted with propyl **1.65**, hexyl **1.66** and octyl **1.67** condense double stranded DNA in compact blobs

which can cross the cell membrane. Conversely, calix[6]- (**1.69**) and calix[8]arenes (**1.70**) give rise to unmasked and large, multimeric aggregates which cannot be delivered into cells, thus explaining the absence of transfection for these larger and conformationally mobile ligands. Interesting behaviour is shown by cone calix[4]arenes compared to mobile calix[6]arenes derivatives such as **1.69**. The former first binds through guanidium phosphate electrostatic interactions and subsequently condenses a single DNA filament through intramolecular hydrophobic interactions of the lipophilic chains at the lower rim. On the contrary, only electrostatic interactions, which give rise to large interfilament networks, operate in the case of calix[6]- (**1.69**) and calix[8]arene (**1.70**) derivatives. An intermediate behaviour is shown by the 1,3-alternate derivatives and by the conformationally mobile calix[4]arenes. This is the first time in which DNA condensation, directly visualized through AFM, has been correlated with transfection and conformational properties of multivalent cationic macrocycles.[59]

1.2.6 Inclusion phenomena

The propensity of calixarenes and related compounds to exhibit inclusion of molecular and ionic guests within the molecular cavity is extremely well known. In this section, we will examine just a few representative examples. Interesting recent work that shows the power of such molecular inclusion follows on from compounds related to **1.68**. A combination of calixarene and cyclodextrin chemistry has been used to target an ambitious supramolecular capsule array on a 'molecular print board', exploiting electrostatic (charge – charge) interactions. A molecular capsule was synthesized by mixing an equimolar amount of a water-soluble calixarene sulfonate and a guanidium based calixarene (**1.71**) related to **1.68**. This resulted in the precipitation of a capsule as a consequence of the neutralization of the charges upon capsule formation and the presence of four lipophilic adamantyl groups, which further decreases the water solubility of the supramolecular assembly.[60]

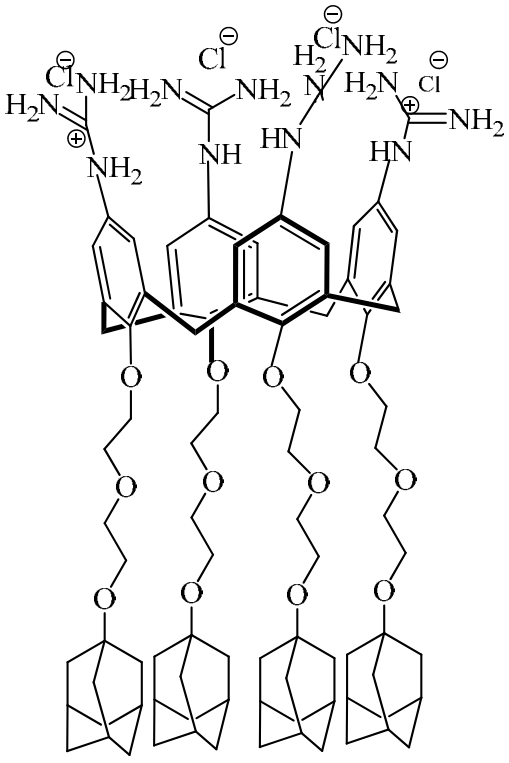

1.71

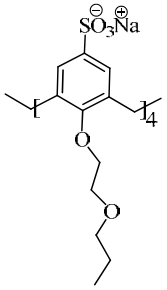

1.72

Upon addition in solution of *β*-cyclodextrin (*β*-CD), which forms an inclusion complex with adamantly units of **1.71**, the capsule dissolves in water and a clear solution is obtained. Evidence for a capsule formation in MeOH and D_2O solution containing 10^{-2} M *β*-CD was obtained by electrospray ionization (ESI) mass spectrometry and ^{1}H-NMR spectroscopy, respectively. The strength of the capsule assembly was evaluated by isothermal titration calorimetry (ITC) in H_2O containing 10^{-2} M *β*-CD. The data obtained from the titration were successfully fitted to a 1:1 binding model giving the association constant $K_a = 7.5 \times 10^5$ M^{-1} for the capsule complex. The tetravalent interaction of the four adamantly groups of the system with the cyclodextrins are shown in Figure **1.12**. Related amphiphilic cyclodextrins form a self-assembled monolayer on gold leading to the 'molecular print board' concept.[60] In 1994, Atwood and Shinkai in a series of papers discussed the preferential inclusion complex formation between C_{60} and calixarenes from a mixture of C_{60} and C_{70}.[61] This is accomplished by the formation of 1:1 complex mixture between the C_{60} guest and the calixarenes.[61] Complexation studies were undertaken between C_{60} and calix[*n*]arenes.[62]

The C_{60} guests could be recovered by the use of chlorinated solvents leading to a method to purify Fullerenes by means of calixarene inclusion. Suzuki and Shinkai also described an efficient way of purification of C_{60} from carbon soot. C_{60} was precipitated out as the calixarene complex from hot toluene in the presence of *p*-tert-butyl calix[8]arene, suggesting that the cavity size, intramolecular hydrogen bonding in the host and the presence of the tert-butyl groups all have a vital role in the selective binding and hence precipitation of the complex.[63]

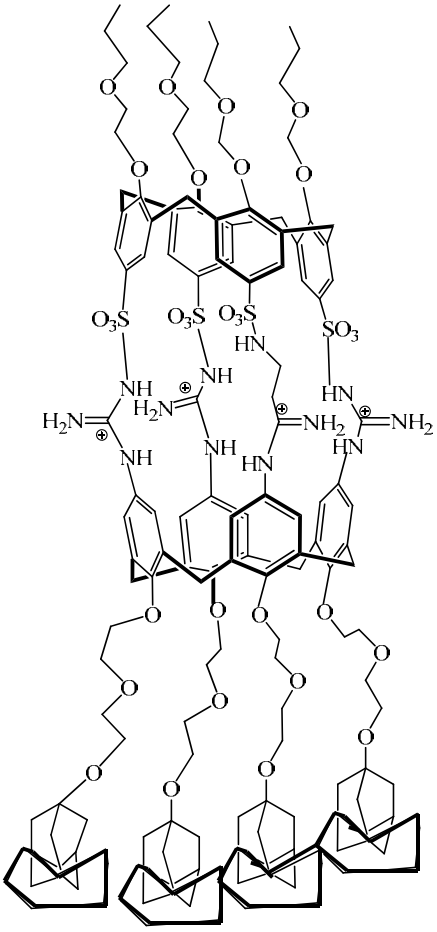

Figure 1.12 Formation of an inclusion complex on β-CD on gold surface.

Georghiou and coworkers have reported possible complex formation between C_{60} and calix[4]naphthalene **1.73**. Association constants were determined in different solvent systems. The highest association constant for the *t*-butyl calix[4]naphthalene and C_{60} complex was reported with CS_2 (K_a = 6920 M^{-1}), toulene (676 M^{-1}) and benzene (K_a = 295 M^{-1}). Debutylated calix[4]naphthalene having bound C_{60} guests complex was reported with CS_2 (K_a = 3390 M^{-1}), toulene (631 M^{-1}) and benzene (K_a = 457 M^{-1}).[83] Georghiou has also concluded that the deeper cavity of the calix[4]naphthalene and cation pi (π) interactions make it more efficient for the selective extraction of C_{60}. Rebek Jr. has also reported the formation of deepened cavities (up to 14 Å) based on the slight modification of the rim of octanitro-cavitands **1.74**.[65] These deepened cavities proved to be an excellent for the selective complexation of C_{60}.[65] Atwood and coworkers have reported that tert-butylcalix[8]arene forms trimeric micelle-like structures in the double cone conformation with C_{60} in toluene solution which may explain the dissolution of the

tert-butylcalix[8]arene complex with C_{60} in the presence of a slight excess of the calixarene.[61] Fukazawa and coworkers have also reported the formation of a C_{60} complex with calix[6]arenes bearing *N*,*N*-dialkylaniline moieties with the highest association constant ($K_a = 7.9 \times 10^2$ dm^3 mol^{-1}) reported so far. Fukazawa has screened the series of calixarenes for possible complexation with C_{60} and to study their interactions.[66]

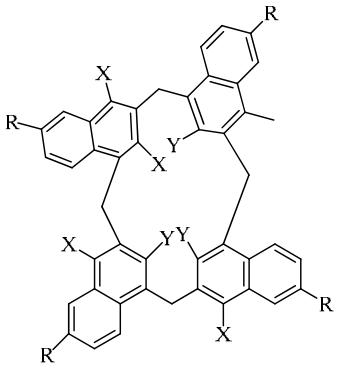

1.73

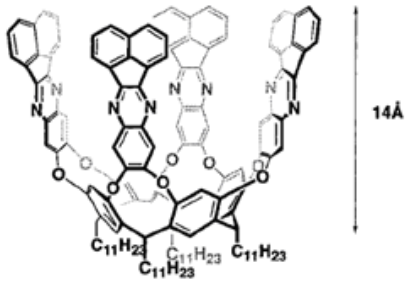

1.74

In this work, comparison of the lower rim substituted and unsubstituted forms showed that the hydroxyl groups play an important role. The internal cavity is also important in forming a complex and the hydroxyl functionalities may serve to rigidify the cavity.

1.2.7 Sulphonated calixarenes

Perhaps the most studied calixarenes are the water-soluble sulphonated derivatives. Complexation of a number of common amino acids by three sulphonato-calix[*n*]arenes (*n* = 4, 6, 8) in water has been determined by Coleman and Desrosiers by microcalorimetry. They determined the thermodynamic parameters for the binding of lysine and arginine by sulphonatocalix[*n*]arenes in water at 298.15 K. Tin derivatives were also studied with a view to catalysis of the hydrolysis of amino acid esters however the hydrolysis rates decreased in the presence of the calixarene complex.[102] Sulphonated calixarenes have been reported as enzyme mimics and calcium blockers,[67] and they also exhibit antiviral and anti-thrombotic properties.[68] Raston and coworkers have reported complex formation with ytterbium chloride and tetraphenylphosphonium ion with hydrated sulphonated calixarenes.[69] Considerable efforts have been devoted over the past decades to developing methods to synthesize functionalized derivatives of sulphonated calixarenes. Shinkai has reported the lower rim substitution of sulphonatocalix[*n*]arenes with hexyl groups, which proved good for the selective extraction of the uranyl ion (UO_2^{2+}) from seawater. The upper rim of sulphonatocalix[6]arene has been functionalized with carboxylate groups and it was found that the stability constant with UO_2^{2+} was greater by two orders of magnitude than for other macrocyclic hosts.[70] Two complex solid state structures of p-sulphonatocalix[8]arene have been described by Coleman's group, one being an almost planar macrocyclic ring and the other showing the double partial cone structure, with each four-membered partial cone directed at 180^0 in relation to the other.[71] Solid state structures have been reported with sulphonated calixarenes and butane-di-ammonium cations.[71]Atwood and Coleman have extensively studied the crystal and packing behaviour of sulphonated calixarenes and showed that the structures can be divided into organic and inorganic layers reminiscent of clays. The organic layer is formed by interlocking calixarenes in an up-down fashion, with a sodium ion and a water molecule interacting simultaneously with a phenolic oxygen atom of the compound. To accommodate this cation, one acidic OH proton of each calixarene is removed; the resultant negatively charged oxygen atom forms a strong electrostatic bond with the sodium ion. The inorganic layer is comprised of the remaining four sodium ions and eleven water molecules.[72] These exist in a vast hydrogen-bonded array that includes the sulphonato head groups of the calixarenes. Characteristics of various types of sulphonated calixarenes is their solubility in organic solvents. Shinkai reported that sulphonated

calix[*n*]arenes (*n* = 4, 6, 8) form highly luminescent complexes with Tb^{3+} complexes.[12] In the past ten years sulphonated calixarenes have been used in highly diverse biomedical applications including anti-viral and antithrombotic activities,[68] enzyme blocking and protein complexation.[102, 68] Because of these interesting properties from inclusion chemistry to medicinal application of sulphonated calixarenes, many groups are focussing on their chemistry and properties. In the past few years sulphonated calixarenes have been shown to act as heparin, mimics. A particular advantage is the fact that sulphonated calixarenes can be synthesized in three relatively simple steps, while heparin saccharide requires some fifty steps![102]

1.3 Metal based anion hosts

1.3.1 Metal based anion hosts

There is currently a need for a rational approach towards ligand design for the selective simultaneous complexation of metal cations and anions in solution.[18, 49] Potential application areas are in the selective extraction of toxic metals from nuclear waste, design of antibiotics that owe their antibiotic action to specific metal complexation, the design of metals complexes to act as an imaging agent in the body, design of functional groups for chelating ion-exchange materials and selective metal extractants in hydrometallurgy.[73] In the body there are lots of processes in which selectivity plays an important role and such cascade receptors often find applications as models for enzyme active sites. Copper complexes are of particular interest because of the naturally occurring haemocyanins; di-copper respiratory proteins that perform a similar role to haemoglobin in most mollusks and some anthropods. Deoxy-haemocyanin is colourless and contains two copper(I) sites coordinated by nitrogen atoms from histidine residues. In the context of designing ligands for selective complexation of cation-anion ion pairs, design can be guided by fundamental principles such as Pearson's hard and soft acid and base concept,[74] steric strain in complex formation, solvation, complimentarily of bond lengths and angles, van der Waals forces, and in some cases dipole-dipole interactions and hydrogen bonding.

Silver and copper metals have d^{10} s^1 electron configurations and hence readily form soft monovalent d^{10} metal ions that bind to different ligands (e.g. S, P, N and O donors).[75] The silver(I) is a versatile building block in supramolecular chemistry because of its various potential coordination geometries; it commonly forms linear, trigonal or tetrahedral complexes and its affinity for soft donor atoms such as sulphur. Silver(I) also binds strongly to nitrogen donors and forms weaker interactions with harder oxygen ligands.[76]

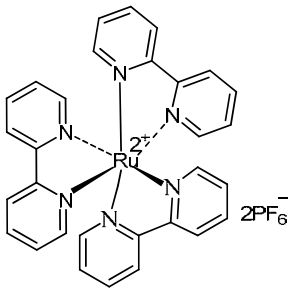

1.75

There is a great deal of chemistry involving the soft Lewis acid Ag^+ and ligands containing sulphur atoms. The binding of anions by organic or metal-based hosts is a process fundamental to many natural systems. There is thus significant interest in synthesizing simple artificial analogues of metal-containing natural hosts that have the same ability to selectively bind anions via intermolecular forces such as hydrogen bonding to ureas and amides.[77] For example, Beer et al., have reported a bipyridyl-based ruthenium complex stabilized by hexaflurophosphate anion. ^{1}H-NMR spectroscopic titration with hexaflurophosphate anion has confirmed the formation of 1:1 complex **1.75**.[78]

Sessler and co-workers have reported analogous dipyrrolylquinooxaline [11] phenanthroline complexes of Ru(II) and Co(III) that act as anion receptors. Their anion binding properties were studied by UV-vis spectroscopy in DMSO and both complexes have strong selectivity for fluoride with association constants of 12,000 M^{-1} for **1.76** and 54,000 M^{-1} for **1.77** compared to 10 – 50 M^{-1} for both complexes with chloride and dihydrogenphosphate.

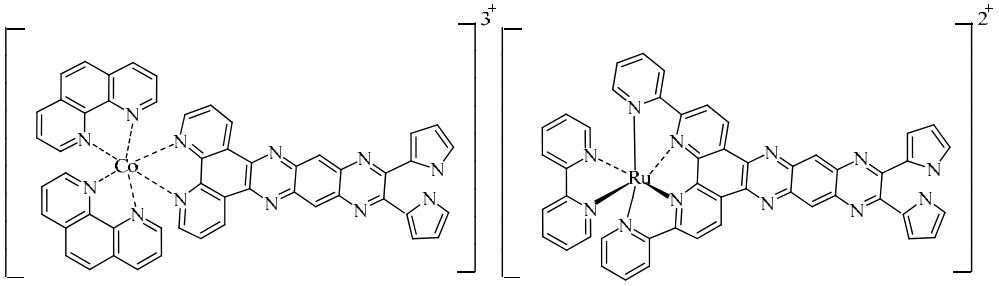

1.76 **1.77**

Loeb and co-workers have reported anion receptors based on square planar platinum complexes. The urea functionalized isoquinoline ligand **1.78** formed a square planar platinum(II) complex that binds both chloride and sulphate, $[Pt(L)]_4(X)_2$ X = Cl, SO_4 (**1.79** and **1.80**). The X-ray crystal structure of the chloride complex shows the host acting as a ditopic receptor while the sulfate complex is a remarkable 1:1 complex with all four urea groups interacting with a single anion, Figure **1.13.** ^{1}H-NMR spectroscopic titration confirms that there is strong binding with both anions.[79]

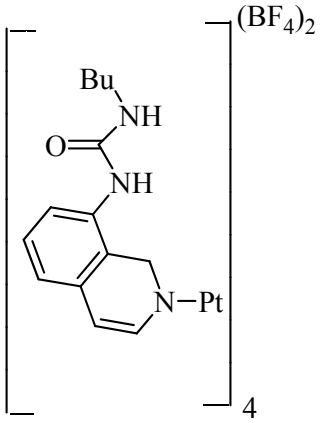

1.78

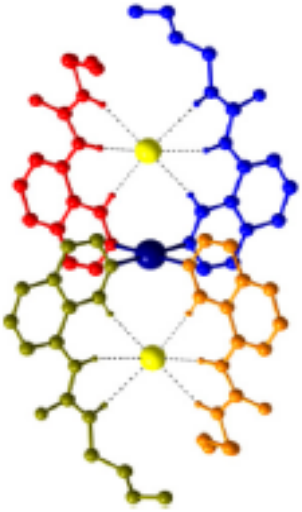

1.79

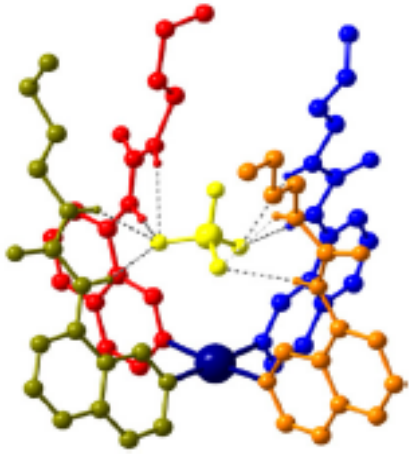

1.80

Figure 1.13 Ball and stick representation of platinum(II) complexes of ligand 1.80 with chloride and sulphate anions.[98, 99]

1.3.2 Ion pair receptors

There is a great deal of interest in designing and synthesizing artificial ion pair receptors, because of their importance in natural biological systems able to simultaneously transport oppositely charged ion such as H^+ and Cl^- across membranes.[107] Ion pair receptors can be classified depending on the type of solvent ranging from polar, less polar to and non-polar. In polar solvents, ion pair receptors can facilitate organic reactions where the cation is solvated. In less polar solvent, ions are poorly solvated and form either contact ion pairs, in which an individual pair of oppositely charged ions are directly bonded via electrostatic interactions, or aggregated contact ion pairs in which a numbers of ions form small clusters, which are solvated by surrounding medium. Classic targets for simultaneous cation/anion receptors are zwitterions of amino acids.[52, 81]

Contact ion pair receptors depend upon the effect of solvent as well as upon binding sites available and relative size, electronic properties and functionality of the ligand. Typical considerations for the anion-recognition portion of the receptor include stereoelectronic effects, Lewis acidic sites, π-π stacking and potential for hydrogen bond formation.[101]

Ion pair binding of simple aryl urea ligands in chloroform solution has been reported by Wilcox and co-workers. Aryl ureas substituted with a nitro group at the meta position are particularly good receptors for anion binding, as reported by Etter.[52, 83] It was concluded that the aryl urea **1.81** is an excellent receptor for ion pairs containing sulphonates, phosphates and carboxylate in solution.[52]

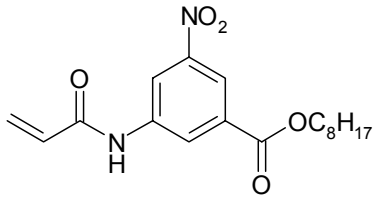

1.81

Beer et al., have reported dithiocarbamate-based thiourea and amide derived hosts as shown in Figure **1.14**. In this work a heteroditopic transition metal dithiocarbamate based on amide-functionalized benzocrown ether were prepared and the complexation of cation-anion ion pairs studied. It was concluded that acetate binds six times more strongly when potassium is co-bound at the benzo-15-crown-5 dithiocarbamate hosts.[84]

Smith has reported contact ion pair binding by macrobicycles **1.82** and **1.83** with alkali metal chloride. In these systems alkali metal cations, particularly sodium and potassium, interact with the oxygen atoms of the diazamacrocycle while halide anions interact with the amide functionalities as illustrated in Figure **1.15**. Bandini et al have reported a related pyrazole derivative.[85 - 89]

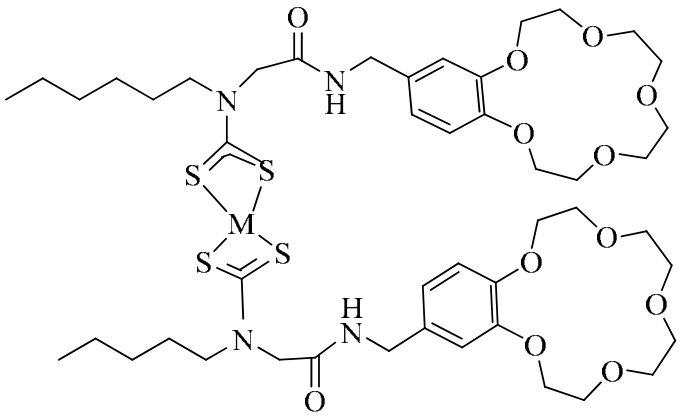

Figure 1.14 M = Ni, Cu dithiocarbamate based hosts capable of alkali metal cation and anion binding.

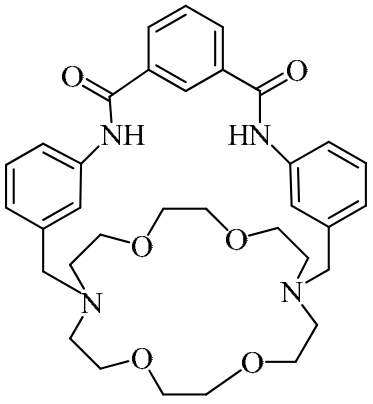

1.82

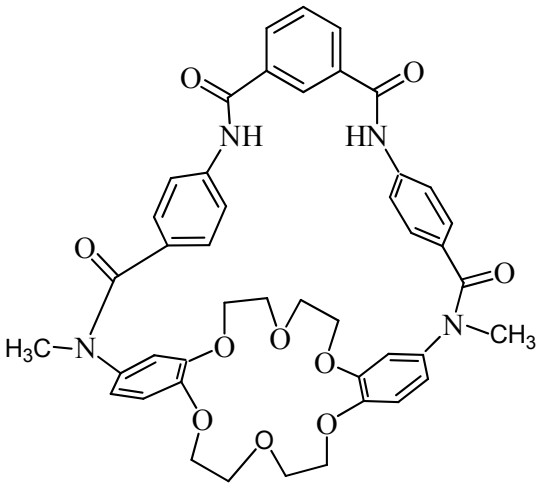

1.83

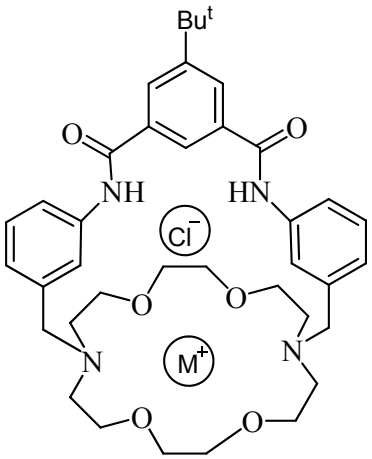

Figure 1.15 An illustration of alkali chloride ion pair binding by a macrobicycle.

1.4 Cystic Fibrosis

1.4.1 The problem

Cystic fibrosis is one of the most common inherited diseases among the Caucasian population.[90] The gene responsible was identified 12 years ago, which enabled extensive studies on the functions of the mutated protein, the Cystic fibrosis transmembrane conductance regulator.[91] There are number of mutations, which cause defective functions of CFTR in epithelial cells, primarily in the respiratory tract, sweat glands and in the gut. CFTR protein acts as a transmembrane chloride transporter and as a regulator of other ion channels.[92] The most common mutations involve three nucleotides that are deleted from the gene causing the transcribed protein to lack phenylalanine at position 508 in its primary structure. The mutation reduces the ability of affected cells, predominantly the epithelial lining of the lungs, to transport chloride and causes them to produce unwanted mucus, which reduces the ability of the lungs to work properly.[91] One approach to treat this condition is to increase transmembrane chloride transport through the introduction of artificial chloride-specific channel forming compounds directly to the affected epithelial cells.[4] Such a channel consists of two layers of molecules meeting 'tail to tail' to form a structure with polar internal and external surfaces and a non-polar region in between.[94] According to the fluid mosaic model, the membrane is host to a variety of macromolecules with specific functions that can penetrate, or bind to its structures. The bilayer may incorporate these macromolecules but remains unbroken unless seriously compromised. The changes in polarity through the bilayer ensure that it forms an effective barrier between extra and intracellular environments. The bilayer thickness (ca. 5 – 6 nm) gives a minimum distance required for a molecule to pass between these regions.[91]

Two general mechanisms for transmembrane ion transport are known: shuttle like movement of a single ion with a carrier molecule, and channel formation allowing a stream of ions to pass through. In the shuttle like process, a carrier molecule binds to a single target ion and the complex passes through the bilayer. To be effective a carrier must bind specifically to only one type of target ion and the complex must traverse the polar and non polar regions of phospholipid bilayer. In the second mechanism one or more macromolecules inserts into the cell membrane; thereby opening a pore through the lipid bilayer. The size of the pore dictates the maximum size of the species that may traverse its length. Transport is extremely rapid with a rate of *ca.*10^8 ions per second

possible in some channels. The ion flow can be controlled by using chemical or electrical signals to open and close the gate.[92]

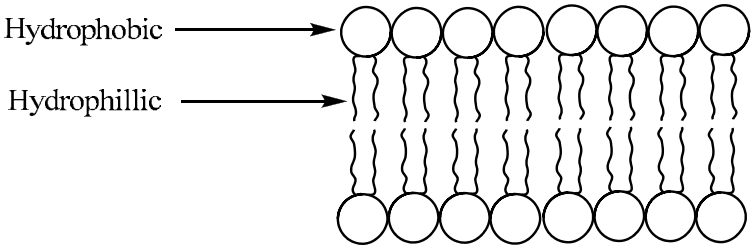

Figure 1.16 Phospholipid bilayer membrane

1.4.2 Solution: Design of chloride hosts based on calixarenes

Qualitatively comparable dermatitis responses have been noted for *p*-tert-butyl phenol-formaldehyde resins, particularly, the linear tetramer. *p*-tert-Butylcalix[4]arenes and *p*-tert-butylcalix[8]arenes give negative responses in the Ames mutagenicity test.[95]An extensive medical and biomedical literature has arisen during the last three decades concerning the oxylalkyl derivatives of simple phenol as well as phenol–formaldehyde condensation products. In the early work of Cornforth, oxyethylated calixarenes were prepared by treating them with ethylene oxide, which yielded a macrocyclic product, which was further tested by Delville and Jacques in the therapy of parasitic diseases.[36] Hart et al have used these oxyethylated calixarenes to induce fusion of erythrocytes.[96] These macrocycles and their related compounds were studied for their effects on phospholipids. A number of research groups have considered cyclodextrins, (from a building block of glucose [97, 98] heparin[99] (a repeating unit of sulphonamide) as powerful tools in many biological transformations with activity towards tuberculosis, viral infections and many others.[100, 102] Recent reviews indicate that phenol derived groups are used as drug target molecules, because they possess a broad range of physiological properties.[100]

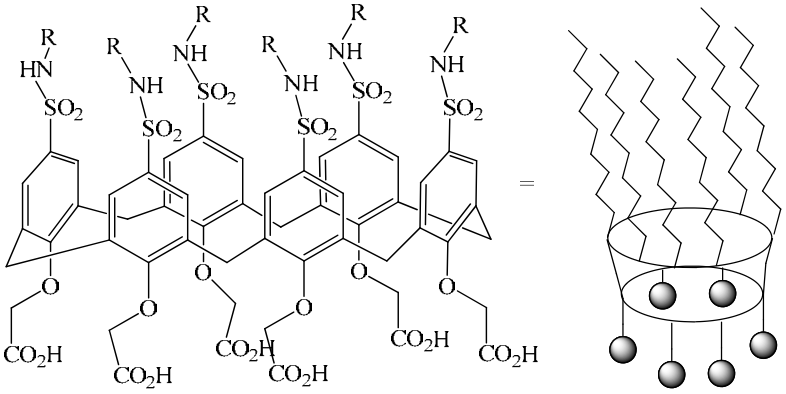

Figure 1.17 Upper rim hydrophobic chain calixarenes R = Alkyl, Aryl

Calixarenes are a versatile class of macromolecule, which have tremendous capability to bind in a variety of different ways due to their large internal cavity, which is suitable to act as an enzyme mimic for example,[101] and hence they can complex proteins and amino acids.[102] One possible application is in the treatment of cystic fibrosis, a disease arising from poor transport of chloride across the lung epithelial membrane that causes the build

up of mucus and hence severe respiratory deficiencies.[91] There are different approaches towards the treatment of cystic fibrosis,[91, 92] but our approach is based on derivatives of the calix[n]arenes. Calixarenes are chalice (bowl) shaped molecules formed by the base catalyzed condensation of tertiary butyl phenol and formaldehyde.[103] Methods to produce calix[6]- and calix[8]arenes are known, and the tert-butyl groups can be removed to give a suitable channel 'mouth' in a couple of steps.[103] The calixarene upper and lower rims can be functionalized to produce a range of candidates for study. Particularly interesting are calixarenes that have overall amphiphilic character where either the upper or lower rims have long-chain alkyl groups acting as hydrophobic tails.[104]

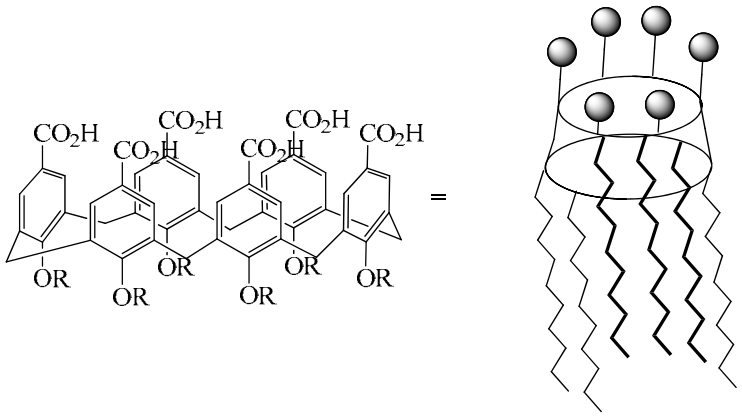

Figure 1.18 Lower rim hydrophobic chain calixarenes R = Alkyl, Aryl

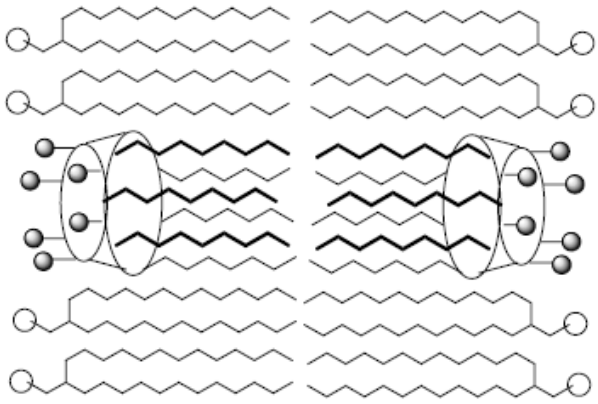

Figure 1.19 Amphiphilic calixarenes within a lipid bilayer forming an end-to-end channel

Calixarenes have been recognized as a good scaffold for chloride binding and hence the construction of artificial chloride ion channels,[93] because of their ready availability,[103] complexation phenomena and the water solubility of some calixarenes.[105] Urea and amide

substituents at the lower rim of the calixarene scaffold have a tremendous capability to bind series of anions especially chloride or related spherical anions.[106] Our approach is to engineer artificial chloride ion channels (or chloride ionophores) based on a calixarene scaffold bearing amide or urea type anion binding functionality.[93, 94, 107] These compounds should facilitate the passage of chloride ion through the phospholipid bilayer thus restoring transmembrane chloride balance as shown in Figure **1.19**. One possible mode of action is the insertion of these compounds should into a bilayer membrane to form an end-to-end channel as shown in Figure **1.19.**

Donald Cram in his visionary statement about the calixarenes said that, large metabolisable molecular cells might be used in drug or agricultural chemical delivery systems or in systems in which very slow release of compounds chemically shielded from their environment are needed. Metabolism- resistant carcerands containing appropriate radiation emitting metal ions or atoms might be attached to immunoproteins that seek out cancer cells.[108] Because of diverse biomedical and medicinal application of the calix[n]arenes, we propose to design such macromolecular scaffolds based on variety of functional groups such as oxyalkyl, alkyl nitrile and urea functionalities. Solubility is also an important parameter in designing the macromolecule. The solubility of the macrocycle varies with slight modification of the upper or lower rim and hence it may be possible to tune the macrocycle for our desired activity and properties. We know that most of calixarene based macrocycles are sparingly soluble in organic solvents. Modification of the upper or lower rim with sulfonate functionality should lead to a water soluble macrocycle to which anion binding functionality can be appended.[102] It is anticipated that such water-soluble calixarenes bearing anion binding functionality such as urea groups will represent a novel approach to the treatment of diseases such as cystic fibrosis.

1.5 Conclusions

In conclusion, the versatile nature of calixarenes means that they are suitable as scaffolds for the design of simple artificial synthetic molecules that can act as a channel in a phospholipid membrane (biological membrane). It is anticipated that such artificial channels based on urea pendant groups will not only facilitate the transport of chloride anion, but help in solubility, transport and binding in solution.

Calixarenes can be tuned at upper or lower rim using the standard procedures of substitution, debutylation to increase their solubility in various media. Our interest is to make urea-based calixarenes functionalized at the lower rim that can facilitate the transport of chloride anion in solution. Chloride anions are excellent guests for urea hosts because of spherical geometry and low charge to mass ratio. The role of chloride in diseases such as cystic fibrosis makes it a particularly attractive target. The lower rim can be modified using different alkyl, aryl, and fluorescent groups to facilitate the desired solubility, binding and transport properties as well as chloride sensing in solution.

We are also interested that how molecules based on simpler urea based ligands bind with metal cations and anions in solid and solution phase as a model for anion binding by calixarenes that are more sophisticated. In particular, we propose to study thiomethyl phenyl urea ligands whose metal and anion binding ability can be determined using the standard solution and solid phase chemistry.

1.6 References

1. C. J. Pedersen, *J. Am. Chem. Soc.*, 1967, **89**, 2495 -2496
2. C. J. Pedersen, *J. Am. Chem. Soc*, 1967, **89**, 7017 - 7036.

.

3. D. F. Shriver and M. J. Biallas, *J. Am. Chem. Soc.*, 1967, **89**, 1078-1085.
4. C. H. Park and H. E. Simmons, *J. Am. Chem. Soc.*, 1968, **90**, 2431-2433.
5 C. H. Park and H. E. Simmons, *J. Am. Chem. Soc.*, 1968, **90**, 2429-2431.
6. E. Graf and J.-M. Lehn, *J. Am. Chem. Soc.*, 1975, **97**, 5022-5024.
7. J.-M. Lehn, E. Sonveaux and A. K. Willard, *J. Am. Chem. Soc.*, 1978, **100**, 4914-4916.
8. B. Dietrich, T. M. Fyles, J.-M. Lehn, L. G. Pease and D. L. Fyles, *J. Chem. Soc., Chem. Commun.*, 1978, **8,** 934-937
9. A. Baeyer, *Ber. Dtsch. Chem. Ges.*, 1872, **5**, 25.
10. J. L. Sessler, D. Q. An, W. S. Cho and V. Lynch, *Angew. Chem. Int. Ed.*, 2003, **42**, 2278-2281.
11. J. L. Sessler, S. Camiolo and P. A. Gale, *Coord. Chem. Rev.*, 2003, **240**, 17-55.
12. P. A. Gale, J. L. Sessler, V. Kral and V. Lynch, *J. Am. Chem. Soc.*, 1996, **118**, 5140-5141.
13. P. A. Gale, P. Anzenbacher Jr. and J. L. Sessler, *Coord. Chem. Rev.*, 2001, **222**, 5 7-102.
14. P. A. Gale, J. L. Sessler and V. Kral, *Chem. Commun.*, 1998, **27**, 1-8.
15. B. Dietrich, T. M. Fyles, M. W. Hosseini, J.-M. Lehn and K. C. Kaye, in *J. Chem. Soc. Chem. Commun.*, Editon edn., 1988, vol. 10, pp. 69-692.
16. P. D. Beer and P. A. Gale, *Angew. Chem., Int. Ed.*, 2001, **40**, 487-516.
17. J. W. Conforth, P. D' Arcy Hart, G. A. Nicholls, R. J. W. Rees and J. A. Stock, *Br. J. Pharmacol.*, 1955, **10**, 73.
18. P. A. Gale, *Coord. Chem. Rev.*, 2001, **213**, 79-128.
19. R. I. S. Diaz, J. Regourd, P. V. Santacroce, J. T. Davis, D. L. Jakeman and A. Thompson, *Chem. Commun.*, 2007, **72**, 2701-2703.
20. G. R. Desiraju, *The Design of Organic Solids*, Elsevier, Amsterdam, 1989.
21. L. J. Prins, D. N. Reinhoudt and P. Timmerman, *Angew. Chem. Int. Ed.*, 2001, **40**, 2383-2426.

22. D. Blazina, S. B. Duckett, P. J. Dyson, R. Scopelliti, J. W. Steed and P. Suman, *Inorg. Chim. Acta*, 2003, **354**, 4-10.
23. M. G. Cacace, E. M. Landau and J. J. Ramsden, *Q. Rev. Biophys.*, 1997, **30**, 241-278.
24. Y. Umezawa, S. Nishizawa, P. Buhlmann and M. Iwao, *Tetrahedron Lett.*, 1995, **36**, 6483-6486.
25. A. Masunov and J. J. Dannenberg, *J. Phys. Chem. B*, 2000, **104**, 806-810.
26. S. J. Brooks, P. A. Gale and M. E. Light, *Chem. Commun.*, 2006, 4344-4346.
27. A. D. Hamilton and B. Linton, *Chem. Rev*, 1997, **97**, 1669-1680.
28. B. R. Linton, M. S. Goodman, E. Fan, S. A. van Arman and A. D. Hamilton, *J. Org. Chem.*, 2001, **66**, 7313-7319.
29 M. P. Hughes, M. Y. Shang and B. D. Smith, *J. Org. Chem.*, 1996, **61**, 4510-4511.
30. M. P. Hughes and B. D. Smith, *J. Org. Chem.*, 1997, **62**, 4492-4499.
31. A. P. Davis and J. B. Joos, *Coord. Chem. Rev.*, 2003, **240**, 143-156.
32. F. P. Schmidtchen, *Angew. Chem. Int. Ed.*, 1977, **16**, 720.
33. F. P. Schmidtchen and M. Berger, *Chem. Rev.*, 1997, **97**, 1609-1646.
34. L. O. Abouderbala, W. J. Belcher, M. G. Boutelle, P. J. Cragg, M. Fabre, J. Dhaliwal, J. W. Steed, D. R. Turner and K. J. Wallace, *Chem. Commun.*, 2002, **99**, 358-359.
35. M. Bochmann, *J. Chem. Soc., Dalton Trans.*, 1996, **5**, 255-270.
36. P. D. Beer, *Acc. Chem. Res.*, 1998, **31**, 71-80.
37. P. D. Beer and J. B. Cooper, *Chem. Commun.*, 1998, **4**, 129-130.
38. A. Ikeda and S. Shinkai, *J. Am. Chem. Soc.*, 1994, **116**, 3102.
39. A. Arduini, M. Fabbi, M. Mantovani, L. Mirone, A. Pochini, A. Secchi and R. Ungaro, *J. Org. Chem.*, 1995, **60**, 1454-1457.
40. M. Conner, V. Janout and S. L. Regen, *J. Am. Chem. Soc.*, 1991, **113**, 9670-9671.
41. J. Scheerder, R. H. Vreekamp, J. F. J. Engbersen, W. Verboom, J. P. M. van Duynhoven and D. N. Reinhoudt, *J. Org. Chem.*, 1996, **61**, 3476-3481.
42. B. R. Cameron and S. J. Loeb, *Chem. Commun.*, 1997, **3**, 573-574.
43. A. Casnati, M. Fochi, P. Minari, A. Pochini, M. Reggiani, R. Ungaro and D. N. Reinhoudt, *Gazz. Chim. Ital.*, 1996, **126**, 99-100.
44. D. N. Reinhoudt, J. Scheerder, R. H. Vreekamp, J. F. J. Engbersen, W. Verboom and J. P. M. van Duynhoven, *J. Org. Chem.*, 1996, **61**, 3476-3481.

45. P. Timmerman, D. N. Reinhoudt and L. J. Prins, *Angew. Chem. Int. Ed.*, 2001, **40**, 2382-2426.

46. J. B. Niederl and I. W. Ruderman, *J. Am. Chem. Soc.*, 1945, **67**, 1176-1177.

47. A. G. Sverkerhogberg, *J. Org. Chem.*, 1980, **45**, 4498-4500.

48. L. M. Tunstad, J. A. Tucker, E. Dalcanale, J. Weiser, J. A. Bryant, J. C. Sherman, R. C. Helgeson, C. B. Knobler and D. J. Cram, *J. Org. Chem.*, 1989, **54**, 1305-1312.

49. P. A. Gale, *Coord. Chem. Rev.*, 2000, **199**, 181-183.

50. M. Dudic, P. Lhoták, I. Stibor, K. Lang and P. Prošková, *Org. Lett.*, 2003, **5**, 149-152.

51. J. Budka, P. Lhotak, V. Michlova and I. Stibor, *Tetrahedron Lett.*, 2001, **42**, 1583-1586.

52. P. J. Smith, M. V. Reddington and Wilcox, Craig S., *Tetrahedron Lett.,* 1992, **33**, 6085-6088.

53. P. D. Beer, *Chem. Commun.*, 1996, **3**, 689-696.

54. D. M. Rudkevich, W. Verboom, Z. Brzozka, M. J. Palys, W. P. R. V. Stauthamer, G. J. van Hummel, S. M. Franken, S. Harkema, J. F. J. Engbersen and D. N. Reinhoudt, *J. Am. Chem. Soc.*, 1994, **116**, 4341-4351.

55. S.-Y. Liu, Y.-B. He, J.-L. Wu, L.-H. Wei, H.-J. Qin, L.-Z. Meng and L. Hu, *Org. Biomol. Chem.*, 2004, **2**, 1582-1586.

56. J. Scheerder, J. F. J. Engbersen, A. Casnati, R. Ungaro and D. N. Reinhoudt, *J. Org. Chem.*, 1995, **60**, 6448-6454.

57. D. N. Reinhoudt, R. Fiammengo, P. Timmerman, J. Huskens, K. Versluis and A. J. R. Heck, *Tetrahedron*, 2002, **58**, 757-764.

58. F. Sansone, L. Baldini, A. Casnati, M. Lazzarotto, F. Ugozzoli and R. Ungaro, *PNAS*, 2002, **99**, 4842-4847.

59. L. Baldini, A. Casnati, F. Sansone and R. Ungaro, *Chem. Soc. Rev.*, 2007, **36**, 254-266.

60. M. J. W. Ludden, D. N. Reinhoudt and J. Huskens, *Chem. Soc. Rev.*, 2006, **35**, 1122-1134.

61. J. L. Atwood, G. A. Koutsantonis and C. L. Raston, *Nature*, 1994, **368**, 229-231.

62 . L. Atwood, L. J. Barbour, M. W. Heaven and C. L. Raston, *Chem. Commun.*, 2003, **13,** 2270-2271.

63. M. Kawaguchi, A. Ikeda, S. Shinkai and I. Neda, *J. Incl. Phenom. Macrocycl. Chem.*, 2000, **37**, 253-258.
64. P. E. Georghiou, S. Mizyed and S. Chowdhury, *Tetrahedron Lett.*, 1999, **40**, 611-614.
65. J. Rebek Jr and D. M. Rudkevich, *Eur. J. Org. Chem*, 1999, **9**, 1991-2005.
66. M. Yanase, T. Haino and Y. Fukazawa, *Tetrahedron Lett.,* 1999, **40**, 2781-2784.
67. Patent US Patent 5489612 Pat.
68. E. De Silva, D. Ficheux and A. W. Coleman, *J. Incl. Phenom. Macrocycl. Chem.*, 2005, **52**, 201-206.
69. M. Makha, Y. Alias, C. L. Raston and A. N. Sobolev, *New J. Chem.,* 2008, **32**, 83-88.
70. S. Shinkai, H. Koreishi, K. Ueda and O. Manabe, *J. Chem. Soc.-Chem. Commun.*, 1986, 233-234.
71. F. Perret, V. Bonnard, O. Danylyuk, K. Suwinska and A. W. Coleman, *New J. Chem.,* 2006, **30**, 987-990.
72. J. L. Atwood, G. W. Orr, N. C. Means, F. Hamada, H. M. Zhang, S. G. Bott and K. D. Robinson, *Inorganic Chemistry*, 1992, **31**, 603-606.
73. P. D. Beer, S. W. Dent, G. S. Hobbs and T. J. Wear, *Chem. Commun.*, 1997, **4,** 99-100.
74. R. G. Pearson, *Chemical Hardness*, John Wiley & Sons, New York, 1997.
75. N. N. Greenwood and A. Earnshaw, *Chemistry of the Elements*, 1st edn., Pergamon, Oxford, 1984.
76. M. Munakata, L. P. Wu, T. Kuroda-Sowa, M. Maekawa, Y. Suenaga, G. L. Ning and T. Kojima, *J. Am. Chem. Soc.*, 1998, **120**, 8610-8618.
77. D. R. Turner, B. Smith, E. C. Spencer, A. E. Goeta, I. R. Evans, D. A. Tocher, J. A. K. Howard and J. W. Steed, *New J. Chem.*, 2005, **29**, 90-98.
78. L. H. Uppadine, F. R. Keene and P. D. Beer, *J. Chem. Soc., Dalton Trans.*, 2001, 2188-2198.
79. C. R. Bondy, P. A. Gale and S. J. Loeb, *J. Supramol. Chem.*, 2002, **2**, 93-96.
80. C. R. Bondy, P. A. Gale and S. J. Loeb, *Chem. Commun.*, 2001, 729-730.
81. C. S. Wilcox, E.-i. Kim, D. Romano, L. H. Kuo, A. L. Burt and D. P. Curran, *Tetrahedron*, 1995, **51**, 621-634.
82. P. A. Gale, *Coord. Chem. Rev.*, 2003, **240**, 191-221.

83. M. C. Etter, Z. Urbanczyk-Lipkowska, M. Zia-Ebrahimi and T. W. Panunto, *J. Am. Chem. Soc*, 1990, **112**, 8415-8426.

84. G. B. Neil, Thomas W. Shimell and Paul D. Beer, *J. Supramolecular Chemistry,* 2002, **2**, 89-92.

85. M. R. A. Mahoney M. J., Beatty, A. M., Smith, B. D., Camiolo, S., Gale, P. A, *J. Supramolecular Chemistry,* 2001, **1**, 289-292.

86. M. D. Lankshear, A. R. Cowley and P. D. Beer, *Chem. Commun.,* 2006, **12,** 612-614.

87. A. V. Koulov, J. M. Mahoney and B. D. Smith, *Org. Biomol. Chem.*, 2003, **1**, 27-29.

88. J. M. Mahoney, A. M. Beatty and B. D. Smith, *J. Am. Chem. Soc.*, 2001, **123**, 5847-5848.

89 J. M. Mahoney, A. M. Beatty and B. D. Smith, *Inorg. Chem.*, 2004, **43**, 7617-7621.

90 E. J. Thomas, S. E. Gabriel, M. Makhlina, S. P. Hardy and M. I. Lethem, *Am. J. Physiol.-Cell Physiol.*, 2000, **279**, C1578-C1586.

91. K. Kunzelmann and M. Mall, *Clin. Exptal. Pharm. Physiol.*, 2001, **28**, 857-868.

92. T. J. Jentsch, T. Maritzen and A. A. Zdebik, *J. Clin. Invest.*, 2005, **115**, 2039-2046.

93. V. Sidorov, F. W. Kotch, J. L. Kuebler, Y. F. Lam and J. T. Davis, *J. Am. Chem. Soc.*, 2003, **125**, 2840-2841.

94. K. S. J. Iqbal, M. C. Allen, F. Fucassi and P. J. Cragg, *Chem. Commun.*, 2007, **38**, 3951-3953.

95. L. Birosova, M. Mikulasova and M. Chroma, *Biomedical Papers (Olomouc)*, 2005, **149**, 405-407.

96. C. D. Gutsche, *Calixarenes Revisited*, Royal Society of Chemistry, Cambridge, 1997.

97. F. Sallas and R. Darcy, *Eur. J. Org. Chem*, 2008, **6**, 957-969.

98. K. Kano and Y. Ishida, *Angew. Chem. Int. Ed.*, 2007, **46**, 727-730.

99. Z. L. Zhong and E. V. Anslyn, *J. Am. Chem. Soc.*, 2002, **124**, 9014-9015.

100. R. Breslow and S. D. Dong, *Chem. Rev.*, 1999, **98**, 1997-2011.

101 A. Ikeda and S. Shinkai, *Chem. Rev.*, 1997, **97**, 1713-1734.

102. E. Da Silva and A. W. Coleman, *Tetrahedron*, 2003, **59**, 7357-7364.

103. C. D. Gutsche, B. Dhawan, H. K. No and R. J. Mhthukrishnan, *J. Am. Chem. Soc.*, 1981, **103**, 3782-3792.
104. C. D. Gutsche, *Calixarenes*, Royal Society of Chemistry, Cambridge, 1989.
105. S. Shinkai, K. Araki, T. Matsuda, N. Nishiyama, H. Ikeda, I. Takasu and M. Iwamoto, *J. Am. Chem. Soc.*, 1990, **112**, 9053-9058.
106. J. Scheerder, F. Fochi, J. F. J. Engbersen and D. N. Reinhoudt, *J. Org. Chem.*, 1994, **59**, 7815-7820.
107. J. L. Seganish, P. V. Santacroce, K. J. Salimian, J. C. Fettinger, P. Zavalij and J. T. Davis, *Angew. Chem. Int. Ed.*, 2006, **45**, 3334-3338.
108. D. J. Cram, *Science*, 1988, **240**, 760-767.

Chapter 2: Calixarene-based anion hosts

2.1 Aim and Targets

The aim of this project is to design artificial calixarene based urea hosts that can selectively bind chloride anion in solution.[1] There is great need of rational design for anion hosts, as anions play ubiquitous role in many biological transformations, but misregulated chloride transport can lead to the genetic disease cystic fibrosis[2] and other problems, as described in Chapter 1. The importance of chloride transport and artificial synthetic chloride ion channels has been discussed in many reviews.[3, 4] Synthetic chloride transporter molecules can help in alleviating the symptoms of this kind of condition. Calixarenes have been recognized as versatile class of supramolecular scaffold, because their large internal cavity, suitable to act as an enzyme mimic for example, and hence they can complex proteins and amino acids.[5] This project specifically aims to produce a selective chloride transporting and or sensing system by tuning the calixarene lower rim with a series of alkyl, aryl and naphthyl moieties in conjunction with urea or amide anion-binding functional groups to make hosts that can selectively bind, transport and detect chloride anion in solution. The hosts' solubility within a lipid bilayer can be enhanced by introducing longer alkyl chains, while their water solubility can be enhanced by sulphonation. In this way amphiphilic, membrane-resident chloride-binding systems, or at least model systems directed to this goal, will be produced.

2.2 Calixarene Based Precursors

2.2.1 Synthesis of nitrile derivatives

The calixarenes are a versatile class of macrocycle owing to their ready availability and low cost starting materials.[6] The one pot synthesis of *p*-tert-butylcalix[4]arene (**2.1**) is accomplished with formaldehyde, a suitable base like sodium hydroxide and *p*-tert-butyl phenol, resulting in a formation of crude calixarene that is further treated with ethyl acetate and toulene to give **2.1**. This procedure was carried out and the product characterisation data matches that reported in the literature.[7] A number of bases were tried to modify the lower rim of this calix[4]arene, and the lower rim was successfully functionalised using K_2CO_3 / bromoacetonitrile to form receptor **2.2** again in accordance with the literature.[8, 9] It was noticed that solvent, amount of base and reaction conditions change the overall yield of the product. Potassium carbonate gives a better yield compared to sodium carbonate even though the overall yield of 28% is disappointing.[10] Macrocycle **2.2** proved to be best synthesized by using the standard procedure of Collin *et al*. in presence of NaI / K_2CO_3 in acetone solvent.[8] The product was refluxed for 16 – 20 h to form a 1,3-distal disubstituted macrocycle. We also tried to use an excess of the electrophile to fully substitute the lower rim, but in all cases compound **2.2** resulted. Spectroscopic techniques confirm the C_{2v} symmetry of the molecule, showing a doublet of doublets of equal intensity at 3.40 and 4.20 ppm for the methylene CH_2 groups, and 4.80 ppm for the OCH_2 groups. The compound was fully characterized by ^1H and ^{13}C NMR spectroscopy. Infrared spectroscopy shows a weak peak confirming the presence of the nitrile group at around 2350 cm^{-1}.

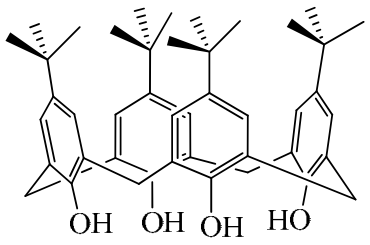

2.1

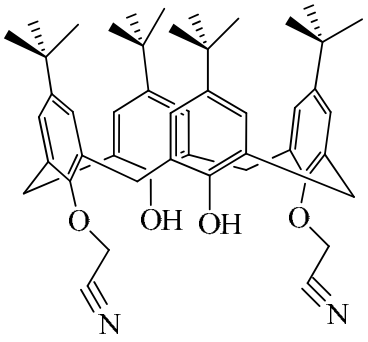

2.2

Our aim is to synthesize a calixarene based macromolecule which is fully substituted, more membrane soluble and facilitates the transport of chloride anion. In order to achieve this we functionalized the remaining two hydroxyl positions (2 and 4) with hexyl substituents. Macromolecule **2.2** was reacted with 6-bromohexane using K_2CO_3 as the base and acetonitrile as the solvent. The reaction mixture was left more than 70 h, resulting in a formation of a new product, **2.3**. The ^{1}H-NMR spectrum of this material shows four single peaks of equal intensity at 6.60, 7.00, 7.10 and 7.40 ppm (Figure **2.1**) assigned to the aryl CH protons suggesting that the product adopts a partial cone conformation. The sharp nature of the peaks suggests that the conformation is fixed at least on the NMR spectroscopic time scale.

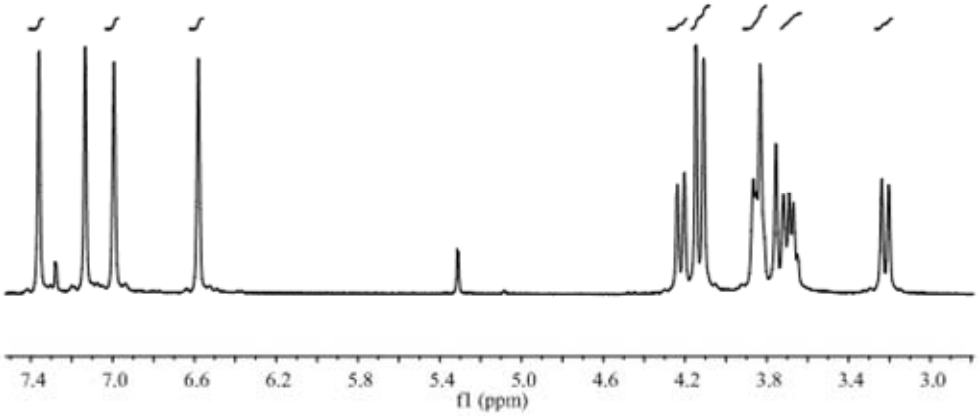

Figure 2.1: ^{1}H-NMR spectrum of 2.3 shown four single peaks of equal intensity at 6.60, 7.0, 7.10 and 7.40 ppm confirming the partial cone conformation

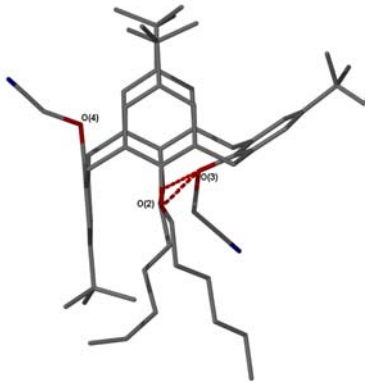

Figure 2.2 X-Ray molecular structure of 2.3 showing the partial cone conformation.

The X-ray crystal structure of **2.3** was determined and confirmed the partial cone conformation. The asymmetry of the molecule is exemplified by the slightly different distances between the two substituted oxygen atoms at the lower rim of calixarene (O3 – O2 = 3.46 Å > O2 – O1 = 2.94 Å). The variable temperature spectrum was recorded in deuterated tetrachloroethane (TCE-d_2) at temperatures ranging from 30 – 90 ^{0}C, but there is no appreciable change in the spectrum to suggest any conformational motion, confirming that the molecule is fixed in the partial cone conformation, indeed the spectrum sharpens with increasing temperature (Figure **2.3**).

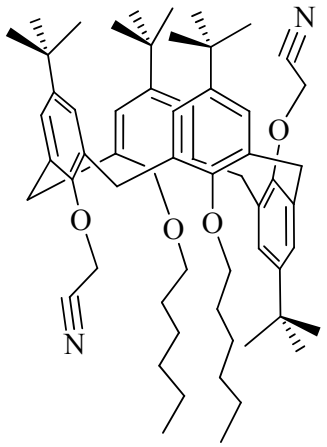

2.3

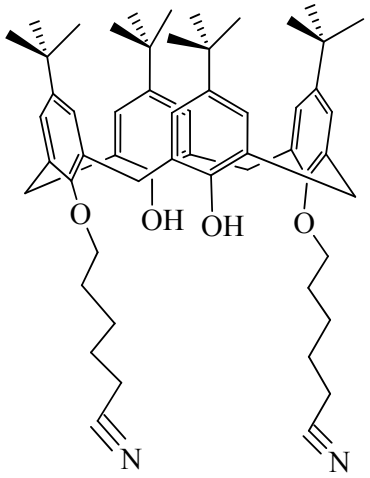

2.4

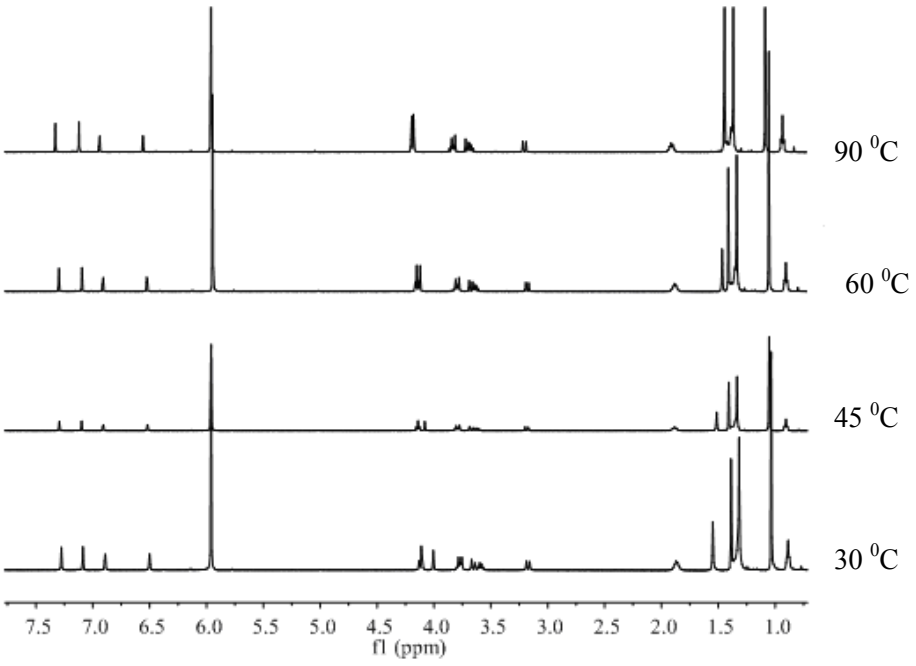

Figure 2.3 Variable temperature spectra obtained for 2.3 in presence of TCE-d_2 ranging from 30 - 90 ^{0}C (bottom to top).

Receptor **2.2** was also treated with 6-bromohexyl nitrile using K_2CO_3 as the base and acetonitrile as the solvent to substitute at 1,3-position of the lower rim of the calixarene to form receptor **2.4**, which was fully characterized by ^{1}H- and ^{13}C NMR spectroscopy and other conventional techniques (see experimental section). The ^{1}H-NMR spectrum of the product shows two peaks at around 6.70 and 7.00 ppm assigned to the aryl CH protons which confirms that **2.4** is in the cone conformation. The ^{1}H-NMR spectrum of **2.4** is shown in Figure **2.4**. The X-ray crystal structure of **2.4** was also obtained and confirms that the 6-cyanohexyl substituents are located at the 1,3-positions of the calixarene lower rim. The molecule adopts a 'pinched cone' conformation, stabilized by intramolecular hydrogen bonding with two very similar length hydrogen bonds (O2 - O3 = O1 - O4 = 3.066 Å). The crystal structure exhibits some disorder of the tertiary butyl groups and aromatic ring of the calixarene. The lack of a significant calixarene cavity means that in contrast to many calixarene crystal structures there is no included solvent molecule either inside or outside the cavity. The crystals are packed in an interlocking fashion as shown in Figure **2.6**.

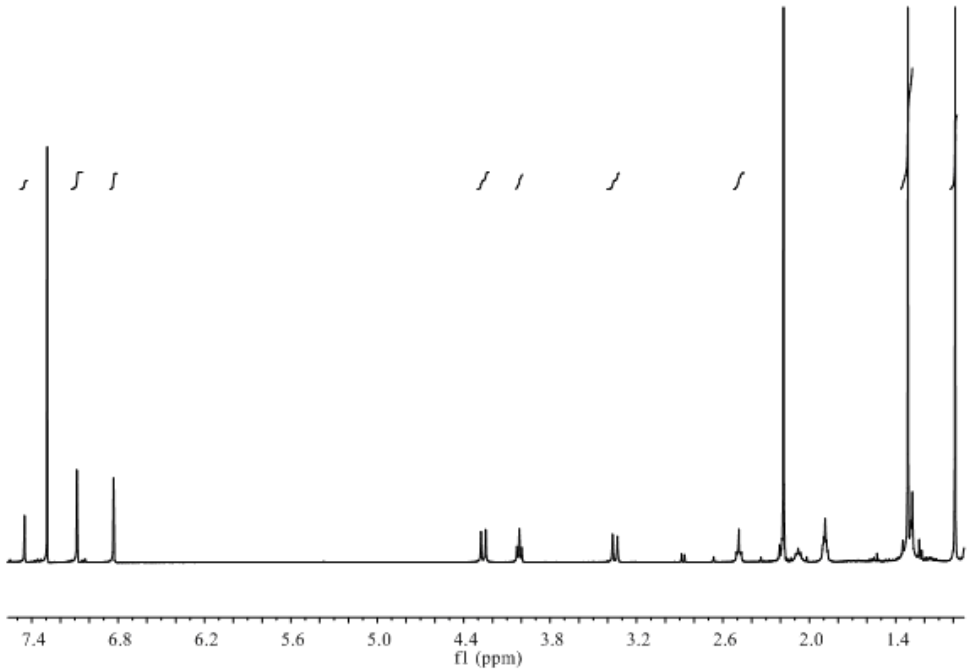

Figure 2.4 ^{1}H-NMR spectrum of 2.4 shown two singlets of equal intensity at 6.70, 7.0 and 7.40 ppm assigned to the aryl CH protons as well as a pair of geminal doublets for the methylene bridges confirming the molecule is in the cone conformation.

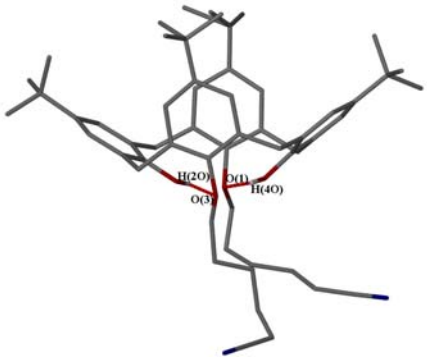

Figure 2.5 X-Ray molecular structure of calixarene 2.4 substituted at the 1,3-positons on the lower rim and demonstrating the pinched cone conformation.

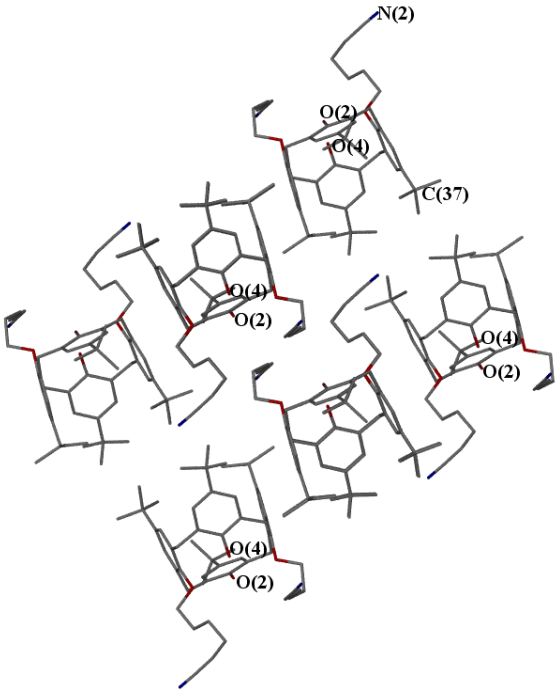

Figure 2.6 Crystal packing in 2.4 viewed along the a-axis showing the 'up-down' arrangement of the calixarenes.

We are interested in how the modification of upper rim can affect the binding, solubility and conformational behaviour of the calixarenes. The starting calixarene **2.1** was debutylated at the upper rim using standard procedures[7] and further reacted with 4-bromobutyronitrile following a similar procedure for **2.2** to give the 1,3-lower rim disubstituted calixarene **2.5**.[7, 9]

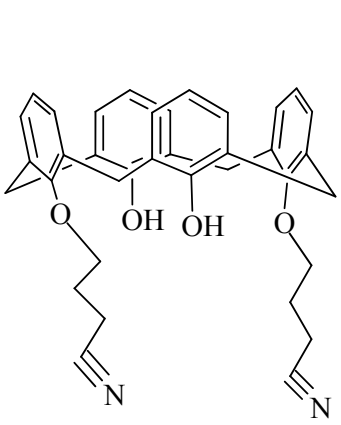

2.5

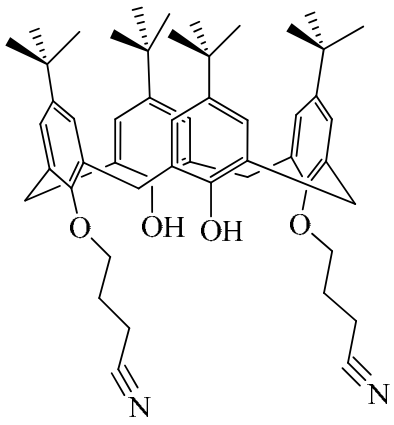

2.6

The crystal structure of **2.5** was determined and shows that it is in the cone form, again stabilized by intramolecular hydrogen bonding as shown in Figure **2.7**a. The crystal includes dichloromethane solvent molecule situated within the calixarene cavity stabilized by Cl_2CH_2···centroid interactions ranging from 2.444 – 2.452 Å as shown in Figure **2.7**a.

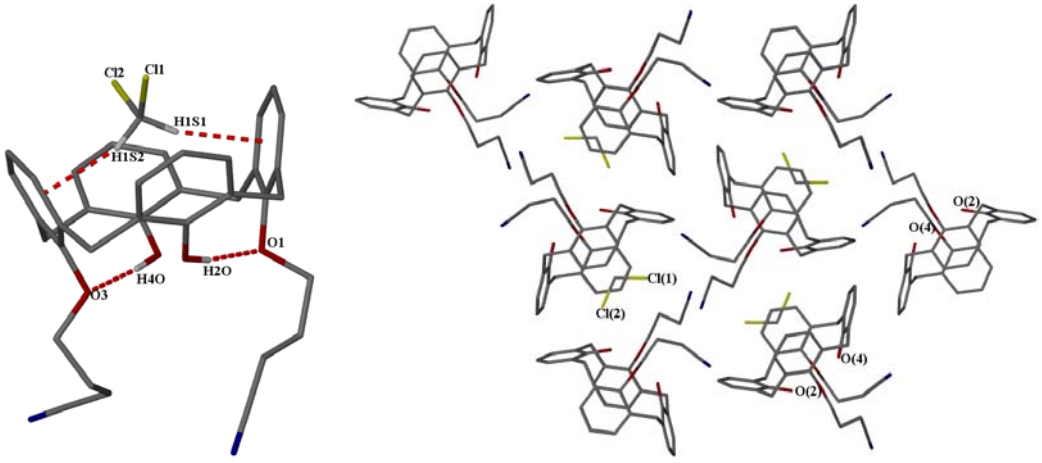

(a) (b)

Figure 2.7: Crystal structures of 2.5 (a) showing the intramolecular hydrogen bonding and dichloromethane solvent molecule situated at the top of the cavity (b) crystal packing along the a-axis (hydrogen atoms are omitted for clarity).

The calixarene **2.1** was also reacted with bromobutyronitrile, a suitable base and acetone solvent to make **2.6** using the standard procedure of Reinhoudt and the data of the product matches with the literature report.[9] The compound was characterised by X-ray crystallography amongst other techniques. The asymmetric unit of the crystal structure comprises of half of the molecule of tertiary butyl calixarene **2.6** and two acetone solvent molecules. These solvent molecules are far apart from each other and one of them is inside and other is outside the cavity. The acetone solvent molecule is severely disordered inside the cavity of the calixarene. There is also some disorder of the tertiary butyl groups as well. The crystal structure confirms that the cyanobutyl substituents are situated at the 1,3-distal positions and that the molecule is stabilized by intramolecular hydrogen bonding at the lower rim of the calixarene. The intermolecular distances at the lower rim of calixarene are the same by symmetry; O1 – O2 = 2.932 Å, and the structure is in the pinched cone conformation. The crystal packing is comprised of tertiary butyl group in an

up and down fashion stabilized by intramolecular hydrogen bonding of adjacent ring (Figure **2 8**).[11]

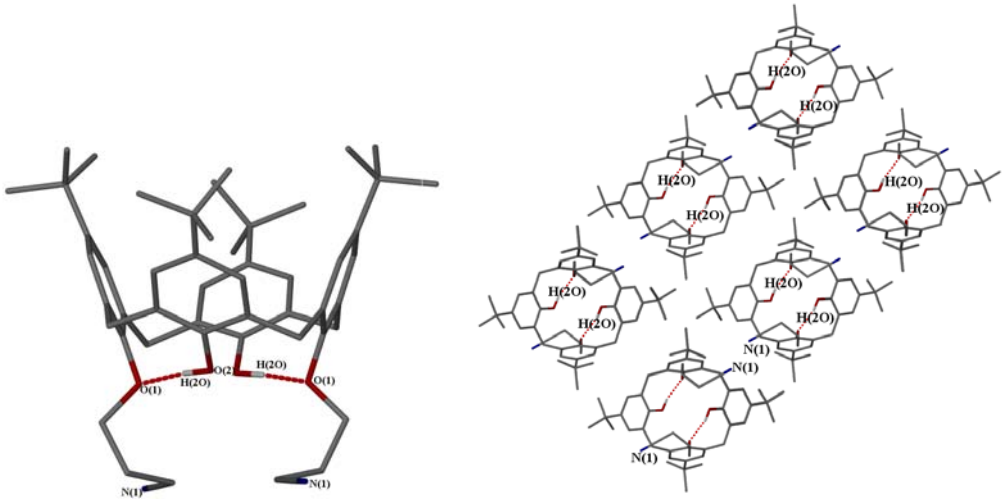

(a) (b)

Figure 2.8 (a) The crystal structure of 2.6 forming cone conformation, selective distance between the O1-O2 = 2.932 Å (b) Crystal structure packing sheet like structure along b-axis (hydrogen atoms are omitted for clarity).

Table 2.1 Crystal structure data from compound 2.3 – 2.6

Compound	**2.3**	**2.4**	**2.5**	**2.6**
Formula	$C_{60}H_{82}N_2O_4$	$C_{56}H_{74}N_2O_4$	$C_{37}H_{36}Cl_2N_2O_4$	$C_{61}H_{84}N_2O_7$
Formula weight	895.28	839.17	643.58	957.30
Crystal system	Monoclinic	Triclinic	Orthorhombic	Monoclinic
Space group	*C*2/*c*	*P*-1	$P2_12_12_1$	*C*2/*c*
a, Å	27.48(2)	13.4692(15)	10.0646(11)	21.951(4)
b, Å	20.311(15)	15.0701(16)	15.6235(17)	12.163(3)
c, Å	19.585(14)	15.3241(16)	20.246(2)	21.185(3)
α, °	90.00	91.994(2)	90.00	90.00
β, °	92.34(6)	115.710(2)	90.00	91.170(10)
γ, °	90.00	109.003(2)	90.00	90.00
Volume	10923(14)	1648.27(6)	3183.5(6)	5654.8(18)
Z	8	2	4	4
ρ (calc.), g/cm^3	1.089	1.075	1.343	1.124
μ, mm^{-1}	0.067	1.519	0.248	0.072
F(000)	3904	1008	1352	2080
Reflections collected	8720	26960	21304	41276
Independent refl., R_{int}	5304, 0.1034	13617, 0.0422	4585, 0.0937	6490, 0.0496
N of parameters	609	595	414	321
Final R_1 [I>2σ(I)]	0.0648	0.0713	0.0470	0.0649
wR_2 (all data)	0.1364	0.1566	0.0789	0.1746
GOF on F^2	0.792	1.016	0.982	1.029

2.2.2 Synthesis of amine derivatives

The next step towards the synthesis of anion binding calixarenes is the reduction of the nitrile derivatives to amines. A number of reducing agents were tried in order to effect this transformation such as sodium borohydride in the presence of cobalt chloride (which results in an observable colour change of the reaction mixture from reddish to pink and blackish on addition of sodium borohydride).[9] Boron hydride in THF solution proved to be an excellent reducing agent in most of the reduction reactions. The intermediate amines **2.7** and **2.8** were synthesized using the selective reduction of nitriles **2.2** and **2.3**. The synthesis of the amine **2.8** was confirmed with the usual spectroscopic techniques (see experimental section), while **2.7** is a known compound and characterization data matches that reported in the literature.[9] These amines proved to be hygroscopic and highly reactive intermediates which were used without further delay. The selective reduction of the calix[4]arene based cyanohexyl derivative **2.4** was accomplished using same standard procedure of Collin to make **2.9**. The ^{1}H-NMR spectruma displayed a broad resonance assigned to the NH protons 3.00 ppm which disappeared on addition of a small amount of D_2O to the NMR sample. The butyronitrile derivative **2.11** and debutylated calixarene **2.10** were also produced using the standard procedure of Collin.[8]

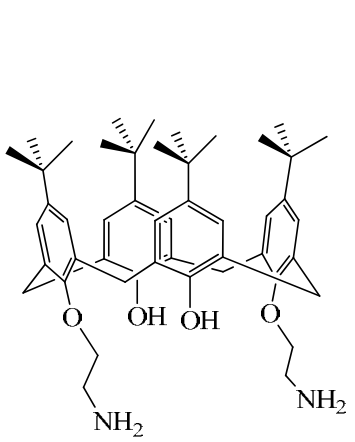

2.7

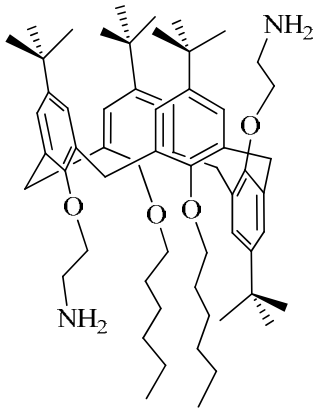

2.8

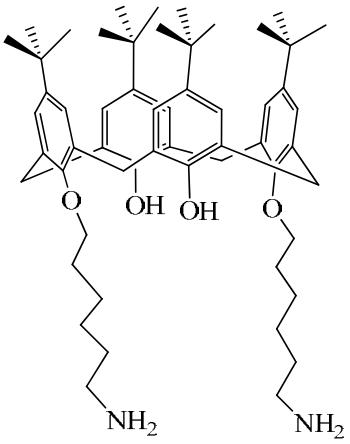

2.9

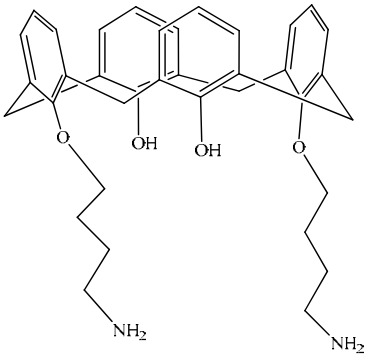

2.10

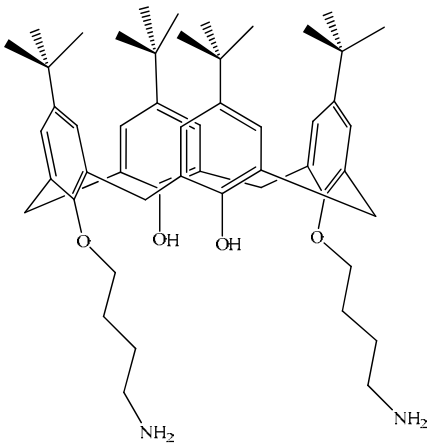

2.11

2.3 Urea Based Calixarenes

2.3.1 Towards a macrocycle host derived from diisocyanates

Our aim is to design artificial molecules based on urea-derivatised calixarene hosts that act as a transmembrane chloride transporters.[4] In order to achieve this we had designed some intermediate amines based on lipophilic chain varying in sizes and substitution pattern. We initially attempted to couple these amines together using diisocyanates to give bis-calixarene urea derivatives of a tube-like shape that might be capable of acting as model ion channels with interior anion binding sites. The synthesis uses the reaction of diisocyanates,[12] under high dilution.[13-15] The intermediate amine **2.7** was reacted with diphenylmethane derived isocyanate **2.12** in dichloromethane solvent at room temperature.

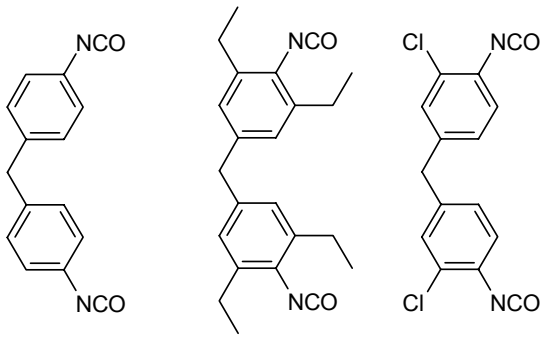

2.12 **2.13** **2.14**

The ^{1}H-NMR spectrum of the resulting product (Figure **2.9**) confirms the presence of two tertiary butyl groups at 1.00 and 1.15 ppm showing the presence of a total of 36H in an unknown structure. Bridging methylene CH_2 doublets are recorded at 4.23 - 4.20 ppm (J = 12 Hz) and 3.43 – 3.40 ppm (J = 12 Hz). The OCH_2 and NH peaks appear at 3.75 and 6.50 ppm, with the NH peaks disappearing on addition of D_2O. The resonances for the aryl CH protons are recorded at 6.80 and 7.20 ppm confirming the two different aryl CH environments and a phenolic OH resonance is present at 8.50 ppm. The crude product was washed with series of different solvents to make a purified product that was only soluble in DMSO solvent however it proved impossible to fully characterise this material. It is expected that the product could be a macrocycle of the type shown in figure **2.10**; however we could not conclusively identify this material.

Having done this reaction, we were interested in making slight modification to give a more soluble product that might prove more tractable. As a result the reaction of **2.7** with 4-methylene bis(phenyl-2,6-diethyl isocyanate) **2.13**.

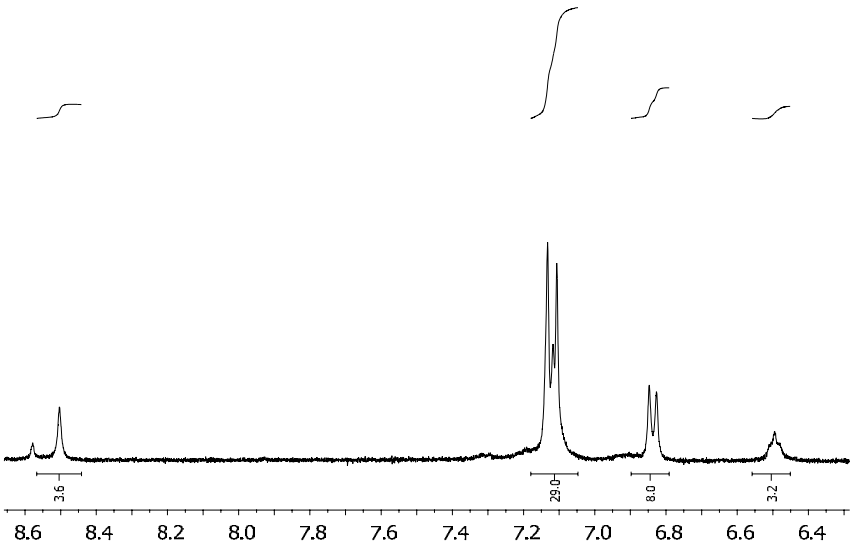

(a)

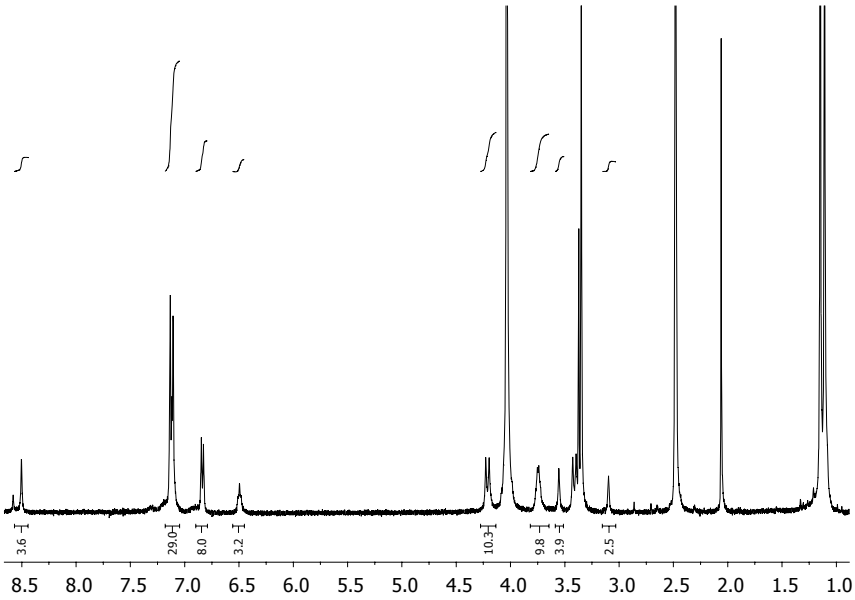

(b)

Figure 2.9 ^{1}H-NMR spectrum obtained by the reaction of calix amine 2.7 with diisocynate 2.12 (a) expansion 6.5 - 8.6 ppm in DMSO-d_6 (b) 1.0 - 8.5 ppm in DMSO-d_6.

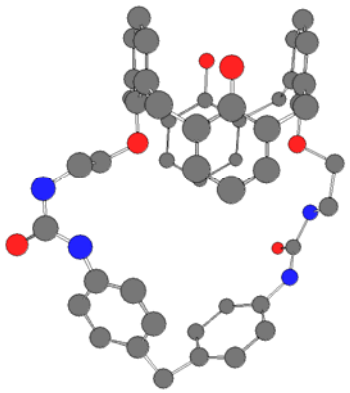

Figure 2.10: Chem-3D model of the possible structure of the product arising from reaction of 2.7 with diphenylmethane-derived diisocyanate 2.12.

Compound **2.7** was reacted with **2.13,** in dichloromethane solvent that was added dropwise in a reaction vessel containing **2.7**. The addition took 2.5 h. The crude product was washed with a small amount of diethyl ether, hexane and petroleum ether to remove excess of isocyanate. The crude product was then analyzed through thin layer chromatography and ^{1}H-NMR spectroscopy. The ^{1}H-NMR spectrum (Figure **2.11**) proved to be very broad, apparently due to restricted intramolecular motion of the product. The spectrum is very confusing and assignment of peaks was very difficult. Variable temperature ^{1}H-NMR spectroscopy in TCE-d_2 ranging from temperature 30 – 90 ^{o}C failed to provide any better understanding of the spectrum apart from some of the peaks became sharper as shown in Figure **2.12**. Mass spectrometry gives a peak at 1140.9 m/z suggesting the formation of a 1:1 product between the calixarene and diisocyanate. Elemental analysis also confirmed a 1:1 ratio.

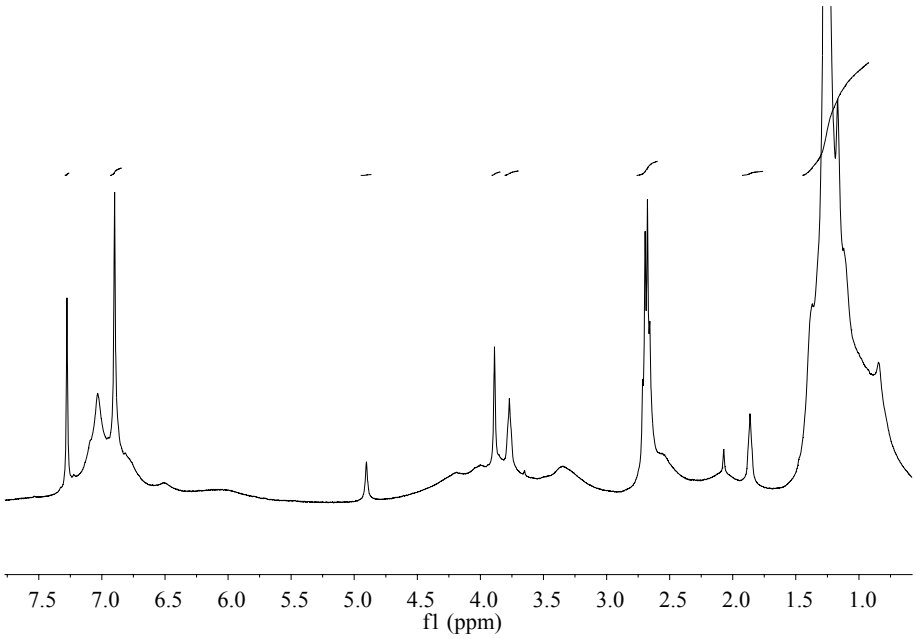

Figure 2.11 ^{1}H-NMR spectrum obtained by the reaction of calix amine 2.7 with diisocynate 2.13

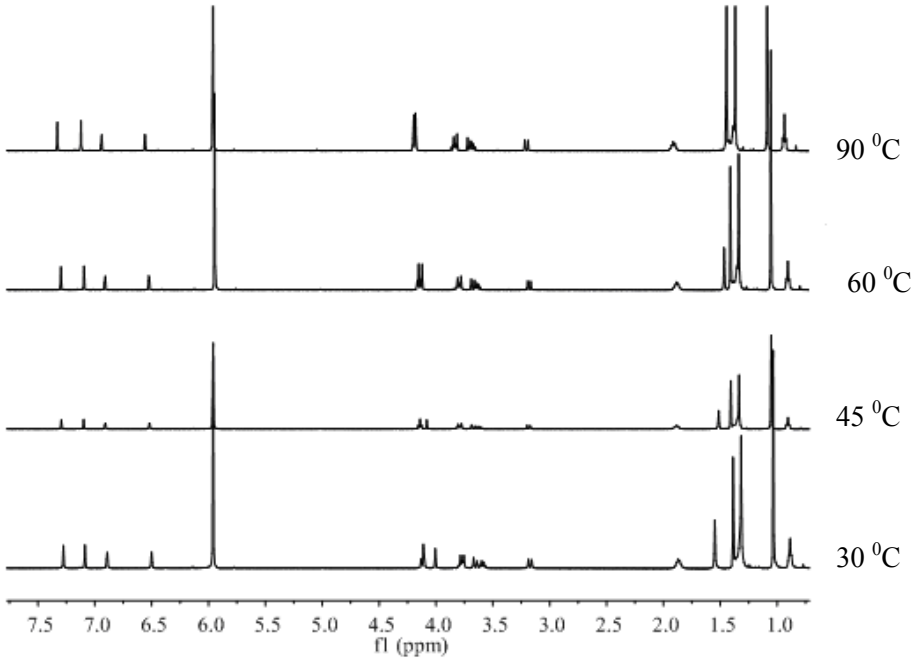

Figure 2.12 Variable temperatures ^{1}H-NMR spectrum in TCE-d_2 obtained by the reaction of calix amine 2.7 with diisocyanate 2.13

Many attempts were made to react diisocyanates **2.12** and **2.13** by slight variation in experimental procedure *e.g.*, dropwise addition of the two reagents simultaneously, high dilution, reacting under an inert atmosphere and cooling to 0 ^{0}C without significant improvement. We also attempted varying the electronic properties of the diisocyanate by using 4,4'-methylene- bis(2-chlorophenylisocyanate) **2.14**. The starting calixarene amine **2.7** was dissolved in dichloromethane and added to **2.14** in dichloromethane. The amine **2.7** was added dropwise at 0 ^{0}C. The reaction mixture was then stirred at room temperature for 8 days resulting in a formation of crude product that was examined by thin layer chromatography and ^{1}H-NMR spectroscopy. The ^{1}H-NMR spectrum (Figure **2.13**) confirms new peaks 8.91, 8.47, 8.05 corresponding to the presence of NH urea and OH groups. The four different environments for the aryl CH protons were recorded at 7.13, 7.00, 6.87 and 6.72 ppm. As usual the presence of two methylene CH_2 and two tertiary butyl groups were recorded at 4.21, 3.73, 1.17 and 1.12 ppm respectively. Some OCH_2 and CH_2 peaks were also observed at 4.03 and 3.42 ppm. Mass Spectrometry (MALDI ToF) resulted in peaks at 1027, 1070.5, 1112.6, 1321.5 and 1613.4 m/z which we were not able to assign.

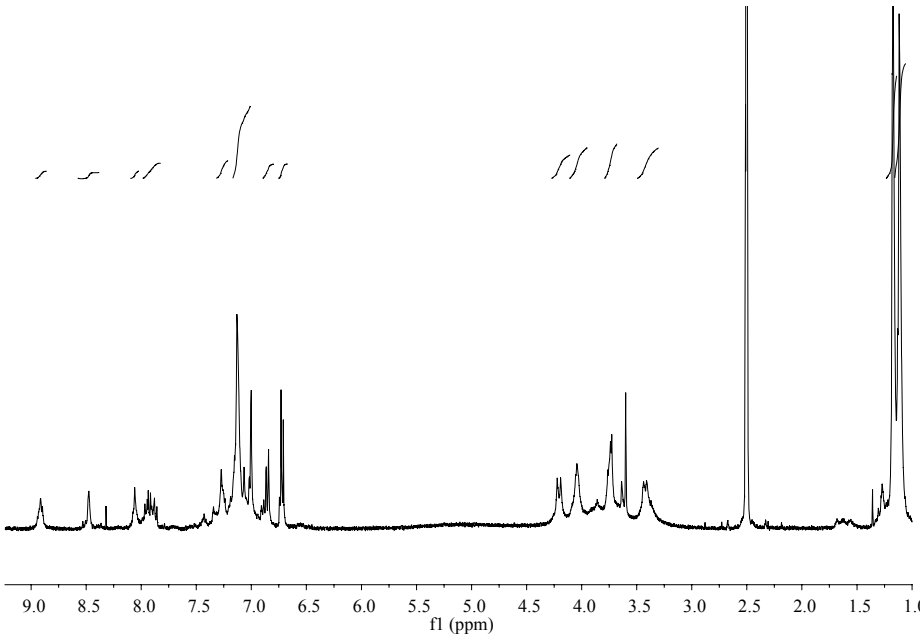

Figure 2.13 ^{1}H-NMR spectrum obtained by the reaction of 2.7 and 2.14 in DMSO-d_6

2.3.2 Bis urea derivatives

Given the intractability of these diisocyanate derived products and their apparent 1:1 nature, we moved to target systems with only a single calixarene bearing pendant urea anion binding groups. Reaction of calix[4]arene diamine **2.7** with 3-methylsulfanylphenyl isocyanate in chloroform solvent to gives **2.15**. The –SMe substituent was included with the possibility of binding soft metal ions such as silver(I) by analogy with previous work.[16-18] The ^{1}H-NMR spectrum of the 3-sulfanylphenyl urea calixarene **2.15** shows two different signals for the protons of the calixarene aromatic rings, as expected on the basis of the substitution pattern. The remaining characterisation data are consistent with the proposed structure (see experimental section). The crystal structure of product **2.15** confirms that sulfanylphenyl urea substituents are attached at the 1,3 position at the lower rim of the calixarene. The structure contains a disordered molecule of acetone within the cavity as well as additional extra-cavity acetone and methanol (Figure **2.14** a). There is also some disorder in the methylsulfanyl and tertiary butyl groups. The urea groups form a bifurcated hydrogen bonding interaction of the $R_2^1(6)$ 'urea tape' type; the distances are slightly more than that proposed by Reinhoudt and co-workers from molecular modelling (Figure **2.14**b).[19]

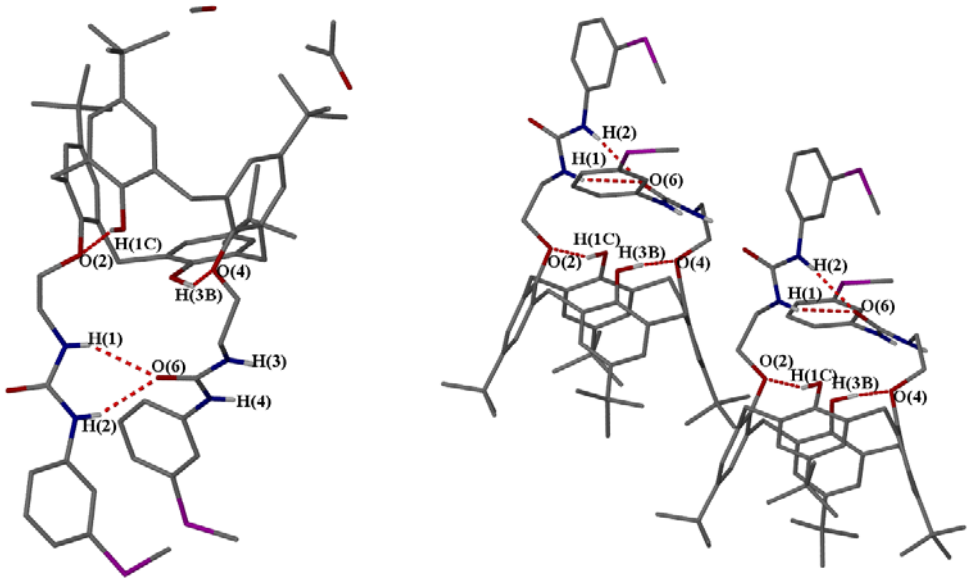

(a) (b)

Figure 2.14 (a) Crystal structure of 2.15 showing the presence of acetone and methanol solvent molecules (b) intramolecular hydrogen bonding selected distances: O6···N1 = 3.070 Å, O6···N2 = 2.889 Å.

Within the crystal compound **2.15** is arranged in an alternating up and down fashion in which the thiomethyl substituent are opposite to each other.[19]

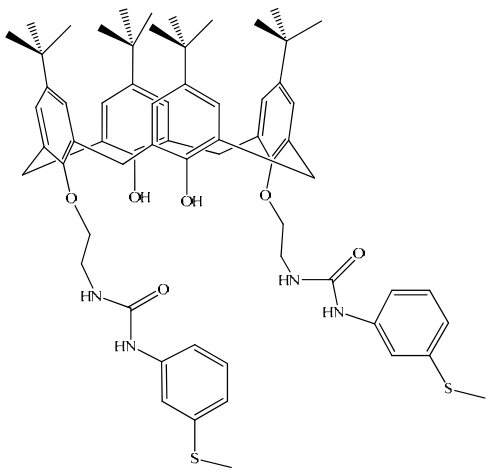

2.15

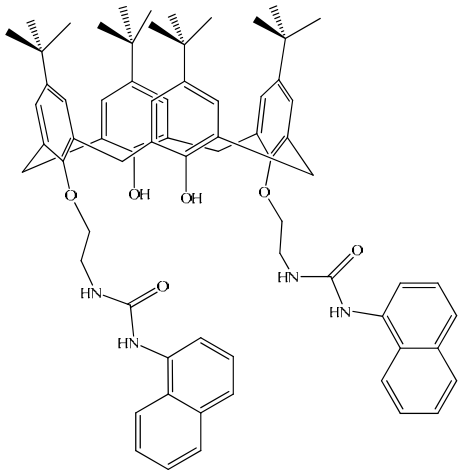

2.16

The anion binding ability of compound **2.15** was assessed by ^{1}H-NMR spectroscopic titration with $TBA^{+}X^{-}$ (X = Cl, OAC, Br, NO_3) anions as guests in acetone solvent.[20] In the case of chloride, anion binding is evident in the chemical shift changes in the NHa and OH resonances, initially at 8.31 and 8.65 ppm; here OH is strongly intramolecularly hydrogen bonded as compared to NHa and hence resonates at lower field. The NHa peak increases chemical shift on chloride addition ($\Delta\delta =$ 1.72 ppm) giving a clean titration curve which can be readily fit to a 1:1 stoichiometric binding model. In contrast the OH resonance does not change chemical shift at all on addition of the first few equivalents of chloride anion guest. It is likely that the OH···O intramolecular hydrogen bonding is retained in the chloride complex, while the urea intramolecular interaction depicted in the crystal structure (Figure **2.14**a) is replaced by a number of $NH\cdots Cl^{-}$ hydrogen bonds.[11, 21] The OH···O interaction apparently becomes weaker as the conformation of the calixarene adapts to accommodate the anion guest, with a gradual shift to higher field being observed for the OH proton as a function of added anion, e.g. from 8.53 to 8.36 ppm after addition of one equivalent of chloride, as shown in Figure **2.15**. The NHb peak occurs at 6.84 ppm; we were unable to follow peaks after 6.97 ppm that disappeared into the aromatic region as shown in Figure **2.16**. ^{1}H-NMR spectroscopic titration was performed with the highly basic acetate anion. The OH peak again moves to high field ($\Delta\delta = -0.32$ ppm), suggesting that anion binding weakens the intramolecular hydrogen bonding

present in the host. More interesting is that NHa proton moves dramatically at downfield ($\Delta\delta = 2.63$ ppm) while the NHb proton moves less ($\Delta\delta = 1.61$ ppm). The shape of the isotherm is consistent with acetate binding in a 1:1 fashion as shown in Figure **2.17**. Here the chloride anion having binding constant log $\beta_{11} = 3.91(3)$ interacts slightly more strongly than acetate log $\beta_{11} = 3.76(4)$ in acetone solvent.

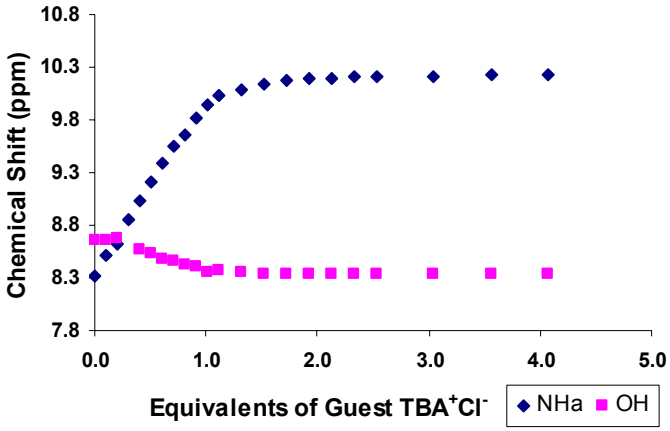

Figure 2.15 Titration of host 2.15 with $TBA^{+}Cl^{-}$ anion in acetone solvent.

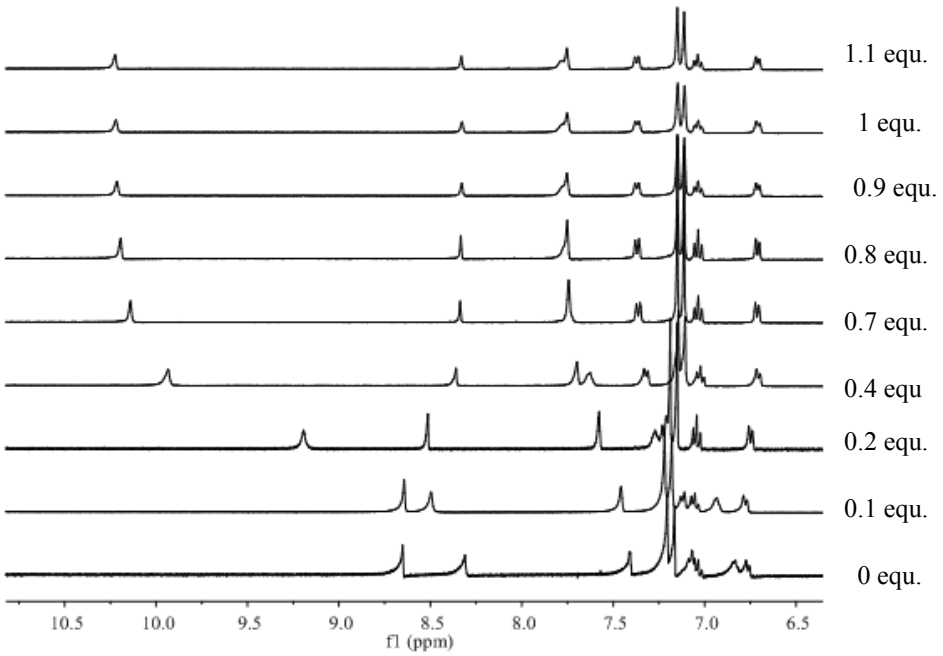

Figure 2.16 Titration of host 2.15 with $TBA^{+}Cl^{-}$ anion in acetone solvent.

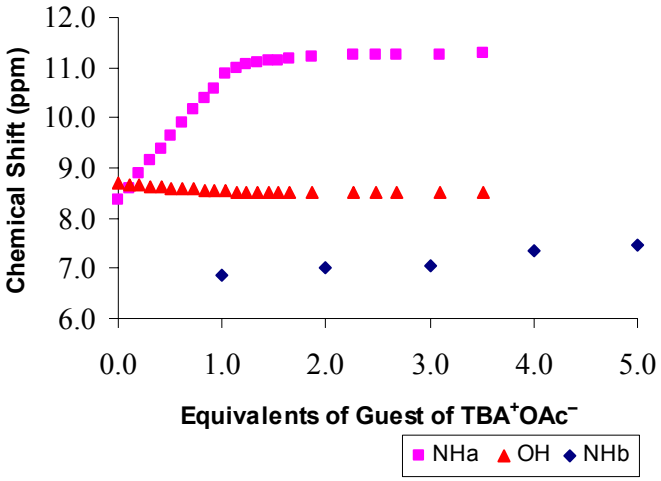

Figure 2.17 Titration of 2.15 hosts with $TBA^{+}OAc^{-}$ anion in acetone solvent

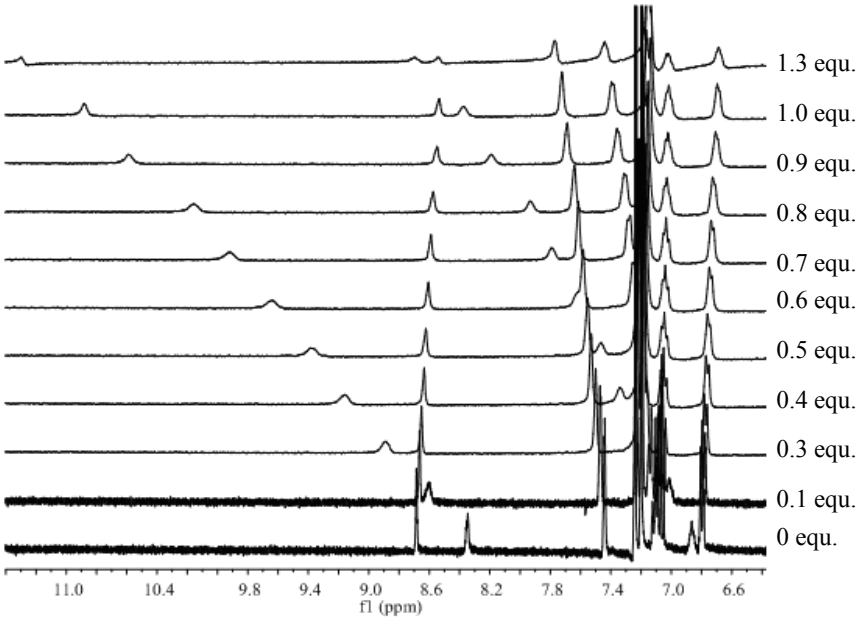

Figure 2.18 Stack plot obtained from titration of 2.15 hosts with $TBA^{+}OAc^{-}$ anion in acetone solvent.

NMR spectroscopic titration with the nitrate anion gives a chemical shift change in the NHa peak from 8.30 to 9.14 ppm ($\Delta\delta = 0.84$ ppm) after addition of five equivalent of nitrate, consistent with a 1:1 stochiometry, as shown in Figure **2.19**. The NHb resonance starts at 6.86 ppm and is masked after 7.03 ppm in the aromatic region. On the contrary the OH peak at 8.68 ppm suggests that the hydroxyl groups do not interact with nitrate,

but again gives evidence for weakened intramolecular interactions ($\Delta\delta = -0.19$ ppm). The ^{1}H-NMR spectroscopic titration behaviour with bromide anion was almost the same, with chemical shift changes for the NHa, OH and NHb peaks of $\Delta\delta = 1.22, -0.24$ and 0.64 ppm, Figure **2.21**. From the binding constants, we concluded that the nitrate anion binds more weakly, log β_{11} 3.03(1) than bromide log β_{11} 3.41(3). The overall selectivity of receptor **2.15** is $NO_3^- < Br^- < OAc^- < Cl^-$. The receptor is thus weakly chloride selective, and hence has some potential as a design for a chloride transporter.

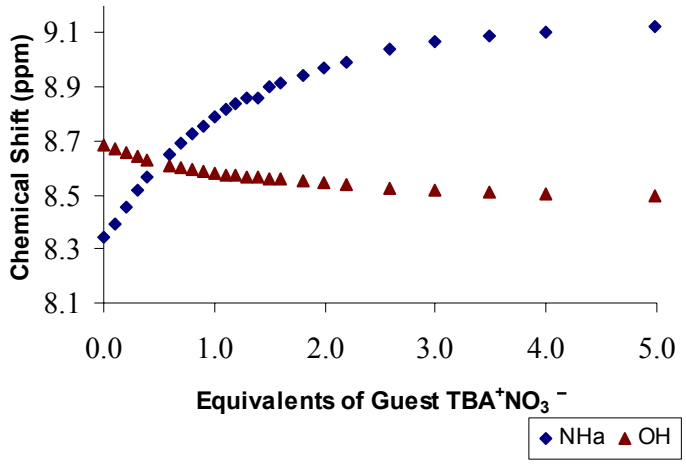

Figure 2.19 Titration of host 2.15 with $TBA^+NO_3^-$ in acetone solvent.

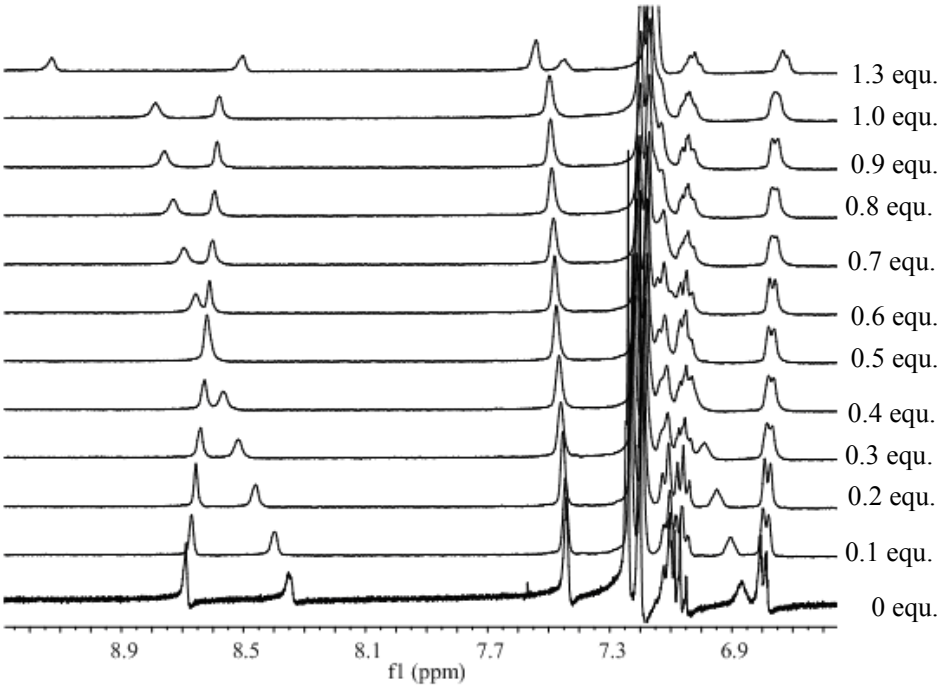

Figure 2.20 Stack plot obtained from titration of 2.15 hosts with $TBA^{+}NO_3^{-}$ anion in acetone.

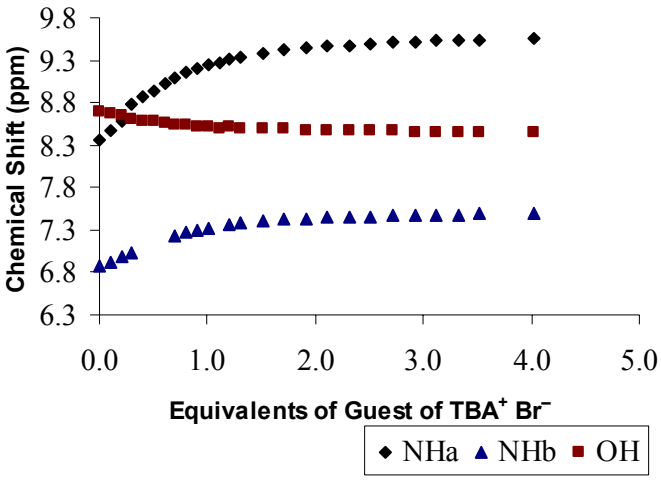

Figure 2.21 Titration of host 2.15 with $TBA^{+}Br^{-}$ in acetone.

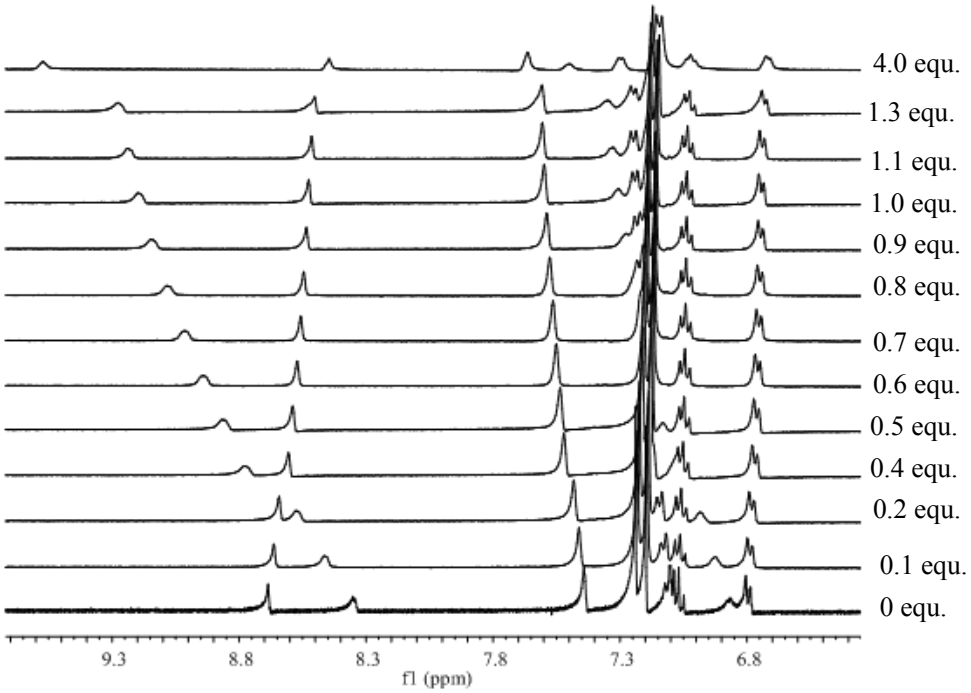

Figure 2.22 Stack plot obtained from titration of host 2.15 with TBA^+ Br^- in acetone.

A related product **2.16** was obtained by the reaction of **2.7** with naphthyl isocyanate in an equimolar ratio in chloroform solvent. Inclusion of the napthyl chromophore offers the possibility of fluorescent detection of anion complexation and enhanced anion binding by π-π stacking effects which could favour the geometry of the anion complex. The identity of the product was confirmed by the usual spectroscopic techniques (see experimental section). The crystal structure of the receptor was also obtained and shows the expected 1,3-disubstitution pattern and a pinched cone conformation. The structure includes two molecules of chloroform and two molecules of acetonitrile, one of which is situated in the calixarene cavity. The crystal structure is stabilized by intramolecular hydrogen bonding interactions involving the hydroxyl groups (O3···O4 = 2.91 Å and O2···O1 = 2.95 Å) as shown in Figure **2.23**. The crystal structure packing shows that the naphthyl aromatic rings are stacked together forming π–π interactions with another naphthyl unit on an adjacent calixarene, as well as intramolecular interactions to the calixarene aromatic rings, Figure **2.24**.[22]

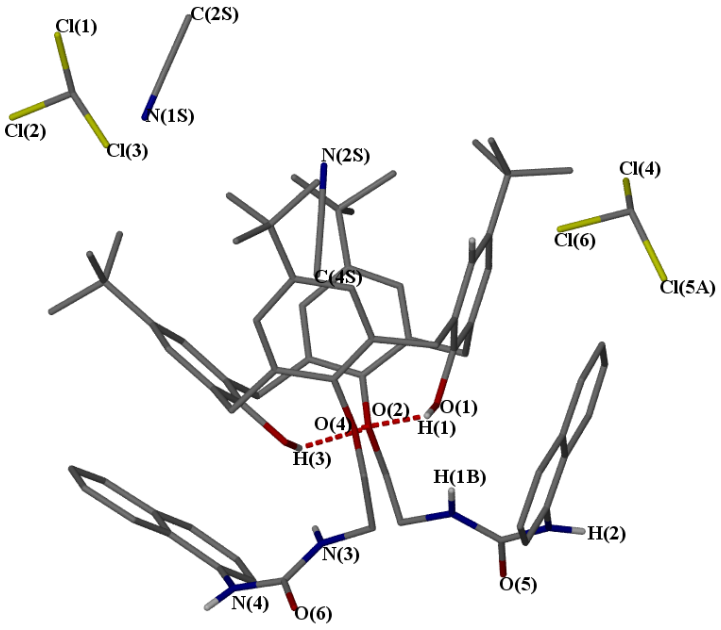

Figure 2.23 (a) X-Ray crystal structure of 2.16 showing positions of solvent molecules.

Interestingly, in contrast to **2.15** the crystal packing exhibits intermolecular $R_2^2(8)$ type hydrogen bonding between α–NH proton and β–oxygen atom (O6···N4) = 2.827Å. The naphthyl moieties are distributed trans to each other in the crystal packing, Figure **2.24**.

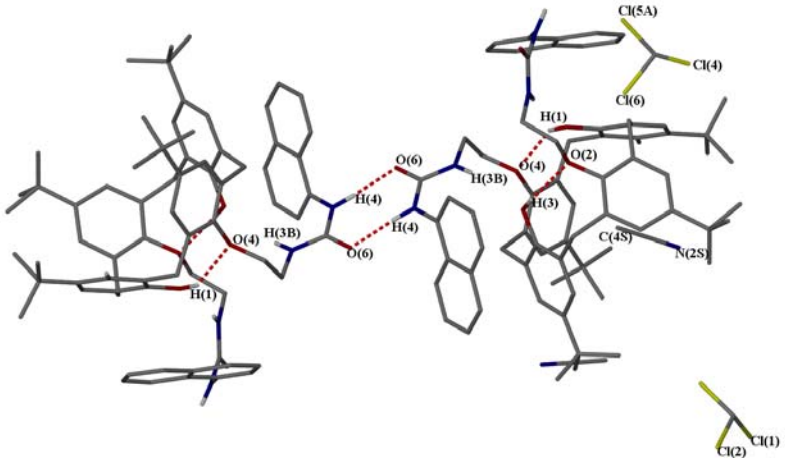

Figure 2.24 Intermolecular hydrogen bonding in 2.16 Selected distances: O6···N4 = 2.827 Å, O3 – O2 = 2.686 Å and O1 – O4 = 2.678 Å.

The anion binding behaviour of host **2.16** was analysed by ^{1}H-NMR spectroscopic titration with TBA^{+} X^{-} (X = Cl, NO_3) in an acetone solvent. The ^{1}H-NMR peaks of the NHb, NHa and OH are initially recorded at 7.30, 8.16 and 8.67 ppm, respectively. The NHb resonance is masked by the aromatic region and is hard to follow during the titration. The NHa peak changes chemical shift markedly to 9.47 ppm ($\Delta\delta = 1.76$ ppm) consistent with 1:1 binding. As with **2.16,** the OH peak shifts upfield ($\Delta\delta = -0.31$ ppm) as shown in Figure **2.25**. The nitrate anion guest has less effect on the chemical shift as compared to chloride. The NHa resonance shows a chemical shift change, $\Delta\delta = 0.486$ ppm, Figure **2.27**. The OH peak again moves upfield suggesting weakening of the intramolecular hydrogen bonding. From the binding constants data, we conclude that chloride anion binds more strongly log β_{11} 3.59(4) than nitrate anion log β_{11} 2.38(8) in acetone.

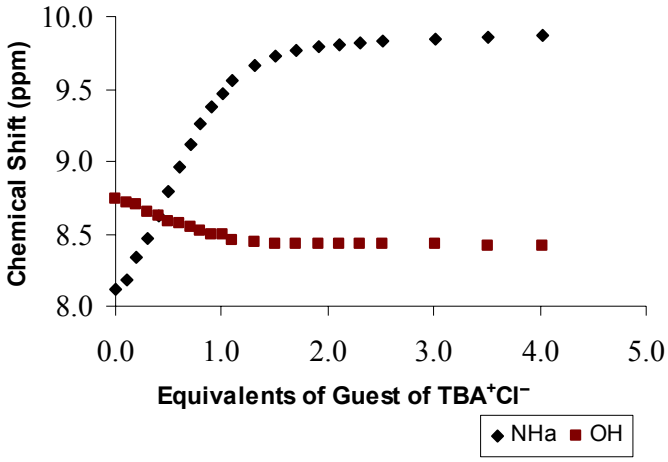

Figure 2.25 Titration of host 2.16 with $TBA^{+}Cl^{-}$ anion in acetone.

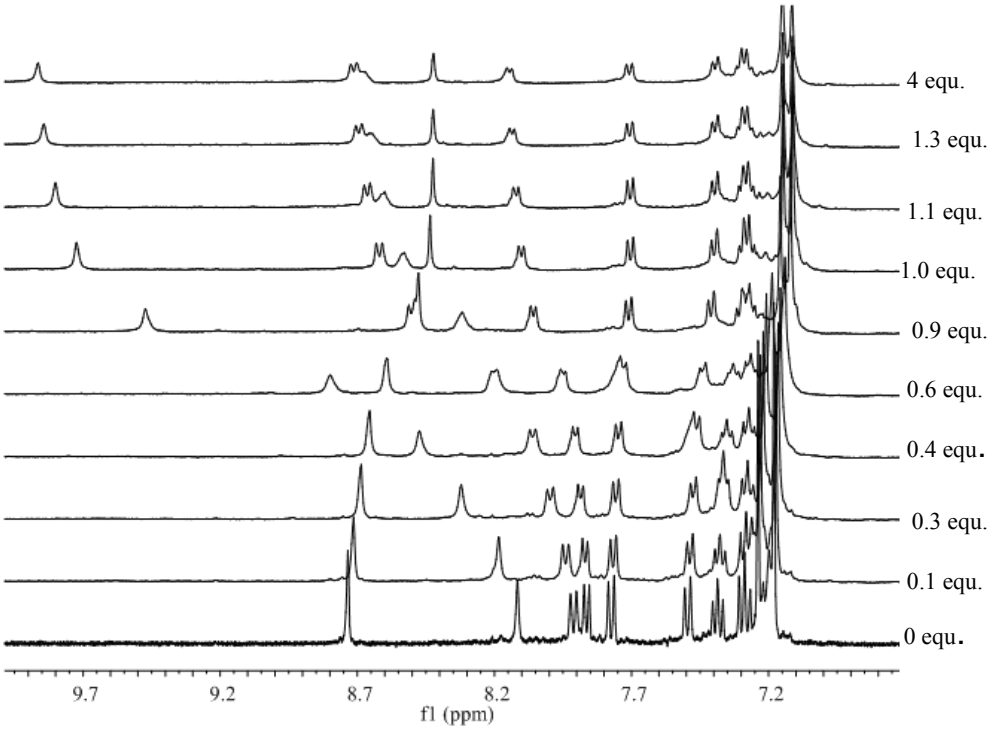

Figure 2.26 Stack plot obtained from titration of 2.16 hosts with $TBA^{+}Cl^{-}$ in acetone

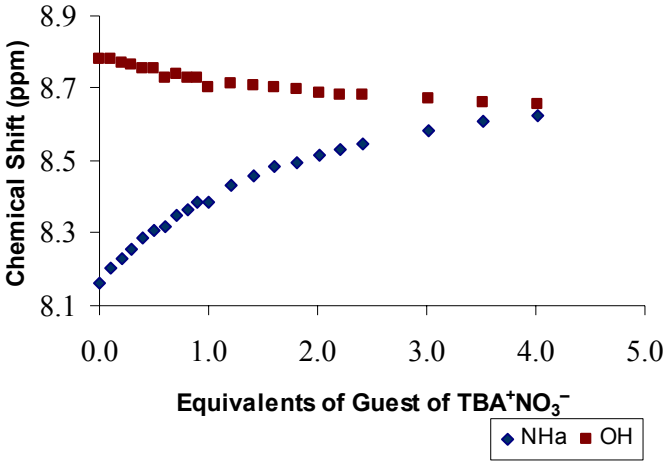

Figure 2.27 Titration of host 2.16 with $TBA^{+}NO_3^{-}$ in acetone.

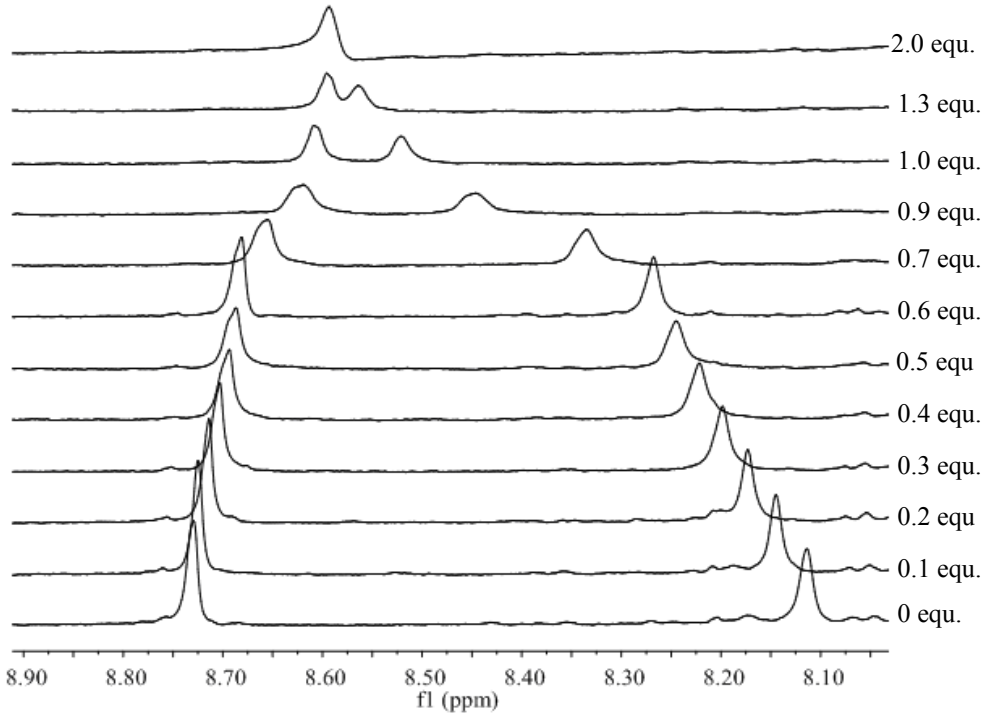

Figure 2.28 Stack plot obtained from titration of 2.16 hosts with $TBA^{+}NO_3^{-}$ in acetone.

The calix[4]arene 4-aminobutyl derivative **2.11** was also reacted at room temperature with naphthyl isocyante in equimolar ratio in chloroform solvent to produce calix[4]arene naphthyl urea **2.17**. The identity of the product was confirmed with the usual techniques (see experimental section). ^{1}H-NMR titration of host **2.17** was performed with tetrabutyl ammonium chloride. While chemical shift changes were observed, severe overlap with the other peaks in the aromatic region made the data difficult to follow quantitatively. The receptor **2.18** was synthesized according the known method[23] by the reaction of para-tolylisocyanate with primary amine **2.7**. The receptor is based on two substituted urea linkages suitable for chloride binding. The pure product **2.18** was obtained by crystallization from hexane and chloroform solvent. Broadening of the ^{1}H-NMR spectrum was observed, which showed a doublet of doublets in the region of 3.45 and 4.10 ppm for the CH_2 bridging protons and three broad peaks were observed for the NH, CH_2 and OCH_2 protons between 3.60, 3.80 and 4.00 ppm. The NH peak at 3.60 ppm disappeared on addition of D_2O. This broadening in ^{1}H- NMR spectrum suggests that there are intramolecular hydrogen bonds resulting in slow molecular conformational motion. A peak at 6.70 ppm is assigned to the OH groups and disappears on addition of D_2O to the

sample. Formation of the product was further confirmed with the help of mass spectrometry, although extra peaks observed at at m/z 1736 could not be assigned. Due to the poor solubility of this product ^{1}H-NMR titration experiments were not performed. In order to make a more soluble, lipophilic receptor we prepared compound **2.19**. The ^{1}H-NMR spectrum of **2.19** shows peaks for the tertiary butyl groups at 0.80 and 1.20 ppm confirming the two different environments expected. Bridging methylene ($ArCH_2Ar$) peaks appeared at 3.38 and 4.38 ppm showing the expected doublet of doublets and series of methylene resonances appeared at 3.15 – 4.10 ppm. Meanwhile CH_2 and OCH_2 peaks appeared at 3.55 and 3.80. NMR spectroscopic titration experiments were attempted to assess chloride affinity in chloroform solution but little chemical shift change was observed.

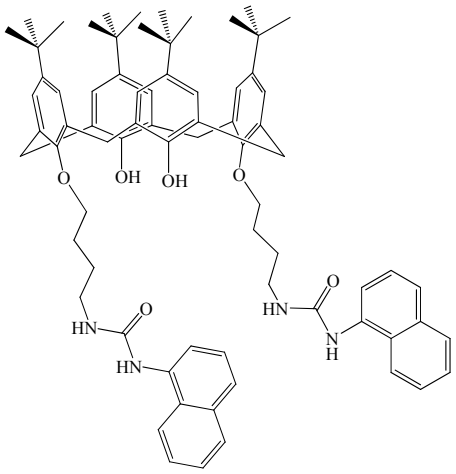

2.17

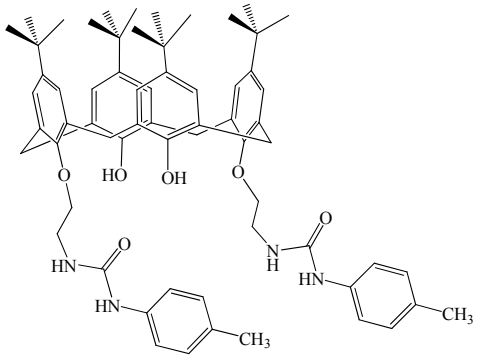

2.18

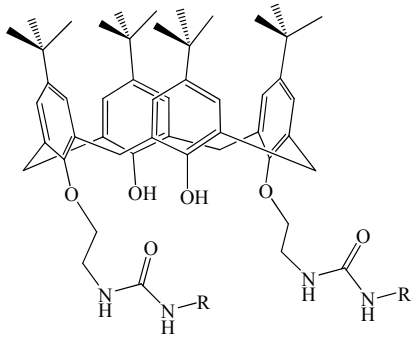

2.19

R = octadecyl

2.3.3 Thiourea derivatives

Given the urea tape type intramolecular hydrogen bonding observed for **2.15** we were interested in preparing thiourea analogues which often exhibit very different hydrogen bonding motifs to their oxygen analogues. Reaction of **2.7** with a slight excess of *m*-tolylisothiocyanate resulted in the clean formation of **2.20** after workup by washing with a small amount of diethyl ether. Thiourea calixarene **2.20** shows two singlet peaks for tertiary butyl groups at 1.05 and 1.18 ppm in its ^{1}H-NMR spectrum, this is at lower field than starting aminoethyl calixarene **2.7**. Methylene bridging ($ArCH_2Ar$) peaks were recorded at 3.18 and 3.80 ppm as a geminal AB pattern. Lower rim substituted CH_2 and OCH_2 peaks were recorded at 4.00 and 4.20 ppm, which is at high field and quite unusual compared to the other urea based macromolecules studied in this work. In the aromatic region, NHa and NHb protons of the thio urea occur at 7.60 and 7.90 ppm, while the OH resonance occurs at 8.00 ppm. The mass spectrum of **2.20** showed a molecular ion peak at *m/z* 1055.5 (assigned to M+Na). A strange peak also occurs at *m/z* 1582.3 corresponding to half of the mass of a trimer (although the isotope progression occurs in integer rather than half integer units), which could be a result of aggregation behaviour, or a calix[6]arene contaminant, as shown in Figure **2.29**. The ^{1}H-NMR spectrum of **2.20** does not show any evidence for a calix[6]arene, however.

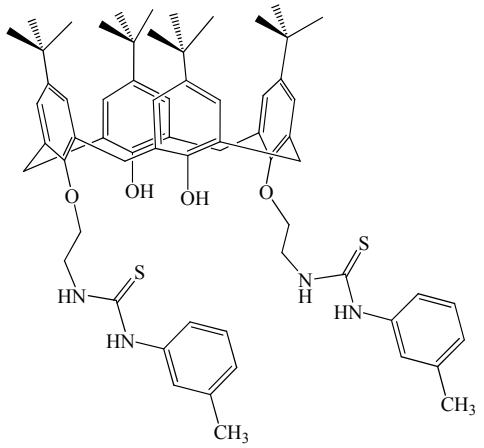

2.20

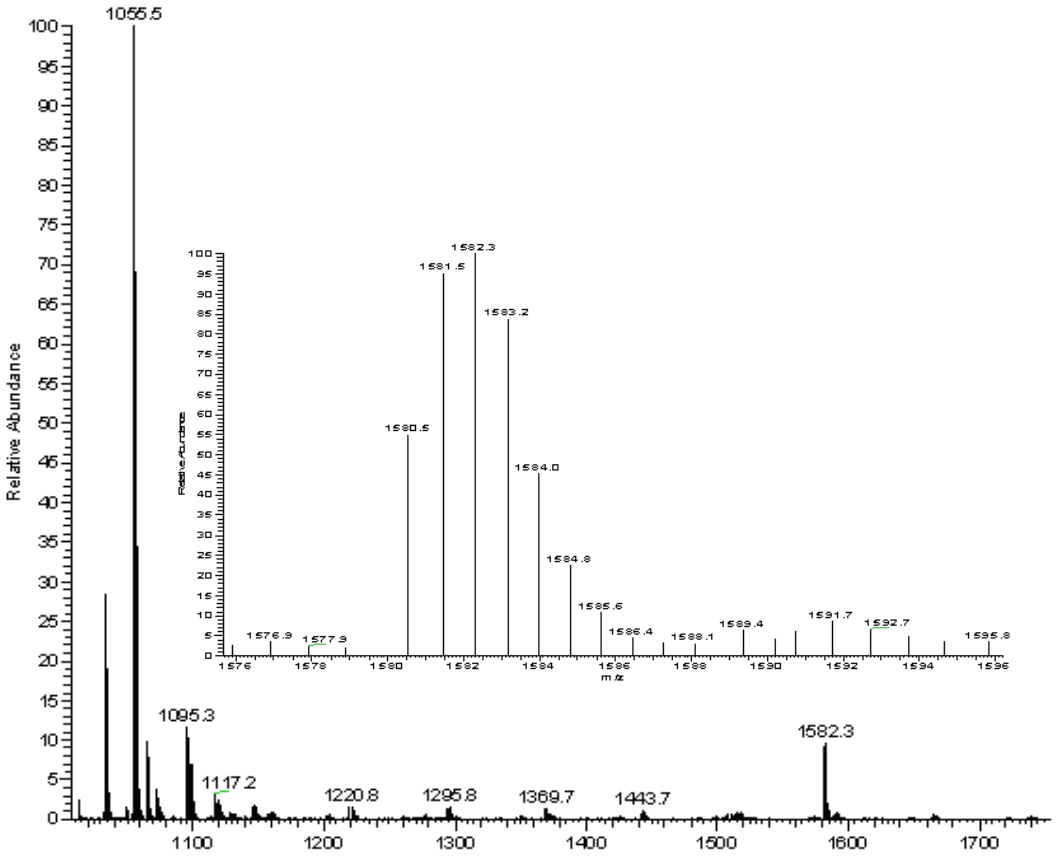

Figure 2.29 Mass spectrum for thiourea-derived calixarene 2.20 showing the molecular ion peak at 1055.5 (M + Na).

The identity of **2.20** was confirmed with the usual spectroscopic techniques (see experimental section). The compound was also characterised by X-ray crystallography. The crystal structure of **2.20** shows that the thiourea substituents are attached at the 1,3-distal positions. In the crystal the molecules are packed together in an up and down fashion and the thiourea groups are far apart from each other making a bent structure that is stabilized by intramolecular hydrogen bonding between the thiourea NH groups and the hydroxyl oxygen atoms. The distances between oxygen atoms of the lower rim of **2.20** are almost same consistent with a regular cone conformation (O2···O1 = O3···O4 = 2.845 Å) as shown in Figure 2.30a. The γ– NH proton with respect to the *meta* methyl phenyl (lower rim substituent) form hydrogen bonds with the phenolic oxygen atom and the phenolic hydrogen is forms a hydrogen bond with the adjacent oxygen atom of the

substituted alkyl spacer as shown in Figure **2.30**a. The crystals are packed together in a slightly tilted alternating fashion as shown in Figure **2.30**b.

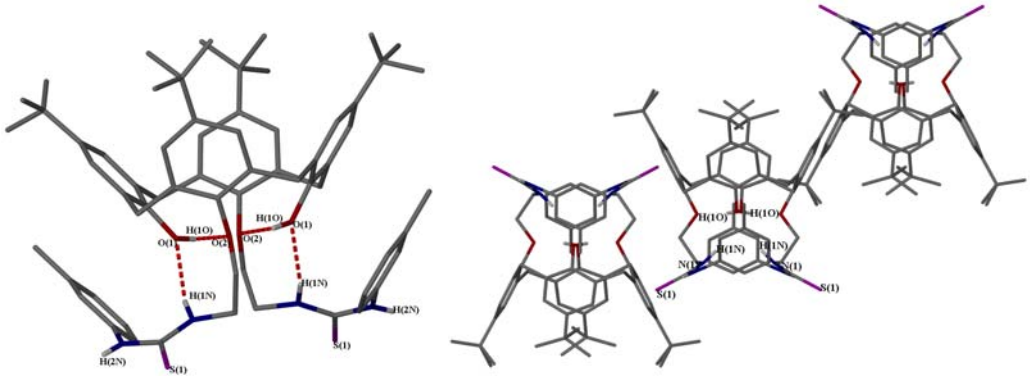

(a) (b)

Figure 2.30 (a) X-Ray structure of compound 2.20. Selected distances are N1- O1 = 3.072 Å, O2···O1 = 2.845 Å, O3···O4 = 2.845 Å (b) crystal packing along the *a*-axis

Due to increased acidity of the NH protons of the thiourea compared to urea (thiourea p*K*a = 21.0; urea p*K*a = 26.9),[24] the anion complexation was expected to be stronger. The increased acidity is evident from the ^{1}H-NMR spectrum of **2.20** where the NHb proton is shifted 0.26 ppm and the NHa proton 0.57 ppm to lower field compared to the urea analogue **2.18**. ^{1}H-NMR titration experiments were performed with $TBA^{+}X^{-}$ (Cl, OAc, NO_3) in acetone. The ^{1}H-NMR peaks of NHa, OH and NHb peaks occur at 7.87, 8.08 and 6.75 ppm in the free host. The urea NHa proton shifts to 9.32 ppm ($\Delta\delta$ = 1.45 ppm) and forms a 1: 1 complex with chloride, having binding constants of log β_{11} 3.16(6), as shown in Figure **2.31**. The NHb peak disappears into the aromatic region and is hard to follow. The OH peak moves from 8.08 ppm to 8.27 ppm ($\Delta\delta$ = 0.19 ppm). This chemical shift change is in the opposite direction to that observed for the oxygen analogues and suggests that intramolecualr hydrogen bonding reinforces anion binding in this case. In the case of acetate anion deprotonation took place in acetone solvent with disappearance of the NH resonances. The nitrate anion was weakly interacting with the chemical shift of the NH resonances still changing up to five equivalents of nitrate anion. The binding constant for nitrate is log β_{11} 1.655(4). From the binding constant data, we conclude that receptor **2.20** binds chloride more strongly than nitrate.

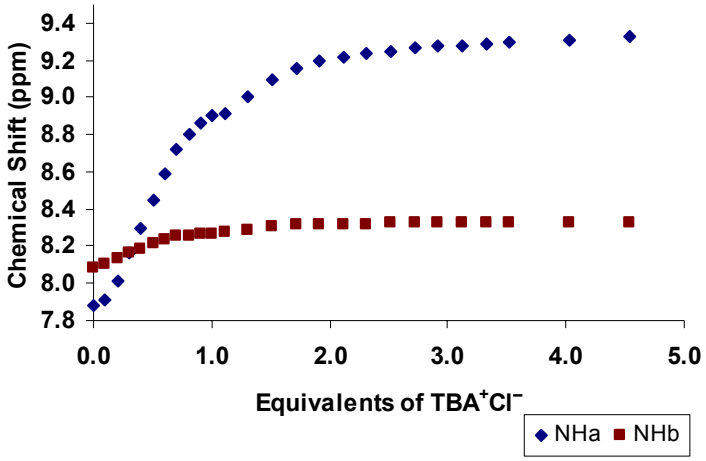

Figure 2.31: ^{1}H-NMR spectroscopic titration of host 2.20 with $TBA^{+}Cl^{-}$ in acetone

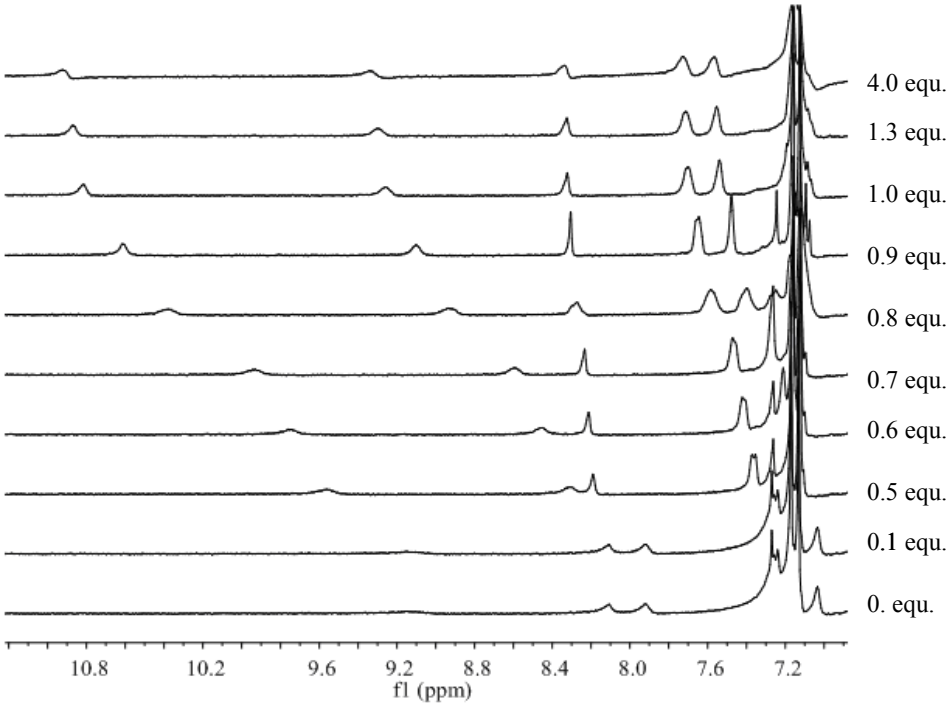

Figure 2.32 Stack plot obtained from titration of host 2.20 with $TBA^{+}Cl^{-}$ in acetone

Table 2.2 Crystal structure data for compounds 2.15, 2.16 and 2.20

Compound	**2.15**	**2.16**	**2.20**
Formula	$C_{64}H_{80}N_4S_2O_6$ ·0.5 CH_3OH · 1.5 C_3H_6O	$C_{70}H_{80}N_4O_6$ · 2 CH_3CN · 1.5$CHCl_3$	$C_{64}H_{80}N_4O_4S_2$ · $CHCl_3$ · $3C_2H_5OH$
Formula weight	1168.58	1334.54	1228.30
Crystal system	Monoclinic	Monoclinic	Monoclinic
Space group	$P2_1/c$	$P2_1/c$	$C2/c$
a, Å	19.5803(5)	12.6122(5)	28.3148(6)
b, Å	20.1679(5)	30.9836(12)	15.8506(3)
c, Å	18.2981(5)	18.6901(7)	18.2260(4)
α, °	90.00	90.00	90.00
β, °	111.82(3)	92.349(10)	118.09(1)
γ, °	90.00	90.00	90.00
Volume/$Å^3$	6708.2(3)	7297.4(5)	7216.3(3)
Z	4	4	4
ρ (calc.), mg/mm^3	1.157	1.215	1.131
μ, mm^{-1}	0.134	0.235	0.181
F(000)	2516	2828	2640
Reflections collected	55928	54294	43374
Independent refl., R_{int}	14623, 0.1568	14329, 0.0926	8708, 0.0464
N of parameters	782	861	420
Final R_1 [I>2σ(I)]	0.0936	0.0852	0.0962
wR_2 (all data)	0.2441	0.2330	0.2708
GOF on F^2	1.056	1.004	1.071

2.4 Amide Based Calixarenes

The calix ethyl amine **2.7** was reacted with dansyl chloride to produce **2.21** using the standard procedure. The product **2.21** is also a florescent molecule, the lone pair on the nitrogen atom can be delocalised into the naphthyl ring. Compound **2.21** was characterised by X-ray crystallography. The crystal structure of **2.21** confirmed that the dansyl groups are substituted at 1,3 distal positions with the amide NH groups forming intramolecular hydrogen bonding with the oxygen atoms of the lower rim of the calixarene. ^{1}H-NMR titration of host **2.21** with $TBA^{+}X^{-}$(Cl, OAc, Br, F, NO_3) in a range of solvents did not produce any significant chemical shift change. It seems that the anion binding is not sufficient to disrupt the intramolecular hydrogen bonding interactions. Because of the short ethylene chain and absence of the second NH group found in the ureas, the intramolecular hydrogen may be particular favourable, Figure 2.33. In order to remove the effect of the intramolecualr hydrogen bonding a longer spacer was introduced. Reaction of aminobutyl calix[4]arene **2.11** with dansyl chloride using the standard procedure gives **2.22**.

Table 2.3 Binding constants (log β_{11}) of receptor 2.15, 2.16, 2.20 and 2.22 with various anions in acetone at room temperatures

Entry	Anion	2.15	2.16	2.20	2.22
1	Cl^-	log β_{11} 3.91(3)	log β_{11} 3.59(4)	log β_{11} 3.16(6)	log β_{11} 1.47(1)
2	OAc^-	log β_{11} 3.76(4)	a	c	b
3	NO_3^-	log β_{11} 3.03(1)	2.38(8)	log β_{11} 1.655(4)	b
4	Br^-	log β_{11} 3.41(3)	b	b	b

a- hard to follow peaks, b- weakly binding, c- deprotonation

The product was fully characterized with the usual spectroscopic techniques (see experimental section). ^{1}H-NMR spectroscopic titration of host **2.22** was performed with $TBA^{+}X^{-}$ (Cl, OAc, Br, F, NO_3) in an acetone solvent. The NHa peak of **2.22** occurs at 6.83 ppm in the free host and does not change significantly until after the addition of 0.5 equivalents of chloride guest anion. After 0.5 equivalents a significant shift is observed in the ^{1}H-NMR titration curve reaching 8.13 ppm at five equivalents, as shown in Figure **2.34**. Other anion guests have significantly less effect. Hence by preventing the formation of strong intramolecular hydrogen bonding, a highly selective and effective chloride host has been produced. This result highlights the importance of careful molecular design. The binding constant for chloride is log β_{11} 1.47(1).

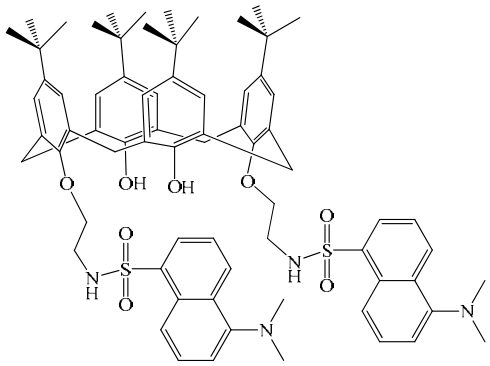

2.21

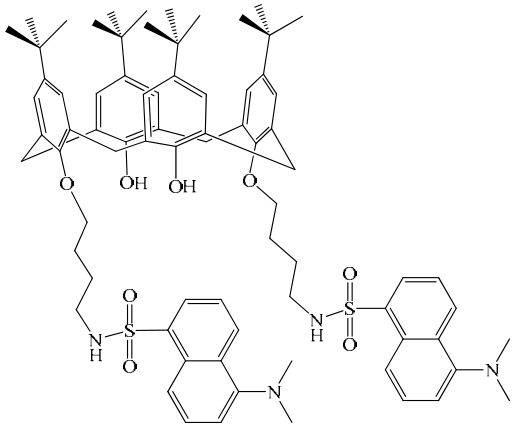

2.22

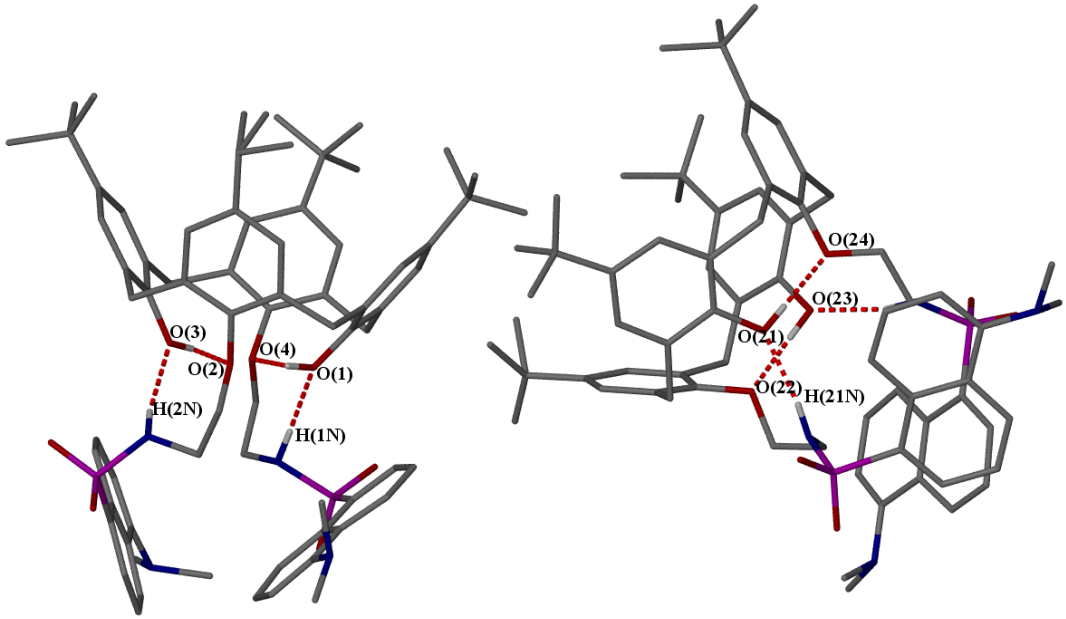

Figure 2.33 The X-Ray molecular structure of 2.21. Selected hydrogen bonding distances are N1···O1 = 2.427, N2···O3 = 2.505 Å

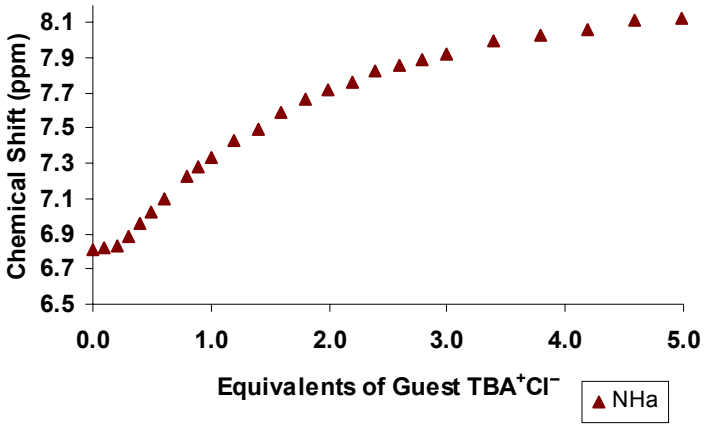

Figure 2.34: ^{1}H-NMR spectra of compound 2.22 with $TBA^{+}Cl^{-}$ anion guest in an acetone.

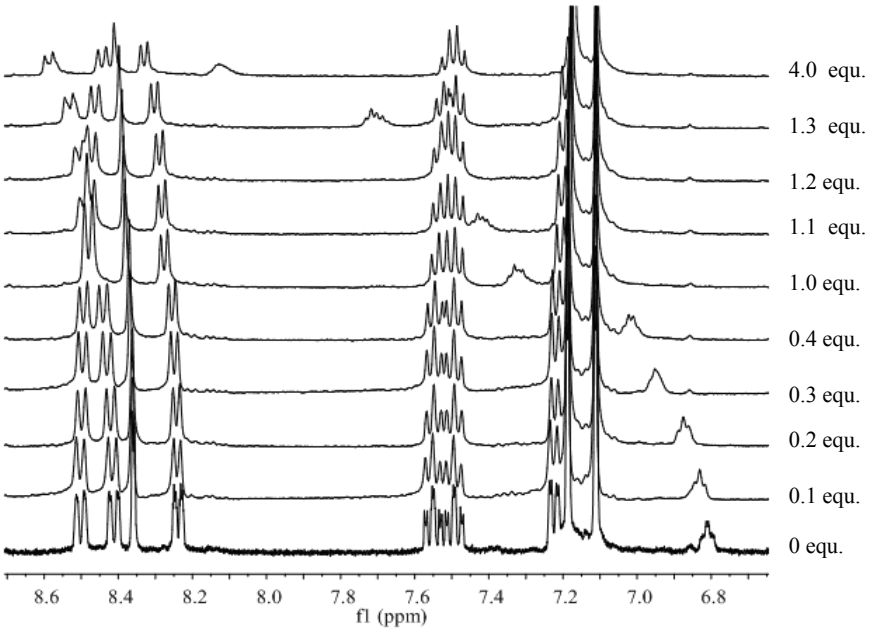

Figure 2.35 ^{1}H-NMR spectroscopic titration of 2.22 with chloride in acetone solution

2.5 Calixarene Sulphonates

It is of key interest to produce amphiphilic or water soluble calixarene derivatives and hence attempts were made to prepare anion hosts based on sulphonated calixarenes. Sulphonated calixarene were synthesized by the two steps, first by deprotection of calix[4]arene **2.1** to form a debutylated calixarene, and further sulphonation in presence of concentrated sulphuric acid to give **2.23**. We tried to use different solvent systems such as DMSO / DMF, and bases such as NaOH and along with bromoalkanes, and bromo and chloro nitriles to modify the lower rim of sulphonated calixarenes **2.23** following different strategies of Shinkai,[25] Reinhoudt[9, 19, 26, 27] and Collin[8] as well by changing the bases from strong NaH to weak K_2CO_3, but all these reactions were not successful. During this work we obtained a crystal structure of the sulphonated calixarene itself. Crystals were obtained from ethanol solvent. The crystal structure is apparently of the calixarene trianion with the charge balanced by three protonated molecules of 3-chloropropylamine, one of which resides in the calixarene cavity as shown in figure **2.36**. The molecule is in a pinched cone conformation and shows internal hydrogen bonding at the lower rim of calixarene (Figure **2.37**).

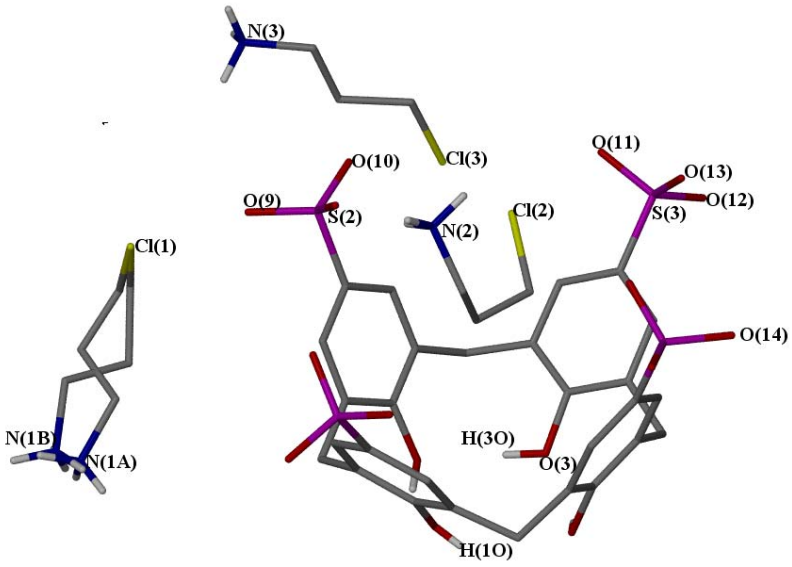

Figure 2.36 Inclusion complex of sulphonated calixarene 2.23

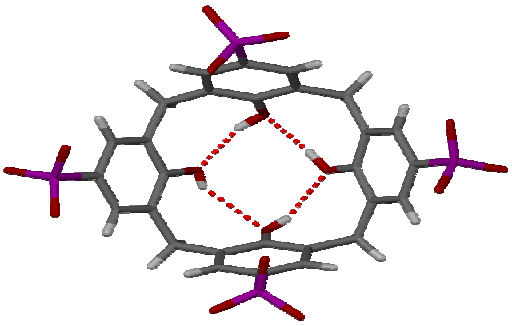

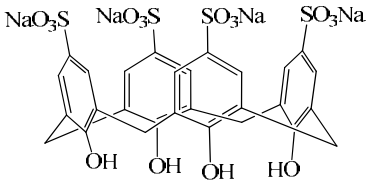

Figure 2.37 Water soluble calixarene 2.23 **2.23**

Table 2.4 Crystal data for compounds 2.21 and 2.23

Compound	**2.21**	**2.23**
Formula	C_{72} H_{88} N_4 O_8 S_2 x 4 CH_3CN	C_{40} H_{64} Cl_4 N_4 O_{20} S_4
Formula weight	1365.80	1190.99
Crystal system	Triclinic	Monoclinic
Space group	*P*-1	I2/a
a, Å	12.1816(3)	21.843(3)
b, Å	24.5969(7	18.485(3)
c, Å	26.7522(7)	27.196(4)
α, °	102.923(10)	90.00
β, °	95.542(10)	107.930(3)
γ, °	98.546(10)	90.00
Volume/Å^3	7655.6(4)	10448(3)
Z	4	8
ρ (calc.), mg/mm^3	1.185	1.514
μ, mm^{-1}	0.129	0.465
F(000)	2928	4992
Reflections collected	85996	7518
Independent refl., R_{int}	35131, 0.0544	7518, 0.0751
N of parameters	1822	690
Final R_1 [I>2σ(I)]	0.0600	0.0484
wR_2 (all data)	0.1502	0.1063
GOF on F^2	1.031	1.038

2.6 Other Calixarene Derivatives

In order to make larger channels we synthesized some calix[8]arene derivatives using the standard procedure.[7] The crystal structure of *p-t*-butylcalix[8]arene itself (**2.24**) was obtained during the course of this work, Figure **2.38**. The calix[8]arene has a flat, pleated loop conformation held together by internal OH···O hydrogen bonding and includes nine chloroform solvent molecules.

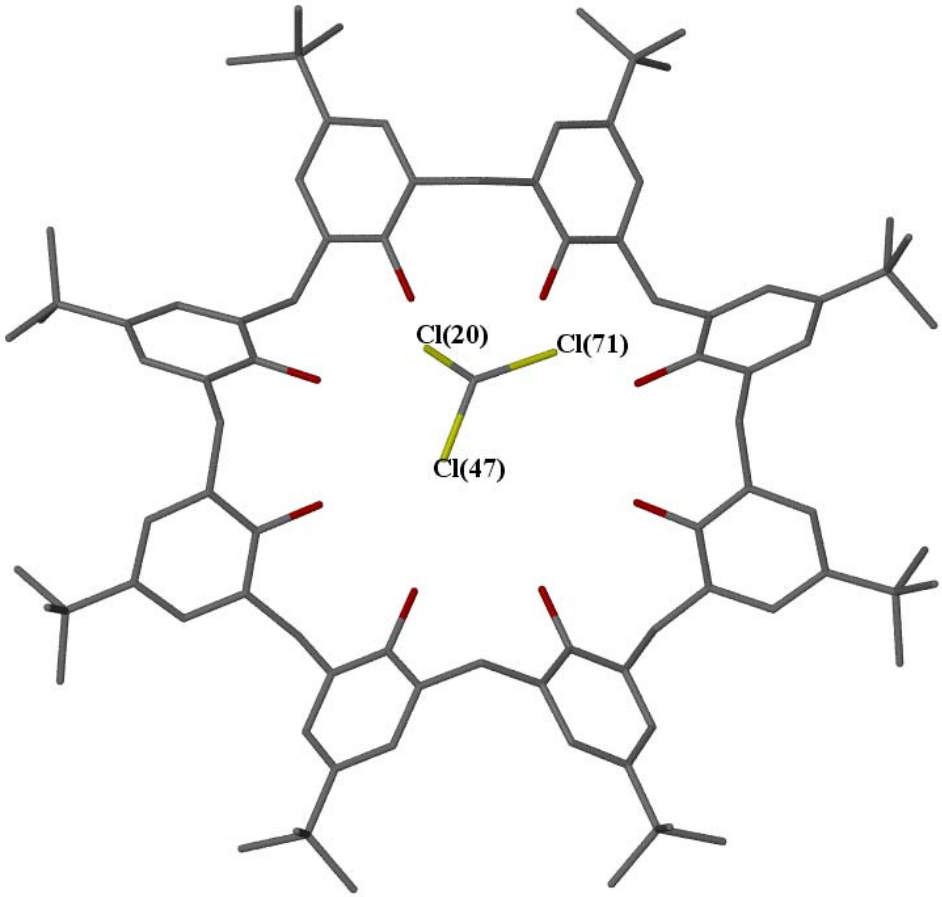

Figure 2.38 Crystal structures of 2.24 forming hydrogen bonds with chloroform solvent.

Receptor **2.24** was reacted with chloroacetonitrile in presence of K_2CO_3/ NaI and acetonitrile leaving the reaction for more than 72 h resulting a molecule with eight substituted acetonitrile moieties **2.25**. Product **2.25** was characterised by the usual spectroscopic techniques (see experimental). Reduction of **2.25** was carried out using BH_3.THF solution resulting in the formation of the amino pendant analogue **2.26**. The

major problem during the reaction and work up of these types of products was the lack of solubility of the product. Most of the substituted calix[8]arenes were partly or not soluble in organic solvents. Some of the products were soluble at higher temperature in DMSO solvent. Broadening of the spectrum was observed in presence of $CDCl_3$ solvent, which suggests that the substituted calix[8]arene is fluxional on the NMR time scale, making interpretation difficult. In order to have better soluble compound, we reacted calix[8]arene with hexyl nitrile using the same standard procedure to make compound **2.26** that was confirmed with all the spectroscopic techniques (see experimental data). Many attempts were made to reduce nitrile moiety using BH_3.THF complex, lithium aluminium hydride and Red-Al, but we failed to obtain a clean sample of the fully reduced product.

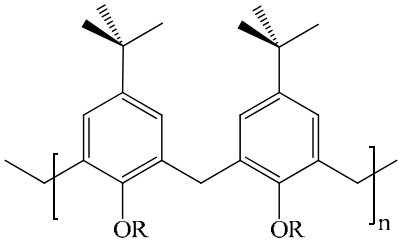

R = H, $n = 4$, **2.24**

R = CH_2CN, $n = 4$, **2.25**

R = $[CH_2]_5CN$, $n = 4$, **2.26**

2.7 Experimental

2.7.1 X-Ray crystallography

Suitable single crystals were grown by slow evaporation in the dark and mounted using silicon grease on a thin glass fibre. Crystallographic measurements were carried out on a Bruker SMART CCD 6000 and Rigaku R-AXIS Spider IP diffractometer using graphite monochromated Mo-Kα radiation (λ= 0.71073 Å). The standard data collection temperature was 120 K, maintained using an open flow N_2 Cryostream (OxfordCryosystems) device. Integration was carried out using the Bruker SAINT and Rigaku FSProcess packages. Data sets were corrected for Lorentz and polarisation effects and for the effects of absorption. Structures were solved using direct methods and refined by full-matrix least squares on F^2 for all data using SHELXTL software. All non-hydrogen atoms were refined with anisotropic displacement parameters. Hydrogen atoms were located on the difference map and refined isotropically. Molecular graphics were produced using the programs X-Seed[28] and POV-Ray[29]. Crystal data for the structures studied are listed in Tables **2.1**, **2.2** and **2.4**.

2.7.2 ^{1}H-NMR Titration Experiment:

^{1}H-NMR titration experiment were carried out at room temperature using Varian Inova-500 spectrometer operating at 500 MHz (Durham University). All chemical shifts are reported in ppm relative to TMS as an internal reference. A solution of the host species of known concentration typically 0.5 – 1.5 mM, was made up in an NMR tube using the appropriate deuterated solvent (0.5 ml). Solution of the anions, as tba salts, were made up in volumetric flasks (2.0 ml) with a concentration five times greater than that of the host. The guest solution was typically added in 10 μl aliquots, representing 0.1 equivalents of the guest with respect to the host. Larger aliquots were used in some cases where no inflection of the trace was evident. Spectra were recorded after each addition and the trace was followed simultaneously. Results were analysed using the curve fitting programme HypNMR.

2.7.3 Variable Temperature (VT) ^{1}H-NMR Experiment:

^{1}H VT-NMR experiments were conducted using a Varian Inova-500 spectrometer operating at 500 MHz (Durham University). Spectra were run in tetrachloroethane TCE-d_6 with TMS as an internal reference. An initial spectrum was run at room temperature

and other spectra were collected at 45, 60 and 90 ^{0}C. The temperature was allowed to equilibrate at each temperature before collecting of the spectra.

5, 11, 17, 23–Tetra-tert-butyl-25, 27-dicyanomethoxy-26, 28-dihydroxycalix[4]arene (2.2):

A mixture of p-tert-butylcalix[4]arene (10 g, 13.7 x 10^{-2} mol), potassium carbonate (8.53 g, 58 x 10^{-2} mol), chloro acetonitrile (4 ml), and sodium iodide (9.25 g, 85.7 x 10^{-3} mol) in dry acetone (250 ml) was stirred and heated under reflux for 12 h. The cooled mixture was filtered through a bed of celite and the filtrate and dichloromethane washings of the celite were combined and contracted to dryness. Recrystallisation of the residue from ethanol furnished the dinitrile (6.4 g, 8.8 mmol, 57%), m.p.> 290 ^{0}C (decomp.) Found: C, 79.2; H, 7.8; N, 3.9. $C_{48}H_{58}N_2O_4$ requires C, 79.3; H, 8.0; N, 3.9%); ν max (KBr) / cm^{-1} 3500 (OH), 3250 (-CN); ^{1}H-NMR ($CDCl_3$) 0.88 (18 H, s, But), 1.34 (18 H, s, But), 3.42 (4H, d, *J* 13.2, $ArCH_2Ar$), 4.24 (4H, d, *J* 13.2, $ArCH_2Ar$), 4.84 (4H, s, OCH_2CN), 5.60 (2H, s, ArOH), 6.83 (4H, s, ArH) and 7.22 (4H, s, ArH).

5, 11, 17, 23–Tetra-tert-butyl-25, 27-bis [(amino ethyl) oxy]-26, 28-dimethoxyhexylaminecalix[4]arene (2.4):

A mixture of p-tert-butylcalix [4] arene (14 g, 21.44 x 10^{-3} mol), potassium carbonate (11.82 g, 85.7 x 10^{-3} mol), bromo hexylnitrile (15.08 g, 85.7 x 10^{-3} mol), and sodium iodide (12.85 g, 85.7 x 10^{-3} mol), in dry acetone (250 ml) was stirred and heated under reflux for 24 h. The cooled mixture was filtered through a bed of celite and the filtrate and dichloromethane washings of the Celite were combined and concentrated to dryness. Recrystallisation of the residue from ethanol furnished the calix hexyl nitrile **2.4** (5.2 g, 28%). ^{1}H-NMR ($CDCl_3$, 400 MHz): 0.96 (18H, s, Bu^t), 1.30 (18H, s, Bu^t), 1.88 (8H, m, CH_2), 2.08 (4H, m. CH_2), 2.48 (2H, m, *J* = 4, 8, 12 Hz, CH_2), 3.35 (4H, d, *J* = 12 Hz, $ArCH_2Ar$), 4.00 (4H, m, *J* = 4, 8, 12 Hz, OCH_2), 4.24 (4H, d, *J* = 12 Hz, $ArCH_2Ar$), 6.82 (4H, s, Ar), 7.07 (4H, s, Ar) and 7.44 (2H, s, OH); ^{13}C{^{1}H}-NMR ($CDCl_3$, 400 MHz): 14.08 (s, CH_2), 17.18 (s, CH_2), 22.61 (d, CH_2), 25.18 (d, CH_2), 30.86 (d, Bu^t), 31.62 (d, $ArCH_2Ar$), 33.87 (d, CH), 75.68 (s, OCH_2), 119.67 (s, CN), 125.11 (s, Ar), 125.51 (s, Ar), 127.76 (s, Ar), 132.44 (s, Ar), 141.63 (s, Ar), 146.96 (s, Ar) and 149.72 (s, Ar); Anal. for $C_{56}H_{72}O_4N_2$ calc. C 80.34, H 8.67, N 3.35, found C 80.13, H 8.33, N 2.74; IR (cm^{-1}) 2358 (s, CN); Mass Spectrum ESI 861.7 ($C_{56}H_{72}O_4N_2$ + H).

5, 11, 17, 23 – Tetra – p – tert – butyl - 25, 27, bis (cyanopropyl) - oxy]-26, 28 dihydroxycalix [4] arene (2.6):

A mixture of p-tert-butylcalix [4] arene (11.46 g, 17.9 x 10^{-3} mol), potassium carbonate (9.90 g, 72 x 10^{-3} mol), bromobutyronitrile (5.30 g, 35.80 x 10^{-3} mol), and sodium iodide (10.70 g, 72 x 10^{-3}) in dry acetone (250 ml) was stirred and heated under reflux for 16 h. The cooled mixture was filtered through a bed of celite and the filtrate and dichloromethane washings of the celite were combined and concentrated to dryness. Recrystallisation of the residue from ethanol furnished the dinitrile **2.6** (9.14 g, 11.68 x 10^{-3} mol) Yield 57 %. ^{1}H-NMR ($CDCl_3$, 400 MHz): 0.93 (18H, s, Bu^t), 1.21 (18H, s, Bu^t), 2.27 (4H, pt, J = 5.6, 6, 11.6 Hz, CH_2), 2.98 (4H, t, J = 6.8, 7.2, 14 Hz, CH_2), 3.29 (4H, d, J = 13.2 Hz, $ArCH_2Ar$), 4.02 (4H, t, J = 5.2, 6, 11.2 Hz, CH_2), 4.082 (4H, d, J = 12.8 Hz, $ArCH_2Ar$), 6.79 (4H, s, Ar), 6.99 (4H, s, Ar), 7.34 (2H, s, OH); $^{13}C\{^{1}H\}$-NMR ($CDCl_3$, 400 MHz): 13.19 (s, CH_2), 25.57 (s, CH_2), 29.97 (s, Bu^t), 30.64 (s, Bu^t) 32.83 (s, $ArCH_2Ar$), 33.00 (s, $ArCH_2Ar$), 72.25 (s, OCH_2), 118.40 (s, CN), 124.27 (s, Ar), 124.78 (s, Ar), 126.49 (s, Ar), 131.49 (s, Ar), 141.08 (s, Ar), 146.59 (s, Ar), 147.79 (s, Ar), 149.31 (s, Ar); Anal. for C_{52} H_{66} N_2 O_4.1.1 $CHCl_3$ calc. C 68.32, H 7.23, N 3.07, found C 68.73, H 7.33, N 3.28; IR (cm^{-1}) 3402 (vbr, OH & NH), 2962.6 (s, OH), 2253 (w, CN), 1484.5 (s, OCH_2), 1362 (s, OH & CO str); Mass Spectrum ESI 783.2 (C_{64} H_{80} N_4 O_6 S_2 + H); Mp. 240 ^{0}C.

5, 11, 17, 23–Tetra-tert-butyl-25, 27-bis [(amino ethyl) oxy]-26, 28-dihydroxycalix [4] arene (2.7):

To a suspension of calix[4]arene **2.2** (2 g, 2.8 x 10^{-3} mol) added 100 ml of THF solvent, which was cooled using ice, then added 60 ml (60 mmol) of BH_3. (1M THF solution) was added dropwise under nitrogen. The mixture was heated then at 80 ^{0}C for 12 h resulting in a formation of product. After cooling, it was quenched with 50 ml of 1 N HCl and the solvent was removed under reduced pressure. The crude product was further stirred in presence 50 ml of 6 N HCl, which was further refluxed for 3 h. After being cooled the product was washed with ether and evaporated to dryness. The residue was washed with dichloromethane and added 2 N NaOH until pH was basic. The organic layer was separated, dried and evaporated to give **2.7** (0.68g, 23%) a foamy product. IR (KBr) 3357 and 3284 cm^{-1} (NH_2); ^{1}HNMR ($CDCl_3$,) 3.10 – 3.30 (br m, -CH_2-), 3.0, 4.0 & 4.20

(br m, NH and CH_2), 4.80 (s, OCH_2, 4H) and 6.90 -7.0 (m, ArH, 8H); Mass Spectrum ESI 737 m/z.

5, 11, 17, 23–Tetra-tert-butyl-25, 27-bis [(amino butyl) oxy]-26, 28-dihydroxycalix [4] arene (2.11):

To a suspension of calix [4] arene **2.6** (2.2 g, 2.8 x 10^{-3} mol) added 100 ml of THF solvent, which was cooled using a dry ice, then added 60 ml (60 x 10^{-3} mol) of BH_3. (1M THF solution) was added dropwise under nitrogen. The mixture was heated then at 80 ^{0}C for 15 h resulting in a formation of product. After cooling, it was quenched with 70 ml of 1 N HCl and the solvent was removed under reduced pressure. The crude product was further stirred in presence 50 ml of 6 N HCl, which was further refluxed for more than 3 h. After being cooled the product was washed with ether and evaporated to dryness. The residue was washed with dichloromethane and added 2 N NaOH until pH was basic. The organic layer was separated, dried and evaporated to give **2.11** (2.56 g, 47%) a foamy product.

^{1}H-NMR ($CDCl_3$, 400 MHz): 0.99 (18H, s, Bu^t), 1.30 (18H, s, Bu^t), 1.86 (4H, m, J = 4.4, 6.4, 11.6, 14.4 Hz, CH_2), 2.04 (8H, m, CH_2), 2.91 (4H, t, J = 6.8, 7.2, 14 Hz, OCH_2), 3.31 (4H, d, J = 13.2 Hz, $ArCH_2Ar$), 3.99 (4H, br, NH_2), 4.27 (4H, d, J = 12, $ArCH_2Ar$), 6.83 (4H, s, Ar), 7.06 (4H, s, Ar) and 7.60 (2H, s, OH); $^{13}C\{^1H\}$-NMR ($CDCl_3$, 400 MHz): 27.30 (s, CH_2), 27.46 (s, CH_2), 30.51 (s, Bu^t), 30.69 (s, Bu^t) 32.78 (s, $ArCH_2Ar$), 32.90 (s, $ArCH_2Ar$), 40.80 (s, CH_2), 76.22 (s, OCH_2), 124.04 (s, Ar), 124.44 (s, Ar), 126.80 (s, Ar), 131.55 (s, Ar), 140.45 (s, Ar), 145.78 (s, Ar), 148.85 and 149.64 (s, Ar); Anal. for $C_{52}H_{74}N_2O_4 . CHCl_3$ calc. C 68.18, H 8.73, N 3.05, found C 68.51, H 8.01, N 2.57; IR (cm^{-1}) 3308 (vbr, OH & NH), 2960.80 (s, Ar), 1601.85, 1483.97, 1016; Mass Spectrum ESI 791 ($C_{52}H_{74}N_2O_4$ + H) and 1627.2 (2 [$C_{52}H_{74}N_2O_4$ + H + Na]); Mp. 78 – 80 ^{0}C.

5, 11, 17, 23 – Tetra – tert - butyl - 25, 27- bis [[(N-phenyl-ureido -3-thiomethyl)-butyl] oxy]-26, 28- dihydroxycalix [4] arene (2.15):

Calix ethyl amine **2.7** (0.5 g, 6.80 x 10^{-4} mol) was mixed with 3-(methylthio) phenyl isoyanate (0.225 g, 1.36 x 10^{-3} mol) in 30 ml of chloroform solution. The reaction mixture was stirred for 4 h resulting in a formation of a product which was confirmed with the

help of T.L.C. The crude product was washed with 2 ml of diethyl ether and hexane solvent to get pure product, which was analyzed through all the spectroscopic techniques.

^{1}H-NMR (Acetone, 700 MHz): 1.05 (18H, s, But), 1.27 (18H, s, But), 2.34 (6H, s, SCH_3), 3.49 (4H, d, *J* = 14 Hz, $ArCH_2Ar$), 3.93 (4H, m, *J* = 7, 14 Hz, CH2), 4.07 (4H, t, *J* = 7 Hz, OCH_2), 4.24 (4H, d, *J* = 14 Hz, $ArCH_2Ar$), 6.80 (2H, d, *J* = 7 Hz, Ar), 6.84 (2H, br, NH), 7.06 (2H, t, *J* = 7, 14 Hz, Ar), 7.11 (2H, d, *J* = 7 Hz, Ar), 7.19 (4H, s, Ar), 7.23 (4H, s, Ar), 7.43 (2H, s, Ar), 8.30 (2H, br, NH) and 8.66 (2H, s, Ar).

^{13}C{^{1}H}-NMR (Acetone, 700 MHz): 15.28 (s, SCH_3), 30.75 (s, But), 31.37 (s, But), 31.85 (s, $ArCH_2Ar$), 31.70 (s, $ArCH_2Ar$), 39.85 (s, CH_2), 76.53 (s, OCH_2), 115.4 (s, Ar), 115.6 (s, Ar), 116.6 (s, Ar), 119.2 (s, Ar), 125.4 (s, Ar), 125.8 (s, Ar), 127 (s, ArOH) and 150 (s, CO); Anal. for C_{64} H_{80} N_4 O_6 S_2 calc. C 72.15, H 7.57, N 5.26, found C 70.47, H 7.39, N 5.0; IR (cm^{-1}) 3338.88 (vbr, OH & NH), 2957.53 (w, CH, str.), 1657.13 (w, CO), 1537.03 (s, NH), 1479.96, 1193; Mass Spectrum ESI 1087.5 (C_{64} H_{80} N_4 O_6 S_2 – H + Na), 1064.3 (C_{64} H_{80} N_4 O_6 S_2 – H); Mp. 142 ^{0}C.

5, 11, 17, 23 – Tetra – tert - butyl - 25, 27- bis [[(N-phenyl-ureido)-butyl] oxy]-26, 28-dihydroxycalix [4] arene 2.16:

Calix ethyl amine **2.7** (0.200g, 2.72 x 10^{-4} mol) was mixed with naphthalene isoyanate (0.092 g, 5.44 x 10^{-3} mol) in 10 ml chloroform solvent at 0 ^{0}C. The reaction mixture was stirred for 1 h resulting in a formation of crude product and washed with 3 ml of diethyl ether, hexane and petroleum ether to get a pure product characterized through all the spectroscopic techniques.

^{1}H-NMR (Acetone, 700 MHz): 1.03 (18H, s, Bu^t), 1.27 (18H, s, Bu^t), 2.43 (4H, d, *J* = 14 Hz, $ArCH_2Ar$), 3.87 (4H, m, CH_2), 4.05 (4H, t, OCH_2), 4.25 (4H, d, *J* = 14 Hz, $ArCH_2Ar$), 7.14 (4H, s, Ar), 7.17 (2H, d, Naph), 7.22 (4H, s, Ar), 7.26 (2H, d, *J* = 7 Hz, Naph), 7.30 (2H, br, NH), 7.37 (2H, t, *J* = 7, 14 Hz, Naph), 7.47 (2H, d, *J* = 7 Hz, Naph), 7.75 (2H, d, *J* = 7 Hz, 14 Hz, Naph), 7.84 (2H, m, Naph), 7.93 (2H, brm, Naph), 8.16 (2H, br, NH), and 8.67 (2H, s, OH); ^{13}C{^{1}H}-NMR (Acetone, 700 MHz): 28.70 (s, CH_2), 28.81 (s, Bu^t), 28.92 (s, Bu^t), 29.03 (s, $ArCH_2Ar$), 29.14 (s, $ArCH_2Ar$), 76.10 (s, OCH_2), 121.75 (s, Naph), 121.85 (s, Naph), 123.45 (s, Naph), 125.19 (s, Naph), 125.30 (s, Naph), 125.40 (s, Naph), 125.58 (s, Ar), 125.95 (s, Ar), 127.45 (s, Ar), 127.60 (s, Naph), 128 (s, Naph), 142.32 (s, Ar), 147.67 (s, Ar), 149.31 (s, Ar), 150.03 (s, Ar), 150.14 (s, Ar), 156.35 (s, Naph), 156.45 (s, Naph) and 156.54 (s, Naph); Anal. for C_{70} H_{80} O_6 N_4 calc. C

78.25, H 7.50, N 5.22, found C 77.14, H 7.67, N 4.80; IR (cm^{-1}) 3356.5 (vbr, OH & NH), 2960.37 (s, CH str.), 1644.98 (s, CO), 1548, 1482.71 and 1046.94; Mass Spectrum ESI 1072.38 ($C_{70}H_{80}O_6N_4$ - H), 1095.7 ($C_{70}H_{80}O_6N_4$ – H + Na); Mp.142 ^{0}C.

5,11,17,23–Tetra-tert-butyl-25,27-bis[[(N-phenyl-ureido)-butyl]oxy]-26,28-dihydroxycalix[4]arene 2.18:

Calix ethyl amine **2.7** (0.700 g, 9.50 x 10^{-4} mol) was mixed with p-tolyl isocyanate (0.51 g, 3.80 x 10^{-3} mol) in 50 ml of chloroform solvent. The reaction mixture was refluxed for more than 12 h resulting in a formation of crude product, which was washed with 4 ml of diethyl ether and hexane solvent to get a pure product.

^{1}H-NMR ($CDCl_3$, 400 MHz): 1.15 (18H, s, Bu^t), 1.27 (18H, s, Bu^t), 2.25 (6H, s, CH_3), 3.41 (4H, d, *J* = 12 Hz, $ArCH_2Ar$), 3.86 (4H, m, *J* = 4 Hz, CH_2), 4.12 (4H, t, *J* = 8 Hz, OCH_2), 4.19 (4H, d, *J* = 12 Hz, $ArCH_2Ar$), 6.66 (2H, br, NH), 6.99 (4H, s, Ar), 7.01 (4H, s, Ar), 7.04 (2H, s, Ar), 7.08 (2H, s, Ar), 7.12 (2H, s, Ar), 7.14 (2H, s, Ar), 7.16 (2H, br, NH) and 7.28 (2H, s, OH).

5, 11, 17, 23–Tetra-tert-butyl-25, 27-bis [[(N-phenyl-thio-ureido] oxy]-26, 28-dihydroxycalix [4] arene 2.20:

Calix ethyl amine **2.7** (0.5 g, 6.80 x 10^{-4} mol) was reacted with m-methyl phenyl isothiocyanate (0.203 g, 1.36 x 10^{-3} mol) in 25 ml of chloroform solvent. The reaction mixture was stirred for 20 h resulting in a formation of a product which was confirmed with the help of T.L.C in a range of solvents. The crude product was washed 5 ml of hexane, diethyl ether, petroleum ether and propanol to get a pure product which was characterized through all the spectroscopic techniques.

^{1}H-NMR ($CDCl_3$, 700 MHz): 1.10 (18H, s, Bu^t), 1.20 (18H, s, Bu^t), 1.96 (6H, s, CH_3), 3.22 (4H, d, *J* = 14 Hz, $ArCH_2Ar$), 3.75 (4H, d, *J* = 14 Hz, $ArCH_2Ar$), 4.08 (4H, m, CH_2), 4.17 (4H, t, *J* = 7, 14 Hz, OCH_2), 6.79 (2H, d, *J* = 7 Hz, Ar), 6.86 (2H, br, NH), 6.90 (4H, s, Ar), 6.92 (4H, s, Ar), 7.03 (2H, t, *J* = 7, 14 Hz, Ar), 7.07 (2H, d, *J* = 7 Hz, Ar), 7.77 (2H, br, NH), 7.93 (2H, t, Ar) and 8.00 (2H, s, OH); $^{13}C\{^1H\}$-NMR ($CDCl_3$, 700 MHz): 21.00 (s, CH_3), 31.09 (s, Bu^t), 31.53 (s, Bu^t), 32.24 (s, $ArCH_2Ar$), 33.78 (s, $ArCH_2Ar$), 34.16 (s, CH_2), 46.21 (s, CCH_3), 74.91 (s, OCH_2), 122.91 (s, Ar), 125.47 (s, Ar), 125.96 (s, Ar), 126.38 (s, Ar), 127.75 (s, Ar), 129.00 (s, Ar), 133.11 (s, Ar), 136.31 (s, Ar), 140.02 (s, Ar), 142.57 (s, Ar), 148.03 (s, Ar), 148.29 (s, Ar), 149.29 (s, Ar) and 182.26 (s,

CS); Anal. for C_{64} H_{80} N_4 O_4 H_2O calc. C 73.10, H 7.67, N 5.32, found C 72.76, H 7.67, N 4.85; IR (cm^{-1}) 3283 (w br, NH), 2985 (m, CH str.), 1657.13 (w, CO), 1484 (s, CS), 1199 (s) and 1033.98 (s); Mass Spectrum ESI 1055.5 (C_{64} H_{80} N_4 O_4 – H + Na), Mp. 178 ^{0}C.

5, 11, 17, 23 – Tetra – tert - butyl - 25, 27- bis [[(N-dansyl sulphonyl)-ethyl] oxy]-26, 28- dihydroxycalix [4] arene (2.21):

Calix ethyl amine **2.7** (0.200 g, 2.72 x 10^{-4} mol) was mixed with dansyl chloride in water and sodium hydrogen carbonate (1:1 v / v: 8 ml) of solution. The reaction mixture was stirred at room temperature for 2 h resulting in a formation of crude product which was washed with slight amount of diethyl ether and hexane to get a pure product which was characterized through all the spectroscopic techniques.

^{1}H-NMR ($CDCl_3$, 700 MHz): 1.12 (18H, s, Bu^t), 1.21 (18H, s, Bu^t), 2.89 (12H, s, NCH_3), 3.01 (4H, m, CH_2), 3.27 (4H, d, *J* = 14 Hz, $ArCH_2Ar$), 3.81 (4H, t, *J* = 7, 14, 21 Hz, OCH_2), 6.98 (4H, s, Ar), 6.99 (4H, s, Ar), 7.11 (2H, d, Naph), 7.29 (4H, m, Naph), 7.49 (2H, d, Naph), 7.50 (2H, br, NH), 7.83 (2H, t, *J* = 7, 14 Hz, Naph), 8.10 (2H, d, *J* = 7 Hz, Naph), 8.39 (2H, d, *J* = 7 Hz, Naph), 8.55 (2H, d, *J* = 7 Hz, Naph) and 8.60 (2H, s, OH); ^{13}C{^{1}H}-NMR ($CDCl_3$, 700 MHz): 30.97 (s, Bu^t), 31.10 (s, Bu^t), 31.45 (s, CH_2), 32.45 (s, CH_2), 42.20 (s, NCH_3), 45.80 (s, CH_2), 76.11 (s, OCH_2), 114.6 (s, Naph), 124 (s, Naph), 125.80 (s, Ar), 126 (s, Ar), 127.8 (s, Naph), 128.5 (s, Naph), 129.80 (s, Naph), 133.50 (s, Ar), 136.31 (s, Naph), 143.04 (s, Ar), 148.18 (s, Naph), 148.50 (s, Ar) and 149 (s, Ar); Anal. for C_{72} H_{88} O_8 S_2 N_4 calc. C 71.97, H 7.38, N 4.66, found C 71.77, H 7.37, N 4.69; IR (cm^{-1}) 3258.1 (br, OH & NH), 2953.9 (s, CH str.), 2869.61 (w, Naph), 1708.20 (s, SO_2), 1462 (m, NCH_3) and 1441.83; Mass Spectrum ESI 1224.4 (C_{72} H_{88} O_8 S_2 N_4 + Na); Mp.142 ^{0}C.

5, 11, 17, 23 – Tetra – tert - butyl - 25, 27- bis [[(N-dansyl sulphonyl)- butyl] oxy]-26, 28- dihydroxycalix [4] arene (2.22):

Calix butyl amine **2.11** (0.724 g, 9.16 x 10^{-4} mol) was mixed with dansyl chloride in water and sodium hydrogen carbonate (1:1 v / v: 8 ml) of solution. The reaction mixture was stirred at room temperature for 2.5 h resulting in a formation of crude product which was washed with 3 ml of diethyl ether and hexane to get a pure product which was characterized through all the spectroscopic techniques.

^{1}H-NMR ($CDCl_3$, 700 MHz): 0.827 (18H, s, Bu^t), 1.24 (18H, s, Bu^t), 1.63 (4H, pt, *J* = 6.4, 13.2 Hz, CH_2), 1.77 (4H, pt, *J* = 6.4, 14, 20 Hz, CH_2), 2.84 (12H, s, NCH_3), 3.180 (4H, m, CH_2), 3.21 (4H, d, *J* = 13.2 Hz, $ArCH_2Ar$), 3.75 (4H, t, *J* = 6.3, 12.4 Hz, OCH_2), 4.11 (4H, d, *J* = 12.8 Hz, $ArCH_2Ar$), 6.04 (2H, br, NH), 6.70 (4H, s, Ar), 7.00 (4H, s, Ar), 7.20 (4H, t, *J* = 7.6, 14 Hz, Naph), 7.42 (2H, t, *J* = 8, 16 Hz, Naph), 7.47 (2H, s, OH), 8.22 (2H, d, *J* = 7.2 Hz, Naph), 8.29 (2H, d, *J* = 7.2 Hz, Naph) and 8.46 (2H, d, *J* = 8 Hz, Naph); $^{13}C\{^{1}H\}$-NMR ($CDCl_3$, 700 MHz): 25.70 (s, CH_2), 25.85 (s, CH_2), 30.65 (s, Bu^t), 31.25 (s, Bu^t), 31.60 (s, $ArCH_2Ar$), 31.80 (s, $ArCH_2Ar$), 42.28 (s, CH_2), 45.80 (s, NCH_3), 76 (s, OCH_2), 124.59 (s, Ar), 125 (s, Ar), 125.40 (d, Ar), 126 (s, Naph), 126.75 (s, Ar), 128.01 (s, Naph), 128.12 (s, Naph), 129.20 (s, Naph), 129.85 (s, Naph), 131.80 (s, Ar), 148.20 (s, Ar), 148.20 (s, Ar) and 148.90 (s, Ar); Anal. for $C_{76}H_{96}O_8S_2N_4$ calc. C 72.58, H 7.69, N 4.45, found C 71.57, H 7.52, N 4.10; IR (cm^{-1}) 3673 (br, H2O), 3311.1 (vbr, NH), 2953.43 (w, NH str.), 1575, 1483.82, 1311, 1073; Mass Spectrum ESI 1279.6 ($C_{76}H_{98}O_8S_2N_4$ - H + Na), 1024.5 ($C_{64}H_{86}O_6SN_3$ – H); Mp.118 ^{0}C.

Tert-butyl-calix [8] arene octa-cyanonitrile (2.25):

A mixture of p-tert-butylcalix [8] arene **2.24** (10 g, 7.6 x 10^{-2} mol), potassium carbonate (8.53 g, 58 x 10^{-2} mol), chloro acetonitrile (4 g, 53.3 x 10^{-2} mol), and sodium iodide (9.3 g, 61.6 x 10^{-2} mol) in dry acetone (250 ml) was stirred and heated under reflux for 72 h. The cooled mixture was filtered through a bed of celite and the filtrate and dichloromethane washings of the celite were combined and concentrated to dryness. Recrystallisation of the residue from ethanol, chloroform and then after ethyl accetate furnished the octanitrile **2.24** (3.07 g, 35%), found: C, 69.34; H, 6.69; N, 5.77 $C_{104}H_{114}N_8O_8$ requires C, 69.3; H, 6.80; N, 5.90); V_{max} (K Br) / cm^{-1} 3500; ^{1}H($CDCl_3$) 1.00 (72H, s, Bu^t), 3.92, 4.20 (16H, s, $ArCH_2Ar$), 5.12 (16H, s, OCH_2), 6.90 (16H, br s,

ArH); $^{13}C\{^{1}H\}$-NMR: 53 (s, OCH_2), 57 (s, $ArCH_2Ar$), 30 – 34 (s, -C-CH_3), 118, 124, 132 (s, ArC);

2.8 Conclusions

In conclusion, we have made simple calixarene based urea and amide based receptors that can specifically bind chloride anion in a 1:1 stoichiometry exclusively through hydrogen bonding. The thiomethyl urea calixarene **2.15** binds chloride anion stronger than other receptors reported above. The crystal structures of intermediate products **2.3**, **2.4**, **2.5** and **2.6** provide better understanding of partial cone, pinched cone and cone conformations respectively. We failed to understand and control the reactions of higher butyronitrile **2.3**, **2.4** and calix[8]arene due to poor solubility and selectivity. The reaction with series of bis –isocyanates also failed to provide any well characterised product. Reactions of amine **2.7** with substituted aryl isocyanate, naphthyl isocyanate, dansyl and octadecyl isocyanate resulted in a formation of clean urea-based products. The solid state structures of these complexes can be compared on the basis of differences between the urea hydrogen bonding. The solid state structure of thiomethyl urea calixarene **2.15** form a bifurcated hydrogen bonding interaction of the $R_2^1(6)$ 'urea tape' type; while crystal packing of **2.16** exhibits intermolecular $R_2^2(8)$ type hydrogen bonding between α–NH proton and β–oxygen atom. The remaining naphthyl moiety trans to each other in crystal structure packing. However in thiourea calixarene **2.20**, the γ– NH proton with respect to meta methyl phenyl (lower rim substituent) forms hydrogen bonds with the phenolic oxygen atom, that in turn bonds to an adjacent oxygen atom of the calixarene lower rim.

2.9 References

1. P. A. Gale, *Coord. Chem. Rev.*, 2001, **213**, 79-128.
2. K. Kunzelmann and M. Mall, *Clin. Exptal. Pharm. Physiol.*, 2001, **28**, 857-868.
3. J. L. Seganish and J. T. Davis, *Chem. Commun.*, 2005, **7**, 5781 - 5783.
4. V. Sidorov, F. W. Kotch, J. L. Kuebler, Y. F. Lam and J. T. Davis, *J. Am. Chem. Soc.*, 2003, **125**, 2840-2841.
5. E. Da Silva and A. W. Coleman, *Tetrahedron*, 2003, **59**, 7357-7364.
6. C. D. Gutsche, *Calixarenes*, Royal Society of Chemistry, Cambridge, 1989.
7. C. D. Gutsche, B. Dhawan, H. K. No and R. J. Mhthukrishnan, *J. Am. Chem. Soc.*, 1981, **103**, 3782-3792.
8. E. M. Collins, M. A. McKervey, E. Madigan, M. B. Moran, M. Owens, G. Ferguson and S. J. Harris, *J. Chem. Soc., Perkin Trans*., 1991, **5**, 3137-3142.
9. J. Scheerder, F. Fochi, J. F. J. Engbersen and D. N. Reinhoudt, *J. Org. Chem.*, 1994, **59**, 7815-7820.
10. D. M. Rudkevich, W. Verboom, Z. Brzozka, M. J. Palys, W. P. R. V. Stauthamer, G. J. van Hummel, S. M. Franken, S. Harkema, J. F. J. Engbersen and D. N. Reinhoudt, *J. Am. Chem. Soc.*, 1994, **116**, 4341-4351.
11. L. J. Prins, D. N. Reinhoudt and P. Timmerman, *Angew. Chem. Int. Ed.*, 2001, **40**, 2383-2426.
12. J. Budka, P. Lhotak, V. Michlova and I. Stibor, *Tetrahedron Lett.*, 2001, **42**, 1583-1586.
13. G. Illuminati and L. Mandolini, *Acc. Chem. Res.*, 1981, **14**, 95.
14. P. Knops, N. Sendhoff, H.-B. Mekelburger and F. Vögtle, *Topics in Curr. Chem.*, 1991, **161**, 1.
15. L. Rossa and F. Vogtle, *Topics in Curr. Chem.*, 1983, **113**, 1.
16. N. Qureshi, D. S. Yufit, J. A. K. Howard and J. W. Steed, *Dalton Trans.*, 2009, **29**, 5708 - 5714.
17. J. M. Russell, A. D. M. Parker, I. Radosavljevic-Evans, J. A. K. Howard and J. W. Steed, *Crystengcomm*, 2006, **8**, 119-122.
18. J. M. Russell, A. D. M. Parker, I. Radosavljevic-Evans, J. A. K. Howard and J. W. Steed, *Chem. Commun.*, 2006, **8**, 269-271.
19. J. Scheerder, R. H. Vreekamp, J. F. J. Engbersen, W. Verboom, J. P. M. vanDuynhoven and D. N. Reinhoudt, *J. Org. Chem.*, 1996, **61**, 3476-3481.

20. C. L. Hannon, D. A. Bell, A. M. KellyRowley, L. A. Cabell and E. V. Anslyn, *J. Phys. Org. Chem.,* 1997, **10**, 396-404.
21. V. Bohmer, O. Mogck and W. Vogt, *Tetrahedron*, 1996, **52**, 8489-8496.
22. B. L. Schottel, H. T. Chifotides and K. R. Dunbar, *Chem. Soc. Rev.*, 2008, **37**, 68-83.
23. J. Scheerder, J. F. J. Engbersen, A. Casnati, R. Ungaro and D. N. Reinhoudt, *J. Org. Chem.*, 1995, **60**, 6448-6454.
24. S. Nishizawa, P. Bühlmann, M. Iwao and Y. Umezawa, *Tetrahedron Lett.*, 1995, **36**, 6483-6486.
25. S. Shinkai, K. Araki, T. Matsuda, N. Nishiyama, H. Ikeda, I. Takasu and M. Iwamoto, *J. Am. Chem. Soc.*, 1990, **112**, 9053-9058.
26. D. M. Rudkevich, W. Verboom, Z. Brzozka, M. J. Palys, W. Stauthamer, G. J. Vanhummel, S. M. Franken, S. Harkema, J. F. J. Engbersen and D. N. Reinhoudt, *J. Am. Chem. Soc.*, 1994, **116**, 4341-4351.
27. J. D. van Loon, J. F. Heida, W. Verboom and D. N. Reinhoudt, *Recl. Trav. Chim. Pays-Bas*, 1992, **111**, 353-359.
28. L. J. Barbour, *J. Supramol. Chem.*, 2001, **1**, 189-191.
29. C. J. Cason, in POV-Ray', 2002.

.

Chapter 3: Synthesis and structures of ureidopyridine ligands

3.1 Aim and Targets

The aim of the project is to design artificial receptors based on urea hosts that can specifically bind chloride anion. The calixarene based synthetic receptors reported in Chapter 2 proved excellent hosts for chloride anion guests in solution. The Steed group has previously reported simple ligands based on 1-(3-methylsulphanyl-phenyl)-3-phenyl-1-urea (MPUP),[1, 2] *p*-tolyl 3-ureidopyridine (TUP) and its 4-pyridyl isomer,[3, 4] bind with series of anions in the presence of a complementary metal cation.[4, 5] The anion is bound through hydrogen bonding to the urea group, while the metal binds to the pyridyl or thioether substituents.[6] Such systems represent cases in which metal cations and anions are far apart from each other forming a separated ion pair and are stabilized through remote hydrogen bonding in the solid state structure and often in solution.[7]

These ligands are of some interest, as there has been potent and selective response reported for 2-pyridyl urea thiomethyl ligand,[8] while others have reported simple urea based receptors as mimics for prodigiosins.[9] While much simpler than the calixarenes reported in Chapter 2, these ligands and their anion and metal cation binding mode will provide preliminary studies about possible behaviour in solution, solid state and metal complexation in the more sophisticated calixarene type systems.[10] From previous work it might be expected that these kinds of ligands will form either contact ion pair or separated ion pair with metal salts in the solid state.[11] Previous work by Reinhoudt has also used a metal centre in a hydrogen bonding ligand as a direct anion binding site, supported by remote hydrogen bonding interactions.[12] A simple ligand related to the *meta* isomer shown in Figure **3.1** but based on a 2-pyridyl substituent and substituted by meta thiomethyl group has been selected for this study. The thioether is a soft Lewis base suitable for binding to silver(I) and the pyridyl nitrogen can donate a lone pair of electron to Lewis acid metal such as silver(I) to form coordination complex that may be stabilized by additional hydrogen bonding to counter anions.[13] The 2-pyridyl compounds prepared in this study are expected to differ from the analogous 3-isomers in their mode of interaction with cation / anion pairs in the way outlined in Figure **3.1**b.[14] In this chapter we report the synthesis and structures of simple ligands of this type including the remarkable polymorphism of

one example, along with metal complexes of **3.1** and **3.2**. Chapter 4 reports more detailed studies on metal-anion ion pair complexes of the 2-pyridyl ligand **3.3**.

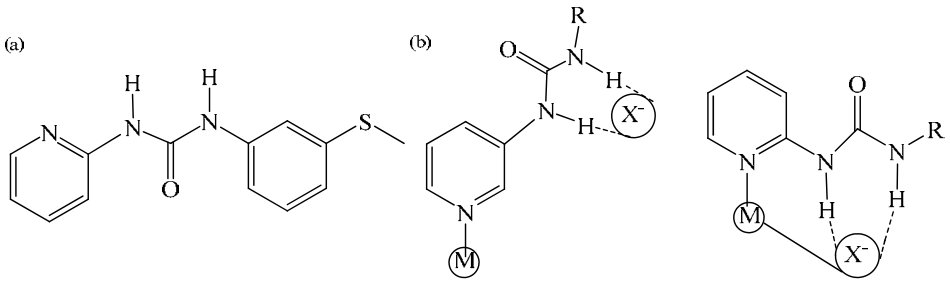

3.3 3-ureidopyridine motif separated ion pair 2-ureidopyridine motif contact ion pair

Figure 3.1 (a) Structure of ligand 3.3 and (b) comparison of the proposed ion-pair binding mode of ligand 3.1 with analogous 3-pyridyl urea complexes.

3.2 Ligand Synthesis and Structure

3.2.1 Ligand synthesis and structure of 3.1

The ligand 1-(3-methylsulfanylphenyl)-3-phenyl-urea (**3.1**) was synthesized by the reaction of aniline with 3-methylsulfanylphenyl isocyanate in chloroform solution resulting in 85% yield.[1] Previously, our group has reported that this compound binds silver metal through the thiomethyl functional group while simultaneously hydrogen bonding to anions.[13] The thioether is a soft base and hence facilitates metal binding remote from the urea anion-binding group.[1]

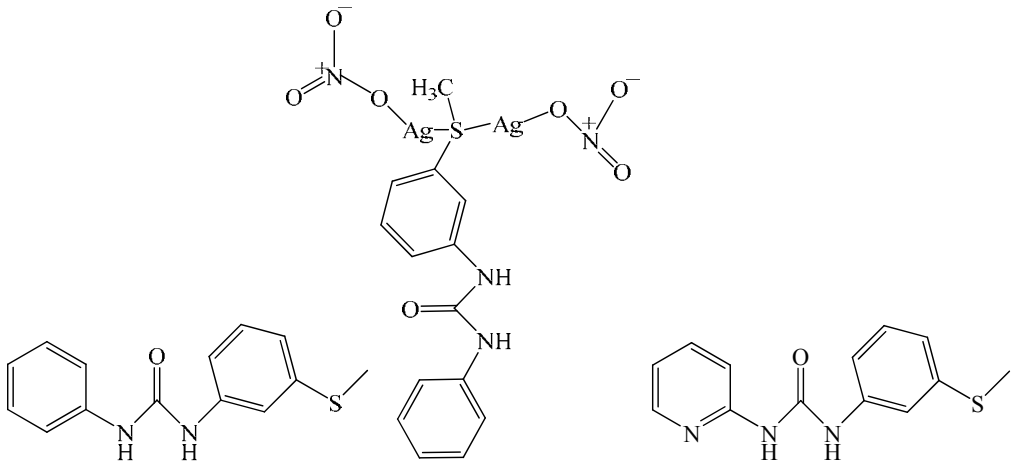

3.1 **3.2** **3.3**

The ligand **3.1** was characterized by the usual spectroscopic techniques (see experimental section) and results agreed well with the literature report.[15] A single crystal was obtained by slow evaporation of a THF: H_2O (1:1) solution of the ligand. The single crystal data confirms that the thiomethyl group is substituted at the *meta* position (Figure **3.2**) and is stabilized by intramolecular hydrogen bonding between the adjacent ring. The crystal structure adopts a herringbone type packing, in which thiomethyl substituents are trans to each other as shown in Figure **3.3**.

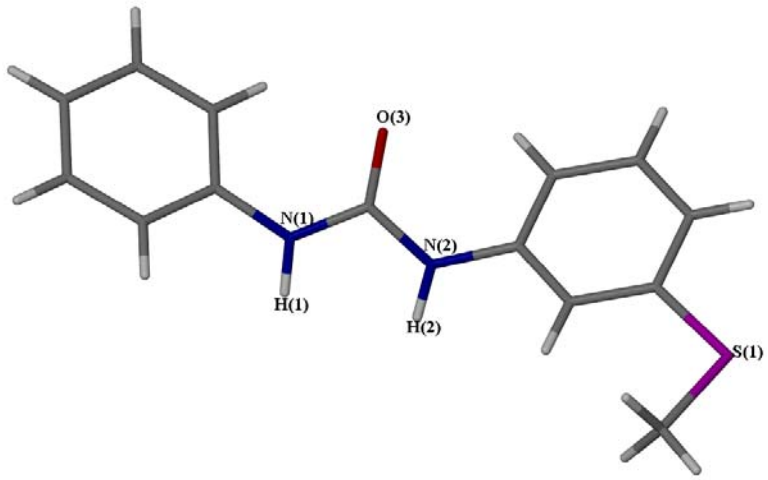

Figure 3.2 X-Ray molecular structure of ligand 3.1

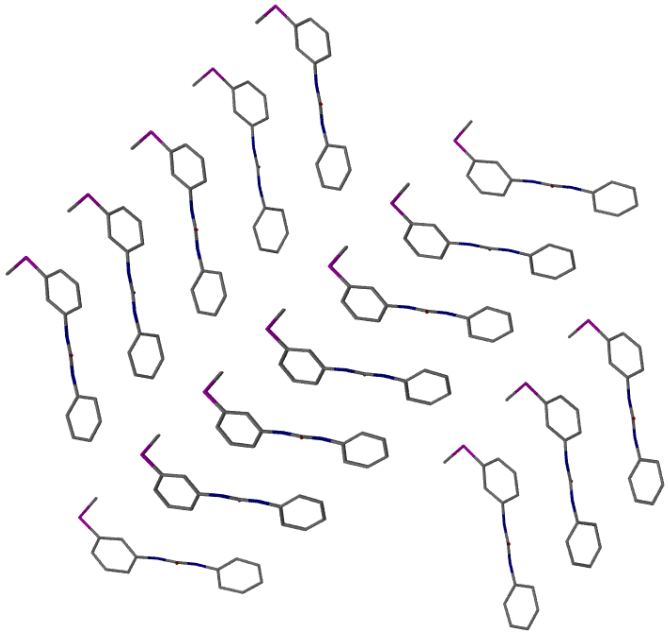

Figure 3.3 Crystal structure of 3.1 showing herringbone packing of phenyl sulphenyl urea complex along the *c*-axis

3.2.2 Reaction of ligand 3.1 with $AgNO_3$ 3.2

We are interested how the ligand binds with silver metal and others forming contact or separated ion pair in the solid state or in solution.[11] Reaction of equimolar amount of ligand **3.1** with silver(I) nitrate in presence of THF: H_2O (1:1 v/v) yields a compound of formula $[Ag_2(\mathbf{3.1})(NO_3)_2]$ (**3.2**) that has been characterized by X-ray crystallography. The asymmetric unit is comprised of one ligand **3.1**, two silver metal cations and two nitrate anion as shown in Figure **3.4**.

The crystal structure suggests that the two silver ions are both bound by sulphur (Ag - S1 = 2.534 – 2.605 Å) forming a wide angle ∟Ag1-S1-Ag2 = 130.40^o between them. The silver metal is further stabilized by interacting with the oxygen atoms of the nitrate anions Ag1–O1 = Ag2–O4 = (2.389 Å) contact angle of ∟Ag1 – O1 – N1 = 109.7 that is slightly more than ∟Ag2 – O4 – N2 = 106.77.

.

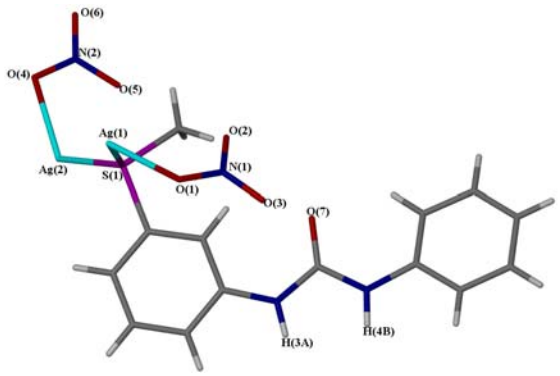

Figure 3.4 Solid state structures of 3.2

The nitrate anion is less basic compared to anions such as acetate and hence the anion does not deprotonate the urea groups. The result is a stable hydrogen bonded polymer.[16] The crystal structure packing along the *a*-axis gives a one dimensional coordination polymer stabilized through $R_2^2(8)$ type hydrogen bonding between the urea NH hydrogen atoms and the oxygen atoms of a nitrate anion H(3A)···O5 = 2.258 Å, N3(H3)···O5 = 3.022 Å as shown in Figure **3.5**a. In the crystal packing silver ion Ag(1) is also stabilized through the formation of Ag-π interactions (Ag1 - C11 = 2.549 Å) forming a trigonal coordination environment as shown in Figure **3.5** b.[17, 18]

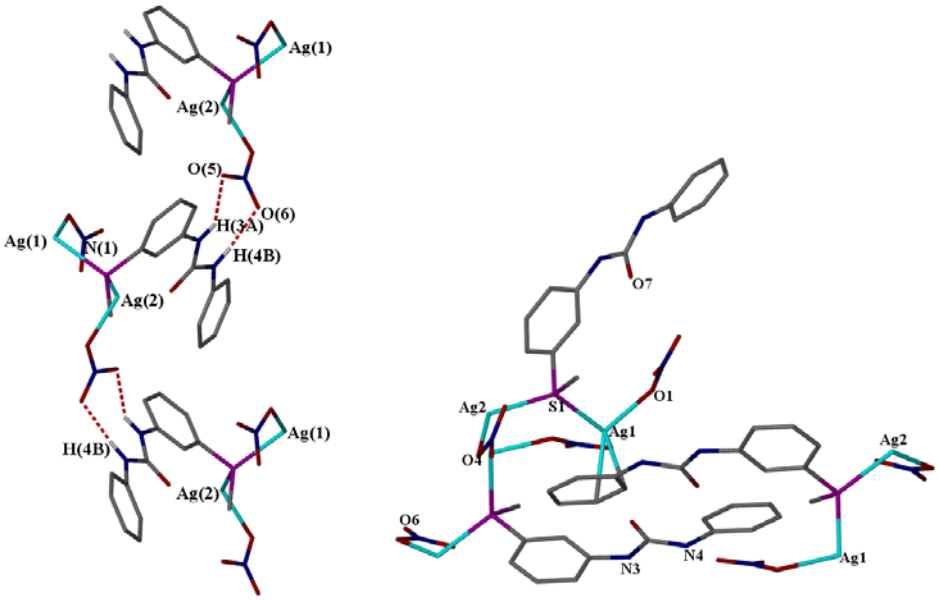

(a) (b)

Figure 3.5 (a) Crystal packing of 3.2 view along *a*-axis H(3A)···O5 = 2.258 Å, N3 (H3)···O5 = 3.022 Å, H(4B)···O6 = 2.048 Å, N4(H4)···O5 = 2.905 Å (b) Crystal packing view along the *b*-axis hydrogen atoms are removed for clarity C(11)–Ag(1) = 2.549 Å, C10–Ag(1) = 2.515 Å, Ag(2)–S(1) = 2.534 Å, Ag(1)–S(1) = 2.605 Å.

Table 3.1 Crystal Structure data for 3.1 – 3.2

Compound	**3.1**	**3.2**
Formula	C_{14} H_{13} N_2 O S	C_{14} H_{14} Ag_2 N_4 O_7 S
Formula weight	258.33	598.09
Crystal system	Orthorhombic	Orthorhombic
Space group	Pca21	P 2_1 2_1 2_1
a, Å	10.414(3)	7.7878(2)
b, Å	4.6028(12)	14.7768(2)
c, Å	26.087(7)	15.2048(3)
α, °	90.00(0)	90.00(0)
β, °	90.00(0)	90.00(0)
γ, °	90.00(0)	90.00(0)
Volume/$Å^3$	1250.5(5)	1749.75(9)
Z	4	4
ρ (calc.), mg/mm^3	1.372	2.270
μ, mm-1	0.247	2.407
F(000)	544	1168
Reflections collected	2614	18487
Independent refl., R_{int}	859, 0.0354	5085, 0.0325
N of parameters	163	253
Final R_1 [I>2σ(I)]	0.0673	0.0296
wR_2 (all data)	0.0887	0.0714
GOF on F^2	0.956	1.032

3.2.3 Synthesis and structure of ligand 3.3

Ligand **3.3** was obtained by reacting 2-amino pyridine with 3-sulfanylphenyl isocyanate in chloroform solvent resulting in 85% yield. The product was characterized by the usual methods including X-ray crystallography.[16] Surprisingly this work showed that ligand **3.3** exists in four polymorphic forms. The conditions under which each form was obtained during attempted crystallizations with metal salts are discussed in section 3.3. All four structures were determined by Dr. D. S. Yufit as part of this project. The structures are all very similar to one another. The molecular conformation in every case shows that these ligands are arranged an anti-conformation for the *N*,*N*′-disubstituted urea moiety that produces S(6) type hydrogen-bonded ring from the urea-NH to pyridyl nitrogen atom as is common with 2-pyridylureas.[19] The remaining carbonyl oxygen and urea NH group form an R_2^2 (8) intermolecular hydrogen bonded ring as shown in Figure **3.6**.[20] A detailed discussion of these four polymorphic structures is given in section 3.3. A follow-on and study of this interesting polymorphs by DSC and hot stage microscopy has been undertaken by Dr. Katharina Fucke within the group and will shortly be published as a full paper showing that it is the weak interactions, particularly of the CH···S type that govern the polymorphism of this system, not the strong hydrogen bonds.[21]

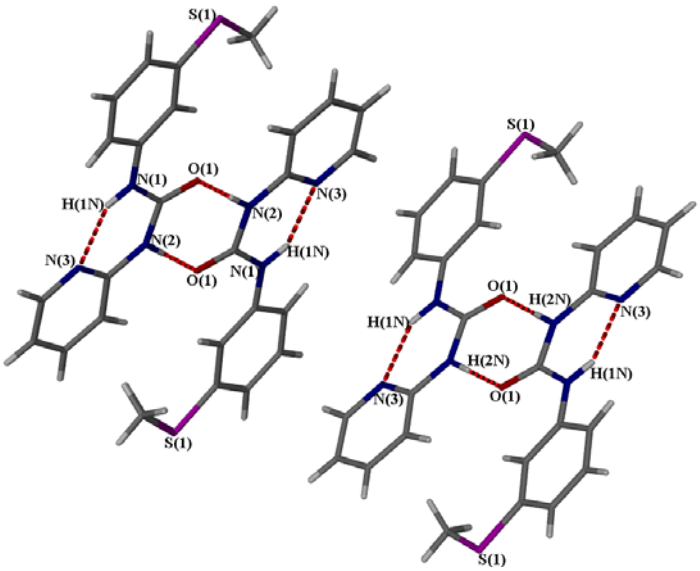

Figure 3.6 Conformation and hydrogen bonding of one representative polymorph of ligand 3.3 derived from X-ray crystallography.

3.2.4 Synthesis and structure of ligand 3.4

3-Amino pyridine reacts with 3-methylsulfnylphenyl isocyanate in chloroform solvent using the standard procedure to give ligand **3.4**. The compound was characterized by the usual methods as discussed in the experimental section, including X-ray crystallography.

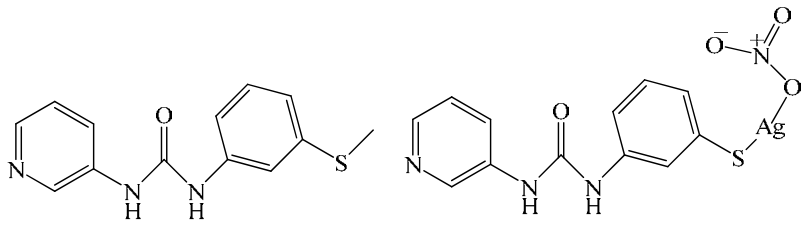

3.4 **3.5**

The crystal structure was obtained by slow evaporation of solvent that was subjected to X-ray crystallography. The asymmetric unit is comprised of a ligand in which the thiomethyl is substituted at meta position as shown in Figure **3.7**a. The crystal packing shows that the nitrogen atom of the pyridyl group forms an intermolecular hydrogen bond with a urea NH group in a $R_2^1(6)$ type hydrogen bonding fashion,[3] in which thiomethyl substituents are trans to each other as shown in Figure **3.7**b.[16]

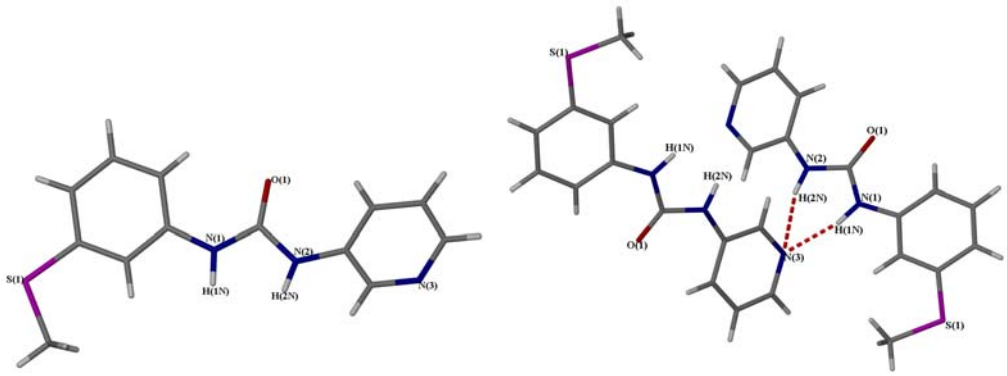

(a) (b)

Figure 3.7 (a) Asymmetric unit of ligand 3.4 (b) Crystal structure packing of ligand 3.4 along b-axis forming hydrogen-bond with pyridyl nitrogen, selected distances are H(2N)-···N3 = 2.60 Å, H(1N)-N(3) = 2.06 Å.

The crystal packing along the *a*-axis forms a herringbone pattern in which crossed ligands are oriented in up and down fashion as shown in Figure **3.8**. The crystal packing along the *b*-axis confirms formation of pair of ligand that has been arranged in a up and down fashion as shown in Figure **3.9**.

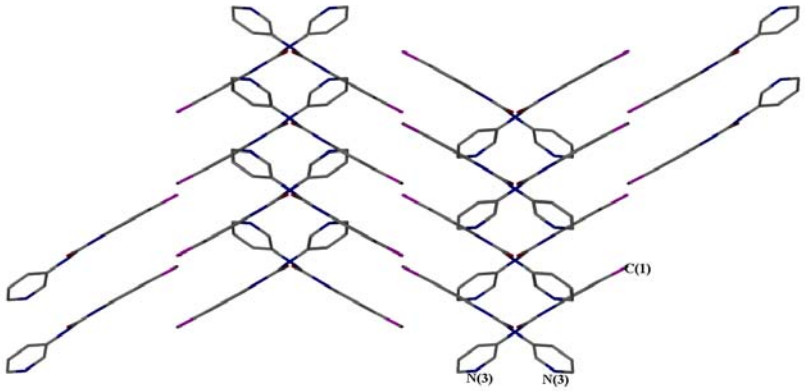

Figure 3.8 Herringbone packing of 3-pyridyl sulphanylphenylurea 3.4 along the *a*-axis hydrogen atoms are omitted for clarity.

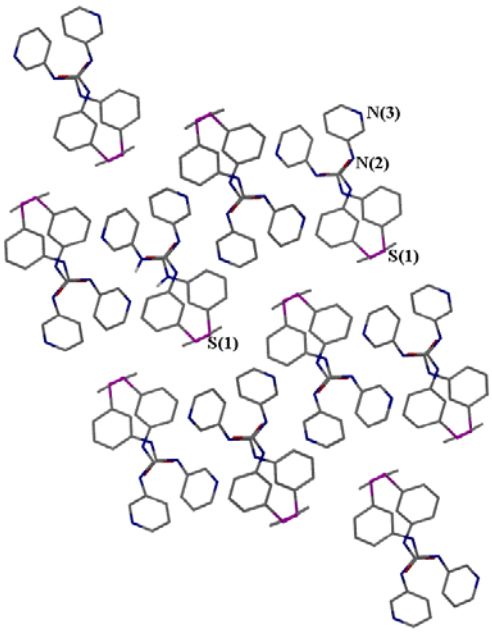

Figure 3.9 Crystal structure packing along b-axis forming a pair of ligand 3.4 (hydrogen atoms are omitted for clarity).

3.2.5 Reaction of ligand 3.4 with $AgNO_3$ 3.5

In the presence of binary metal salts of univalent cations (MX) ligand **3.4** should either form an N,S-bound coordination polymer or a discrete $M_2X_2L_2$ assembly, possibly templated by suitable anions. Because of the relatively soft donor ability of the thioether, we expect that the pyridyl urea bound MX should be stable in solution and fragments should dimerise or assemble *via* labile metal-sulfur interactions.[1]

The ligand **3.4** was reacted with silver nitrate in a mixture of THF: H_2O: CH_3CN (3: 1: 1 v/v) resulted in a formation of single crystals of [Ag(**3.4**)NO_3](**3.5**). The asymmetric unit is comprised of ligand **3.4**, silver metal and nitrate anion, in which both the sulphur and nitrogen atoms from different ligands coordinate to the metal centre. The Ag-S bond length (S(1)-Ag(1) = 2.418 Å) is shorter that those reported previously.[16] The silver ion also bonds with an oxygen atom of the nitrate anion (Ag(1)-O(2) = 2.435 Å) with a wide angle of 120.68^o (S-Ag-O) as shown in Figure **3.10**a. The crystal packing shows that the oxygen atoms of the nitrate anion form an $R_2^2(8)$ type hydrogen bonding motif (Figure **3.10**b) in which the thiomethyl substituents and nitrate anion are opposite each other.[22] The crystal packing along the *a*-axis confirms that the silver metal adopts a distorted trigonal geometry.

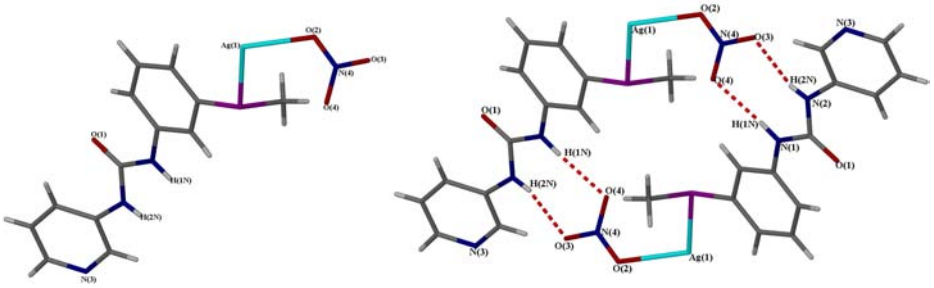

(a) (b)

Figure 3.10 (a) Asymmetric unit of 3.5 selected bond distances are Ag1-S1 = 2.418 Å, Ag1-O1 = 2.435 Å (b) Crystal structure packing along c-axis forming a dimmer with 3.5 selected bond distances are H1N-O4 = 2.154 Å, H2N-O3 = 2.129 Å

The crystal structure comprises a one dimensional coordinated polymer chain in which nitrate and thiomethyl substituents are trans to each other linked by the $R_2^2(8)$ type hydrogen bonding between the urea NH protons and the oxygen atoms of the nitrate anion as shown in Figure **3.11**.[23]

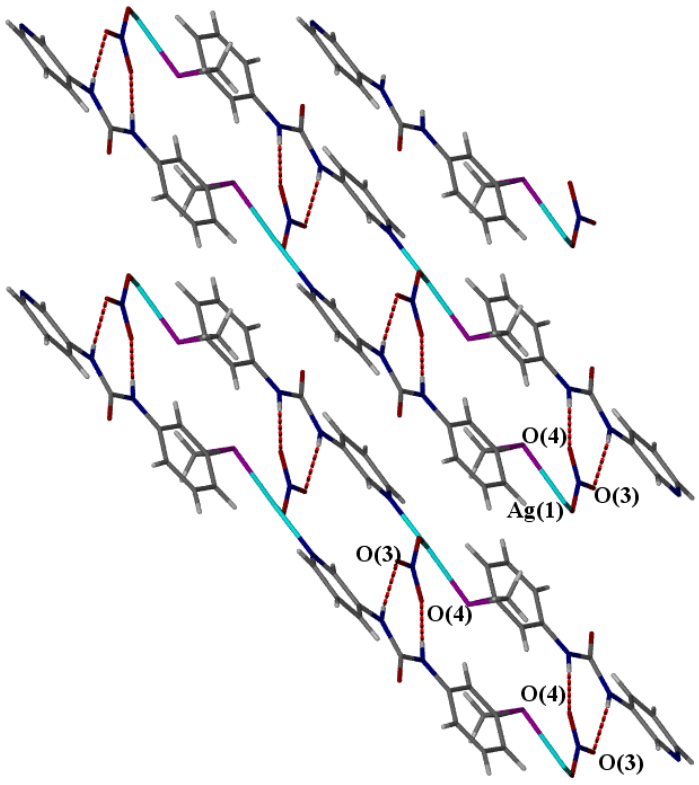

Figure 3.11 Crystal structure packing of 3.5 along a-axis forming one coordination polymer chain, selected distances are H1N-O4 = 2.154 Å, H2N-O3 = 2.129 Å.

3.2.6 Synthesis and structure of ligand 3.6

2-Aminopyridine was reacted with 3-sulphanylphenyl isothiocyanate in chloroform solvent to give the thiourea derivative **3.6** that has been characterized by all of the usual spectroscopic techniques (see experimental section).[16] The thiourea derivative should result in due to increased acidity of the NH protons compared to urea (thiourea pK_a = 21.0; urea pK_a = 26.9) and hence anion complexation is expected to be stronger.[24, 25]

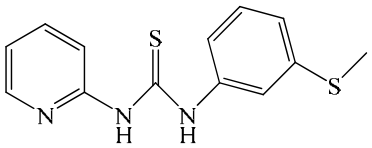

3.6

A single crystal of **3.6** was obtained by slow evaporation of chloroform solvent. The molecular conformation of single crystal suggests that the urea NH protons are anti in orientation forming an S(6) type hydrogen bonding with pyridyl nitrogen as reported for related 2-ureidopyridine ligands.[19] The thiomethyl groups are substituted in an up and down fashion in crystal structure packing as shown in Figure **3.12**a and arranged parallel to the *c*-axis direction as shown in Figure **3.12**b.[16] No metal complexes of this ligand were isolated.

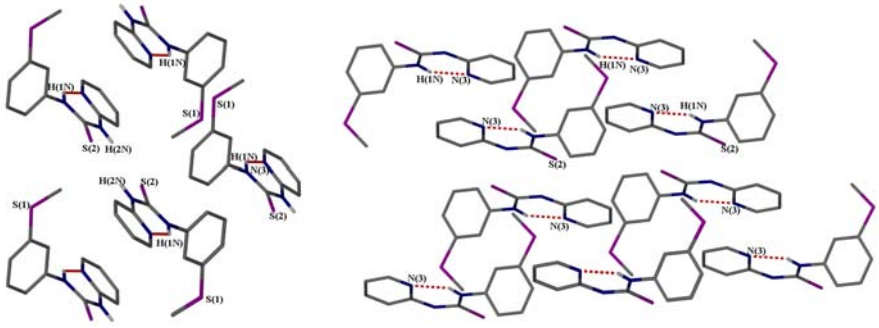

(a) (b)

Figure 3.12 (a) Crystal structure packing along a axis N3-H1N = 2.014 Å (b) crystal structure packing along *c*-axis

Table 3.2 Crystal Structure data for 3.4 – 3.6

Compound	**3.4**	**3.5**	**3.6**
Formula	C_{13} H_{13} N_3 O S	C_{13} H_{13} N_3 O S, Ag, NO_3	$C_{13}H_{13}N_3S_2$
Formula weight	259.32	429.20	275.38
Crystal system	Orthorhombic	Triclinic	Triclinic
Space group	P b c a	P -1	P-1
a, Å	12.1422(4)	8.3419(2)	9.0775(2)
b, Å	8.0387(6)	9.8566(3)	9.3132(2)
c, Å	25.2301(10)	9.9195(3)	9.4360
α, °	90.00(2)	85.729(10)	102.78(2)
β, °	90.00(2)°	81.028(10)	103.25(2)
γ, °	90.00(2)°	65.908(10)	114.64
Volume/$Å^3$	2462.6(2)	735.40(4)	659.03
Z	8	2	2
ρ (calc.), mg/mm^3	1.399	1.938	1.388
μ, mm-1	0.254	1.539	0.389
F(000)	1088	428	288
Reflections collected	16797	9616	5575
Independent refl., R_{int}	0.0395	0.0288	0.0424
N of parameters	215	260	215
Final R_1 [I>2σ(I)]	0.0751	0.0388	0.0535
wR_2 (all data)	0.1266	0.0760	0.1169
GOF on F2	1.064	0.962	1.030

3.3 Polymorphism of 2-Ureidopyridine Ligand 3.3

The ligand 2-ureidopyridine ligand 3.3 exists in four polymorphic forms which were obtained on crystallization from various solvents in the presence of metal salts according to the conditions shown in Table 3.3. These polymorphs adopt very similar hydrogen bonding patterns in which the N,N′-disubstituted urea groups are oriented in trans arrangement, that has been stabilized through forming S(6) type hydrogen bonding[26] while the remaining urea NH and carbonyl oxygen is forming $R_2^2(8)$ type interaction. In three polymorphic forms (forms I - III) the thiomethyl groups adopt a trans type mutual disposition about the central $R_2^2(8)$ motif.[27] The remaining polymorph, designated IVº, is a conformational polymorph with the thiomethyl substituent in a syn arrangement. Subsequent DSC measurements by Dr. Katharina Fucke show that this form is the most thermodynamically stable at all temperatures.21 Her measurements indicate that the stability of polymorphic form can be described as I< III< II <IV.

Table 3.3 Crystallization setup for the different modifications using salts.

Form	I	II	III	IVº
Solvent (1 mL)	THF	THF	THF	THF
Salt	$AgCF_3SO_3$	$AgCF_3SO_3$	$AgNO_3$	$AgMeCO_2$
Solvent for salt (1 mL)	THF	THF	H_2O/EtOH (1:1)	H_2O/EtOH (1:1)
Evaporation time	10 days	15 days	20 days	10 days

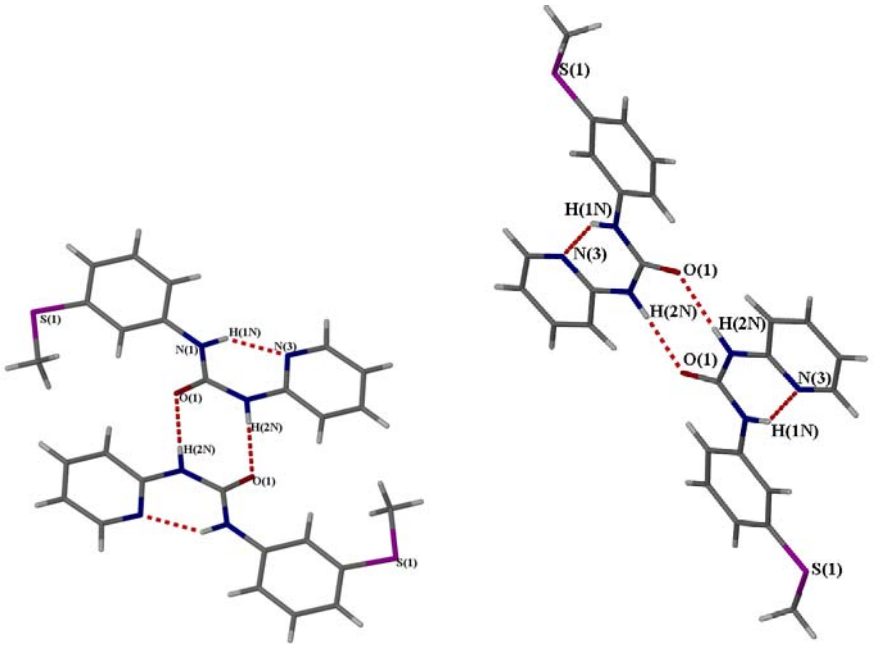

(a) (b)

Figure 3.13 Crystal structure packing along *b*-axis of polymorphs I – III. Selected distances of polymorph I O1 – H2N = 3.933 Å, N2 – O1 = 3.492 Å, N3 – H1N = 5.263 Å (b) Crystal structure packing along *b*-axis of polymorph IV° selected distances O1···H2N = 1.958 Å, N2···O1 = 1.958 Å, N3···H1N = 1.994 Å

The thiomethyl substituents having almost same angle ranging from ∟C2 - S1 - C1 (103.2 -104.0) but the different forms show a variety of different modes of CH···S hydrogen bonding. Polymorphs I, II and III are closely related to forms I and II exhibiting pyridyl CH···S interactions, while an aryl CH···S interaction dominates in form III. The conformational polymorph, form IV°, is the odd one out, exhibiting interesting hydrogen bonded ring made up of two face-to-face SCH_3 groups based on H2CH···S interactions (Figure **3.14**). This case highlights the importance of overall crystal packing considerations and weak interactions in the crystal in determining solid state structure, as opposed to the more obvious strong hydrogen bonds, as suggested by Nangia, Etter and Desiraju.[27-29] All these polymorphic forms having strong hydrogen bonding that results in dimer formation.

Table 3.4 polymorphic forms of ligand 3.3

Compound	**I**	**II**	**III**	**IV**
Formula	$C_{13}H_{13}N_3OS$	$C_{13}H_{13}N_3OS$	$C_{13}H_{13}N_3OS$	$C_{13}H_{13}N_3OS$
Formula weight	259.32	259.32	259.32	259.32
Crystal system	Monoclinic	Monoclinic	Orthorhombic	Monoclinic
Space group	*C*2/*c*	$P2_1/n$	$Pca2_1$	$P2_1/n$
a, Å	26.8102(7)	5.4862(3)	17.2320(14)	11.5968(4)
b, Å	5.4333(2)	13.9388(8)	5.4830(4)	5.3174(2)
c, Å	17.7090(5)	16.1959(9)	26.478(2)	20.2874(8)
α, °	90	90	90	90
β, °	107.09	93.59	90	93.45(2)
γ, °	90	90	90	90
Volume/$Å^3$	2465.79(13)	1236.08(12)	2501.7(3)	1248.75(8)
Z	8	4	8	4
ρ (calc.), mg/mm^3	1.397	1.393	1.377	1.379
μ, mm-1	0.253	0.253	0.250	0.250
F(000)	1088	544	1088	544
Reflections collected	15733	9188	16248	9592
R_{int}	0.0378	0.0393	0.1134	0.0314
No. of parameters	215	215	404	215
Final R_1 [I>2σ(I)]	0.0576	0.0640	0.0977	.039
wR_2 (all data)	0.1180	0.1153	0.1068	0.1257
GOF on F^2	1.020	1.062	1.069	1.039

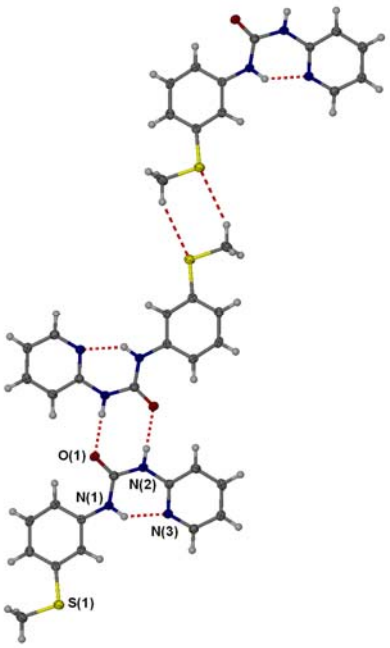

Figure 3.14 Conformational polymorph form IV° showing the $R_2^2(6)$ CH···S motif.

3.4 Experimental

3.4.1 1-(3-Methylsulfanyl-phenyl)-3-phenyl-urea (3.1): Aniline (4.00 g, 43.0 x 10^{-3} mol) was reacted with 3-sulphanylphenyl isocyanate (6.97g, 43.0 x 10^{-3} mol) in 50 ml of chloroform solvent at room temperature resulting in a formation of white solid. The product was isolated by filtration and washed with 4 ml of diethyl ether to give 7.00 g (89 %) of the product. ^{1}H-NMR ($CDCl_3$): 7.35 (bs, 1H, NH), 7.34 (bs, 1H, NH), 7.31 (1 H, t, Ar, J = 4 Hz), 7.25 -7.21 (2 H, m, Ar), 7.10 (2 H, d, ArH, J = 8 Hz), 7.01 (2 H, d, ArH, J = 8 Hz), 2.45 (3 H, s, CH_3). IR (ν /cm^{-1}) 1740 (s, C=O), 3314 (br, NH). M.p. 158 ^{0}C. Anal. Calcd (%) for $C_{14}H_{14}N_2OS$: C, 64.86; H, 5.83; N, 10.79. Found (%) C, 64.84; H, 5.73; N, 9.67.

3.4.2 1-(3-Methylsulfanyl-phenyl)-3-pyridin-2-yl-urea (3.3): 2-Amino pyridine (2.84 g, 30.2 mmol) was reacted with 3-sulphanylphenyl isocyanate (4.95 g, 30.2 x 10^{-3} mol) in 25 ml of chloroform solvent at room temperature resulting in a formation of white solid. The product was isolated by filtration and washed with small amount of diethyl ether to give 7.00 g (89 %) of the product. ^{1}H-NMR (DMSO-d_6): 10.55 (bs, 1H, NH), 9.46 (bs, 1H, NH), 8.29 (1 H, d, PyH, *J* = 5.2 Hz), 7.73 (1 H, dt, PyH, 1.6 & 7.2 Hz), 7.51 (2 H, m, ArH), 7.24 (2 H, m, ArH), 7.01 (1 H, dd, PyH, *J* = 4.8 & 6.4 Hz), 6.91 (1 H, dt, PyH, *J* = 3.2 & 6.0 Hz), 2.45 (3 H, s, CH_3). IR (ν /cm^{-1}) 1683 (s, C=O), 3214 (br, NH). M.p. 141 ^{0}C. Anal. Calcd (%) for $C_{13}H_{13}N_3OS$: C, 60.21; H, 5.05, N, 16.20. Found (%) C, 60.17; H, 5.07; N, 16.03.

3.4.3 1-(3-Methylsulfanyl-phenyl)-3-pyridin-2-yl-thiourea (3.6): 2-Amino pyridine (2.58 g, 27.5 x 10^{-3} mol) was reacted with 3-sulphanylphenyl isothiocyanate (5.00 g, 27.5 x 10^{-3} mol) in 100 ml of dichlorometane solvent at room temperature resulting in a formation of white solid. The product was isolated by filtration and washed with small amount of diethyl ether to give 2.65 g (36 %) of the product. ^{1}H-NMR (400 MHz, $CDCl_3$): 13.81 (s, 1H, NH), 9.77 (s, 1H, NH), 8.24 (d, 1H, *J* = 8 Hz, Ar), 7.70 (d, 1H, Ar, *J* = 1.6 Hz), 7.67 (m, 1H, Ar), 7.46 (d, 1H, Ar, *J* = 8 Hz), 7.36 (t, 1H, Ar, *J* = 8, 16 Hz), 7.17 (d, 1H, Ar), 7.05 (s, 1H, Ar), 7.01 (m, 1H, Ar) and 2.45 (s, 3H, CH_3). ^{13}C{H}-NMR (400 MHz, $CDCl_3$): 145.81 (s, Ar), 138.97 (s, Ar), 128.55 (s, Ar), 124.20 (s, Ar), 122.72 (s, Ar), 121.71 (s, Ar), 118.35 (s, Ar), 112.79 (s, Ar) and 15.93 (s, CH_3). IR (ν /cm^{-1}) 1599 (s, C=S), 3172.09 (br, NH). M.p. 127 ^{0}C. Anal.

Calcd (%) for $C_{13}H_{13}N_3S_2$: C, 56.70; H, 4.76, N, 45.26. Found (%) C, 56.64; H, 4.78; N, 15.38.

3.5 References:

1. J. M. Russell, A. D. M. Parker, I. Radosavljevic-Evans, J. A. K. Howard and J. W. Steed, *Cryst. Eng. Comm.*, 2006, **8**, 119-122.
2. J. M. Russell, A. D. M. Parker, I. Radosavljevic-Evans, J. A. K. Howard and J. W. Steed, *Cryst. Eng. Comm.*, 2006, **8,** 125–127.
3. D. R. Turner, B. Smith, A. E. Goeta, I. R. Evans, D. A. Tocher, J. A. K. Howard and J. W. Steed, *Cryst. Eng. Comm.*, 2004, **6**, 633-641.
4. D. R. Turner, B. Smith, E. C. Spencer, A. E. Goeta, I. R. Evans, D. A. Tocher, J. A. K. Howard and J. W. Steed, *New J. Chem.*, 2005, **29**, 90-98.
5. P. Byrne, D. R. Turner, G. O. Lloyd, N. Clarke and J. W. Steed, *Crystal Growth & Design*, 2008, **8**, 3335-3344.
6. L. J. Prins, D. N. Reinhoudt and P. Timmerman, *Angew. Chem. Int. Ed.*, 2001, **40**, 2383-2426.
7. D. R. Turner, E. C. Spencer, J. A. K. Howard, D. A. Tocher and J. W. Steed, *Chem. Commun.*, 2004, **6,** 1352-1353.
8. S. M. Bromidge, S. Dabbs, D. T. Davies, S. Davies, D. M. Duckworth, I. T. Forbes, A. Gadre, P. Ham, G. E. Jones, F. D. King, D. V. Saunders, K. M. Thewlis, D. Vyas, T. P. Blackburn, V. Holland, G. A. Kennett, G. J. Riley and M. D. Wood, *Bioorg. Med. Chem.*, 1999, **7**, 2767-2773.
9. P. A. Gale, M. E. Light, B. McNally, K. Navakhun, K. E. Sliwinski and B. D. Smith, *Chem. Commun.*, 2005, **7,** 3773-3775.
10. J. W. Steed and K. J. Wallace, in *Advances in Supramolecular Chemistry*, 2003, vol. 5.
11. M. J. Deetz, M. Shang and B. D. Smith, *J. Am. Chem. Soc.*, 2000, **122**, 6201-6207.
12. D. M. Rudkevich, Z. Brzozka, M. Palys, H. C. Visser, W. Verboom and D. N. Reinhoudt, *Angew. Chem., Int. Ed.*, 1994, **33**, 467-468.
13. J. M. Russell, A. D. M. Parker, I. Radosavljevic-Evans, J. A. K. Howard and J. W. Steed, *Chem. Commun.*, 2006, **8**, 269-271.
14. J. M. Mahoney, A. M. Beatty and B. D. Smith, *J. Am. Chem. Soc.*, 2001, **123**, 5847-5848.
15. J. M. Russell, A. D. M. Parker, I. Radosavljevie-Evans, J. A. K. Howard and J. W. Steed, *Cryst. Eng. Commun.*, 2006, 119 - 122..

16. N. Qureshi, Dmitry S. Yufit, Judith A. K. Howard and Jonathan W. Steed, *Dalton Trans.*, 2009, **29**, 5708 - 5714.
17. C. G. Claessens and J. F. Stoddart, *J. Phys. Org. Chem,*. 1997, **10**, 254-272.
18. C. A. Hunter and J. K. M. Sanders, *J. Am. Chem. Soc.*, 1990, **112**, 5525-5534.
19. J. T. Lenthall, K. M. Anderson, S. J. Smith and J. W. Steed, *Crystal Growth & Design*, 2007, **7**, 1858-1862.
20. L. S. Reddy, S. Basavoju, V. R. Vangala and A. Nangia, *Crystal Growth & Design*, 2006, **6**, 161-173.
21. N. Qureshi, K. Fucke, D. S. Yufit, J. A. K. Howard and J. W. Steed, *Cryst. Growth & Des*. accepted. .
22. P. R. Schreiner, *Chem. Soc. Rev.*, 2003, **32**, 289-296.
23. L. Applegarth, A. E. Goeta and J. W. Steed, *Chem. Commun.*, 2005, **7,** 2405-2406.
24. R. Custelcean, *Chem. Commun.*, 2008, **9,** 295-307.
25. M. D. Hollingsworth and K. D. M. Harris, in *Comprehensive Supramolecular Chemistry*, eds. J. L. Atwood, J. E. D. Davies, D. D. MacNicol and F. Vögtle, Pergamon, Oxford, Edn., 1996, **6,** 177-237.
26. J. T. Lenthall, K. M. Anderson, S. J. Smith and J. W. Steed, *Crystal Growth & Design*, 2007, **7**, 1858–1862.
27. M. C. Etter, *Acc. Chem. Res*, 1990, **23**, 120-126.
28. N. J. Babu, A. Nangia, *Cryst. Growth. Des.*, 2006, **6**, 1995 - 1999.
29. G. R. Desiraju and T. Steiner, *The Weak Hydrogen Bond*, OUP/IUPAC, Oxford, 1999.

Chapter 4: Ion-pair binding by mixed N,S-donor 2-ureidopyridine ligands

4.1 Aim and targets

Metal fragments are increasingly being used in the construction of hosts for anions and neutral molecules. Metals act as a Lewis acidic binding sites or as sensing units, carry positive charge and can increase the strength of non–covalent interactions such as hydrogen bonds.[1] As discussed in section **1.4** recent work by the groups of Gale,[2] Loeb,[3, 4] and Steed[5-7] have elegantly shown that simple coordination compounds containing a combination of a cationic metal centre and monodendate ligands featuring hydrogen bond donor groups can be used as hosts for selective binding of particular counter anions. Simple compounds based on 3-aminopyridine,[5] 3-(aminomethyl)pyridine and 3-ureidopyridine[8, 9] type ligands have shown a range of separated ion pair binding behaviour. In particular previous work by the Steed group has resulted in the isolation of compounds of the type shown in Figure **4.1** in which simple 3-pyridyl urea-based ligands interact simultaneously with labile Ag(I) ions and nitrate counter ions. Related compounds have also been discussed in the previous chapter. The geometry of the ligand is such that the metal and its accompanying counter ion are bound as a separated ion pair.[5, 7] Such systems in which the cation and anion ion are far apart are in contrast to Smith's macrobicycle **1.82**, **1.83** which form a contact ion pair with alkali metal halides[10-15] and related work by Wilcox.[16] Previous work by Reinhoudt has also used a metal centre as a direct anion binding site, supported by remote hydrogen bonding interactions.[17] A simple ligand related to the meta isomers shown in Figure **4.1** but based on 2-pyridyl and substituted by meta thiomethyl group has been selected for this study, as described in the previous chapter. The thioether is a soft Lewis base suitable for binding to silver(I) and the pyridyl nitrogen atom can donate lone pair of electron to a Lewis acidic metal centre to form coordination complexes with silver that may be stabilized by additional hydrogen bonding to counter anions. The choice of ligand is particularly relevant as there has been potent and selective response reported for 2-pyridyl urea thiomethyl ligand, against,[18] while others have reported simple urea based receptors as mimics for prodigiosins,[19, 20] as well as in the context of anion binding, [21, 22] gels[23] and biomimetic chloride transport.[24] The 2-pyridyl compounds prepared in this study (reported in Chapter

3) are expected to differ in their mode of interaction with cation / anion pairs in the way outlined in Figure **4.1**b.

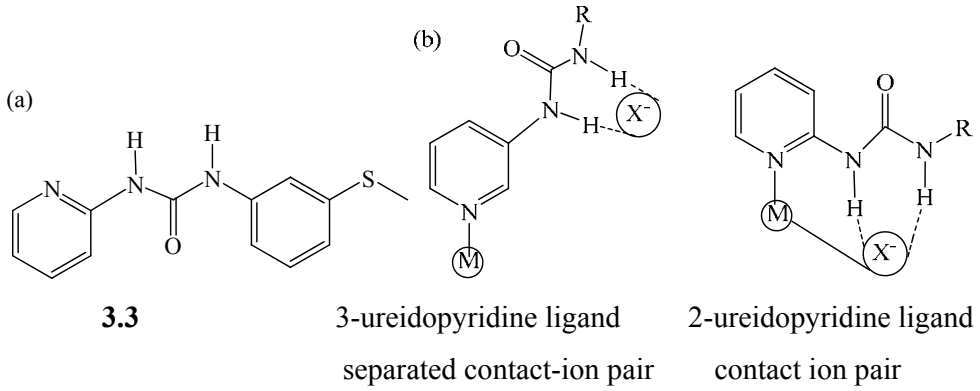

Figure 4.1 (a) Structure of ligand 3.3 and (b) comparison of the proposed ion-pair binding mode of 3.3 with analogous 3-pyridyl urea complexes.

4.2 Structures of Silver Complexes

4.2.1 Structure of [Ag (3.3)](CH_3CO_2) 4.1

The ligand **3.3** was mixed with AgX (X = OAc, NO_3, PF_6 and BF_4) in a range of solvents to prepare silver complexes with various counter anions. Colourless single crystals of each of the products were subjected to analysis by X-ray diffraction. The solid state structure confirms a 1: 1 complex of formula [Ag(**3.3**)](CH_3CO_2) **4.1**.Crystallisation vials were completely wrapped with aluminium foil in order to exclude light due to photosensitivity of silver(I); leaving the mixture to evaporate slowly.

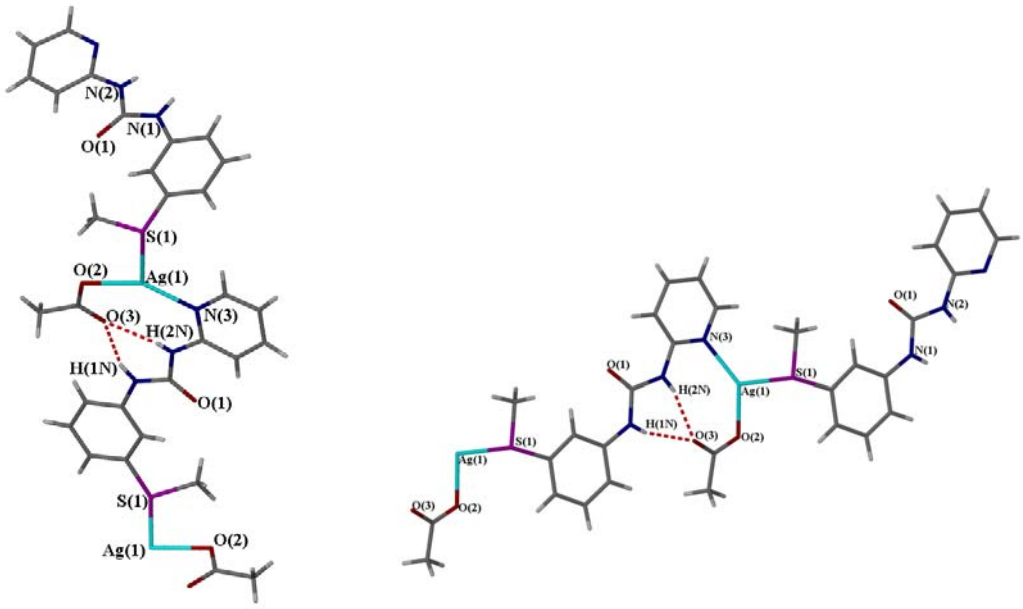

(a) (b)

Figure 4.2 (a) Silver (I) acetate contact ion pair binding motif in two polymorphs of [Ag (3.3)] (CH_3CO_2) (4.1) (a) monoclinic form A and selected bond lengths, form A: Ag(1) N(3) 2.254(2), Ag(1) O(2) 2.280(2), Ag(1) S(1) 2.5905(7). Selected hydrogen bond distances, form A: N(1) O(3) 2.759(3), N(1) O(3) 2.759(3); (b) form B Ag(1) O(2) 2.2357(15), Ag(1) N(3) 2.2383(15), Ag(1) S(1) 2.5828(5) Å. Selected hydrogen bond distances, form B: N(1) O(3) 2.819(2), N(2) O(3) 2.857(2) Å.

The acetate complex **4.1** was obtained from slightly different solvent mixtures as two polymorphs (monoclinic and triclinic forms A and B, respectively). In both polymorphs, the anion is simultaneously bound to urea hydrogen bonding contact ion pair binding. In both of these polymorphs silver metal is bound the pyridyl nitrogen atom and the sulphur atom of an adjacent ligand as well as an oxygen atom of the acetate counter anion in an irregular fashion. There is an $R_2^1(6)$ type hydrogen bonding motif involving the urea group and acetate ligand in both of these polymorphs of the contact ion pair type illustrated in Figure **4.1**b.[25] In both polymorphs the silver–sulphur distances are almost same (S–Ag, ca. 2.58 Å), but there are additional argenophilic (Ag…Ag, 3.013 Å) interactions observed in polymorph B,[26] which are longer than 2.886 Å found in metallic Ag,[27] but shorter than the sum of the van der Waals radi of Ag atoms. This may suggest the existence of weaker metal bonding between Ag(I) ions. Both of these polymorphs form sheet–like structures as part of a one dimensional coordination polymer. There is some difference in the orientation of the thiomethyl substituents in the two forms, which form a zig–zig like polymeric chain. In polymorph A, the thiomethyl substituents are antiparallel in the one dimensional polymeric chain, while in polymorph B the thiomethyl substituents are parallel. The hydrogen bond distance is slightly longer in polymorph B as shown in Figure **4.2**,and polymorph B is less dense than polymorph A (1.78 g cm^{-3} *vs.* 1.81 g cm^{-3}), hence it may be that polymorph B is a kinetic form, while form A is the stable polymorph. The crystal packing diagram of these polymorphs along the *c*-axis shows that polymorph A comprises a bent polymeric chain arranged in up and downward orientation while polymorph B forms a more linear polymeric chain. In this orientation the thiomethyl, acetate and nitrogen atom of the pyridyl group are orientated in a trans manner as shown in Figure **4.3**.

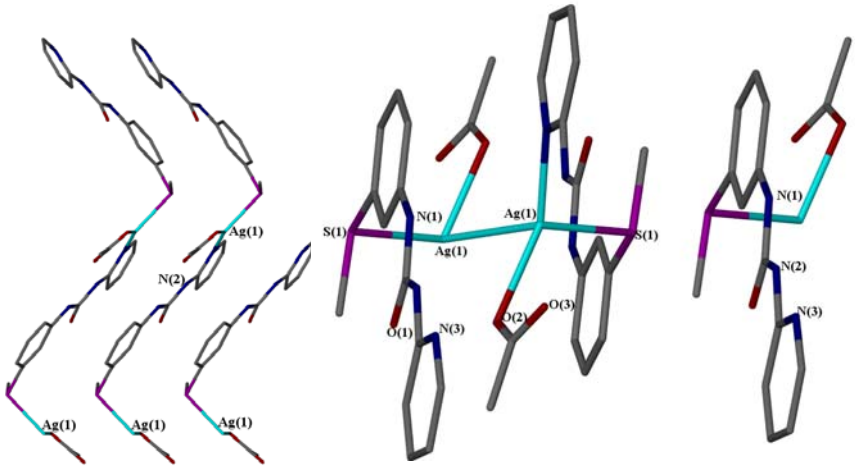

(a) (b)

Figure 4.3 (a) Crystal structures packing of polymorph A forming bent like structure (b) form B having linear polymeric chain.

.

4.2.2 Structure of [Ag (3.3)](NO$_3$) 4.2

Ligand **3.3** was dissolved in THF and added to a solution of silver nitrate in water (1:1 v/v) and the vial was completely wrapped with aluminium foil in order to exclude light due to the photosensitivity of silver metal. The mixture was left to slowly evaporate for five days resulting in a formation of colourless single crystals. The X-ray crystal structure of the nitrate complex [Ag (**3.3**)] (NO_3) **4.2** is based on an asymmetric unit comprised of ligand **3.3** and a silver nitrate contact ion pair, in which the sulphur and pyridyl nitrogen atoms are bonded with the silver metal ion, which is further and stabilized by forming bond with an oxygen atom of the nitrate anion as shown in Figure **4.4**a. The remaining two oxygen atoms of the nitrate anions are form an $R_2^2(8)$ hydrogen bonding motif as shown in Figure **4.4**b.

The silver nitrate complex **4.2** exhibits a very similar ion pair binding motif to that found for **4.1** consistent with the similarity of the nitrate and acetate ions. The silver nitrate metal is much less basic than acetate, however, and hence the Ag–O anion distances are much longer than in the acetate complex structures and the single short Ag–O_2CCH_3 bond of *ca.* 2.23 Å is replaced by two much longer Ag–ONO_2 contacts each *ca.* 2.5 Å long. As the nitrate is able to coordinate on all the three edges also means that the extended geometry of the structure is rather different. While it is again a coordination

polymer, the structure is based on an infinite network of dimeric[28] units linked together by bridging nitrate anions and Ag–S interactions. The coordination geometry of the Ag(I) centres is thus distorted tetrahedral rather than distorted trigonal (Figure **4.5**)

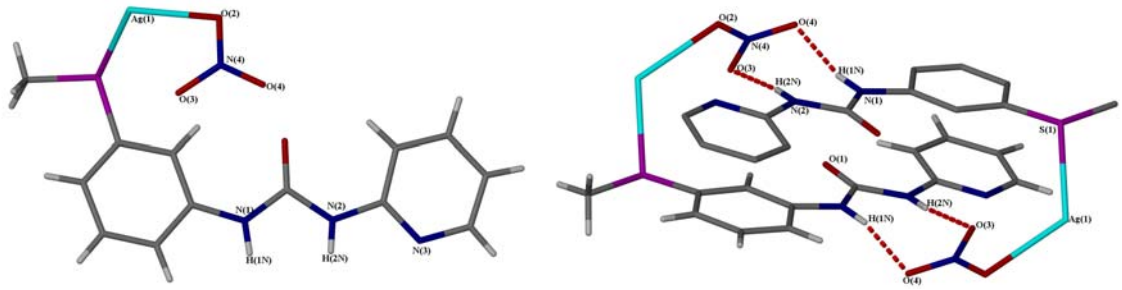

(a) (b)

Figure 4.4 (a) Asymmetric unit of crystal structure 4.2 (b) crystal structure showing hydrogen bonding in an $R_2^2(8)$ fashion selected hydrogen bond distances are H1N1-O4 = 2.116 Å, H2N2- O3 = 2.133 Å.

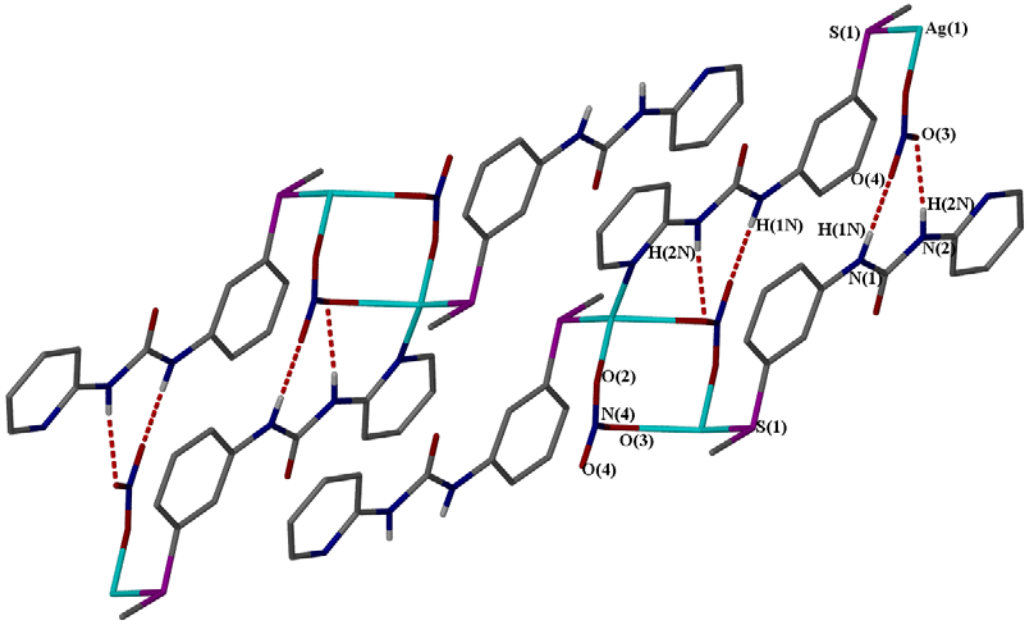

Figure 4.5 Silver(I) nitrate contact ion pair binding motif in [Ag(3.3)](NO_3) (4.2) (a) extended structure. Selected bond lengths: Ag N(3) 2.2636(16), Ag(1) S(1) 2.4674(5), Ag(1) O(2) 2.4957(17), Ag(1) O(3) 2.5789(15) Å. Selected hydrogen bond distances: N(1) O(4) 2.920(2), N(2) O(3) 2.946(2) Å.

4.2.3 Structure of [Ag(3.3)](BF$_4$) 4.3

Ligand **3.3** was dissolved in THF and added to a solution of silver tetraflouoroborate in water (1:1 v/v) and the vial was completely wrapped. The mixture was left to slowly evaporate for five days resulting in a formation of colourless single crystals. Efforts were made to make a 1:1 complex, but final product turned out to be 1: 4 metal to ligand complex containing THF solvent, [Ag(κ-*S*-**3.3**)$_4$](BF$_4$)·thf (**4.3**) Decomposition of the silver(I) to give silver metal in the vial was observed over time and is likely responsible for the 1:4 stoichiometry, as AgBF$_4$ is hygroscopic and photosensitive in nature. The BF_4^- anion poor hydrogen bond acceptor and hence the urea groups do not bond to the anion; their coordination is satisfied with the soft sulphur atoms by forming 1: 4 complexes with silver metal. The silver metal adopts a distorted tetrahedral geometry with Ag –S distances 2.55 – 2.61 Å, which is slightly higher than in 2- and 3-coordinate polymer systems. The thiomethyl groups are arranged in an anti-conformation in crystal structure. The γ–NH proton to pyridyl ring forms S(6) type hydrogen bonding with nitrogen of pyridyl ring H4A – N6 (1.94 Å) that satisfies the Etter's rule,[30, 31] which says that anti conformation of protons prefer to form hydrogen bond with pyridyl nitrogen in substitution S(6) type hydrogen bonding. The remaining NH hydrogen atom bond of the urea group is not involved in an $R_2^2(8)$ type motif similar to that found in the free ligand to give a infinite hydrogen bonded polymer in the crystal structure.

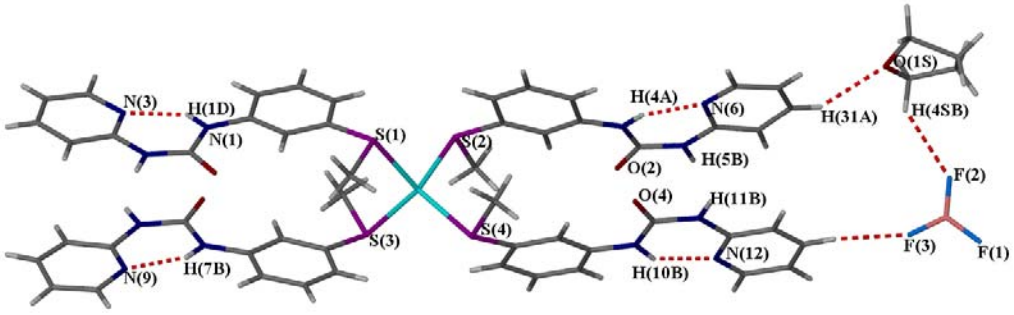

Figure 4.6 The 1:4 silver (I) tetrafluoroborate complex [Ag (κ-*S*-3.3)$_4$](BF$_4$)·thf (4.3) view along the *a*-axis.

The BF_4^- anion and THF solvent is not involved in any type of hydrogen bonding with urea NH hydrogen atoms, but one of the fluorine atoms of the BF_4^- anion interacts with the γ–H proton of pyridyl ring forming a CH···F interaction (H71A···F3 = 2.41 Å) and a second fluorine atom forms a hydrogen bond with the α–H of the THF solvent molecule H4SB···F4 (2.65 Å).

The oxygen atom of the THF solvent is interacting with the γ–H proton of pyridyl ring forming a CH···O1S interaction (H31A···O1S = 2.37 Å). The crystal packing is shown in Figure **4.7**.

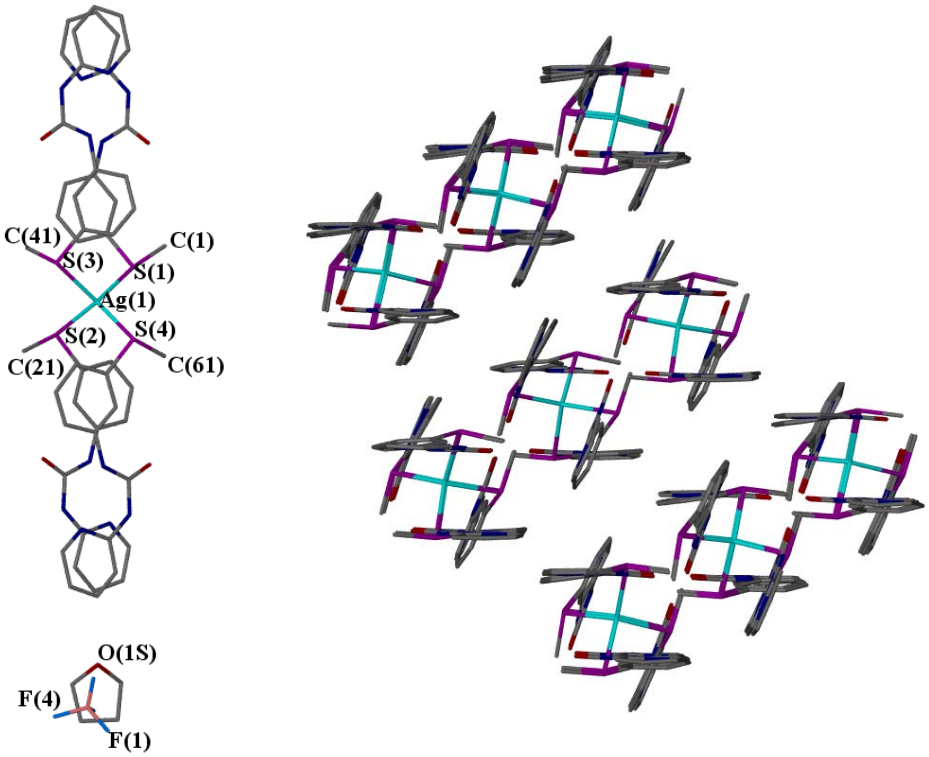

(b)

Figure 4.7 The 1:4 silver (I) tetrafluoroborate complex [Ag(κ-*S*-3.3)$_4$](BF$_4$)·thf (4.3) view along *c*-axis (b) crystal structure packing along *b*-axis (hydrogen bonds, thf solvent and BF$_4$ anion is removed for clarity purpose).

4.2.4 Synthesis and structure of [Ag (3.3)] (PF_6)

Ligand **3.3** was dissolved in THF and added to a solution of silver hexafluorophosphate in water (1: 1, v/v) and the vial was completly wrapped with silver foil in order to exclude light due to the photosensitivity of silver metal. The mixture was left to slowly evaporate for seven days resulting in a formation of colourless single crystals. Having made complexes with coordinating anion like acetate and nitrate, we are interested how the 1:1 solid state structures will look in the presence of a non-coordinating anion since clearly the 1:4 complex obtained with BF_4^- is not informative in this regard. The colourless crystal structure confirms the complex formula as [Ag(**3.3**)](PF_6) (**4.4**), in which the silver ion is coordinated with a sulphur atom of the thiomethyl ether group Ag–S = 2.432 Å, a distance slightly less than the other coordinated complexes, but the PF_6^- anion does not interact with the urea hydrogen bonds due to non-coordinating nature of the anion. The crystal structure shows that a carbonyl oxygen atom of the ligand forms a $R_2^1(6)$ type hydrogen bonding H2N···O = 2.08 Å and H1N···O = 2.76 Å in a bifurcated hydrogen bond motif. The crystal structure shows a linear coordination polymer based on coordination by the sulphur atom of the thiomethyl ether and nitrogen atom of the pyridyl ring, which is further stabilized by long interactions of silver and hydrogen atoms of the aryl rings (Ag…CH, 3.765Å). Fluoro groups of the anion also form long interactions (CH···F = 2.71 Å). In the absence of a strong hydrogen bond acceptor anion, the oxygen atom of the urea group forms a hydrogen bond NH···O motif in a $R_2^1(6)$ fashion, which involves the carbonyl oxygen atom as a bifurcated acceptor.[30-33]

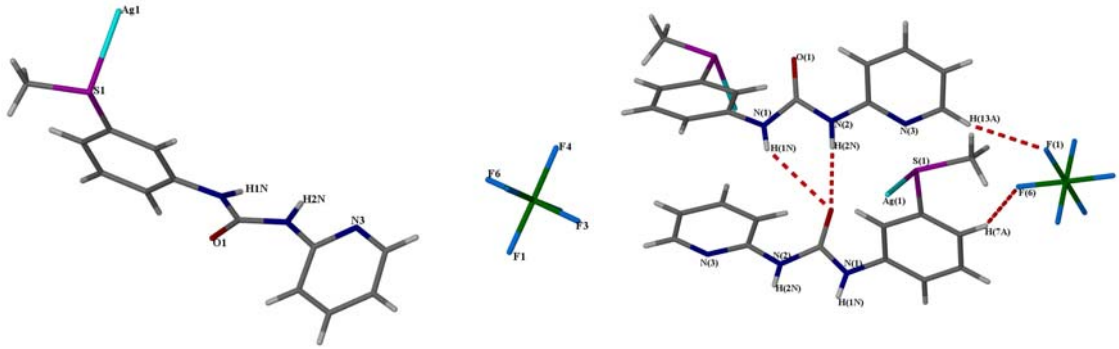

(a) (b)

Figure 4.8 The 1:1 silver hexaflurophosphate complex [Ag (3.3)](PF_6) (4.4) showing the bifurcated hydrogen oxygen bond and polymer chain.

The crystal structure packing along b-axis shows that the thiomethyl ether groups are arranged in a trans manner and packing is stabilized through forming $R_2^1(6)$ type hydrogen bonding in an alternating way in the crystal packing, Figure **4.9**.

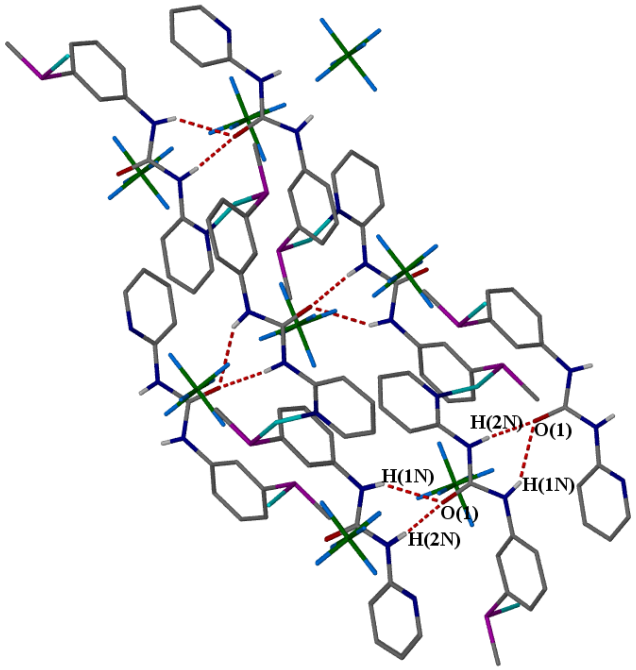

Figure 4.9 The crystal structure packing along *b*-axis forming hydrogen bond motif (hydrogen bonds are removed for clarity).

4.3 Solution Binding Behaviour

4.3-^{1}H-NMR spectroscopic titration

The aim of the project is to design synthetic molecules that can specifically bind chloride anion in solution and in the solid state. Having made solid state structures of ligand **3.3** with AgX (X = NO_3, PF_6, BF_4, OAc) in a range of solvents, we are further interested in how the molecule behaves in solution. Unfortunately solution binding studies were severely hampered by the precipitation of the complex from a range of solvents upon titration with anions. Problems with the photosensitivity of silver(I) were also encountered. Ligand **3.3** itself is soluble in a range of organic solvents, however. So, the ^{1}H-NMR spectroscopic titrations with metal salts had to be carried out in the highly competitive DMSO–d_6. Binding studies of free ligand **3.3** with $NBu_4^+X^-$ (X = NO_3, PF_6^-) did not result in significant chemical shift changes, suggesting weak binding in DMSO–d_6 and the complexes formed precipitates in acetone-d_6. However in both acetone-d_6 and DMSO-d_6 solution addition of tetrabutylammonium acetate resulted in the formation of a 1:1 complex as confirmed by Job plot in figure **4.10**(c). In DMSO-d_6 conventional binding isotherm behaviour was observed for both NH resonances (NH_a and NH_b, Fig. **4.10**(b); in acetone the resonance at 8.37 ppm (NH_b) is affected dramatically more than the NH_a signal at 11.53 ppm (Fig. **4.10**(a)). From this we can deduce that there is an intramolecular hydrogen bond between pyridyl nitrogen and urea of hydrogen to make an S(6) type hydrogen bonding pattern as shown in Figure **3.1**. When the ^{1}H-NMR titration was performed with ligand **3.3** in the presence of silver trifluromethane sulphonate in DMSO-d_6 solvent, as there was only 0.1 ppm change observed after the addition of 5.0 equivalents of guest, as shown in Figure **4.11**

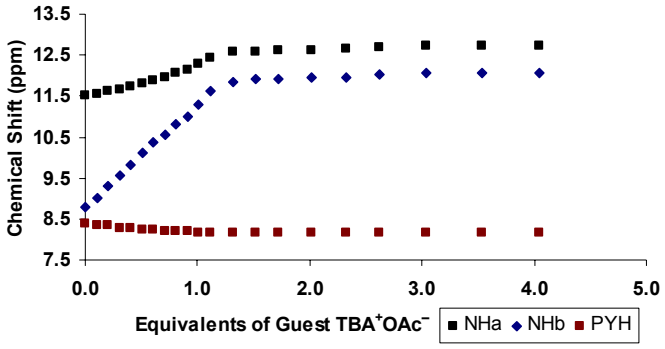

(a)

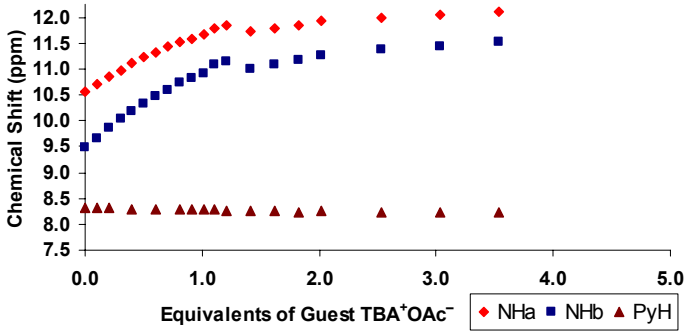

(b)

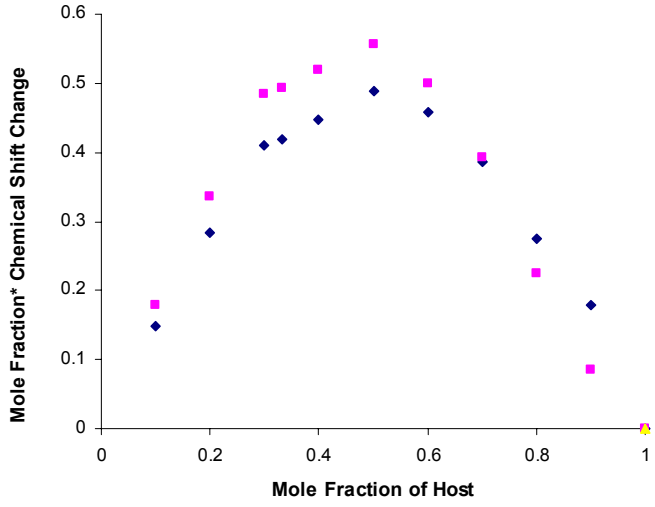

(c)

Figure 4.10: ^{1}H-NMR spectroscopic titration of 3.3 with $TBA^{+}OAc^{-}$ (a) in acetone-d_6 and (b) in DMSO-d_6 (c) Job plot

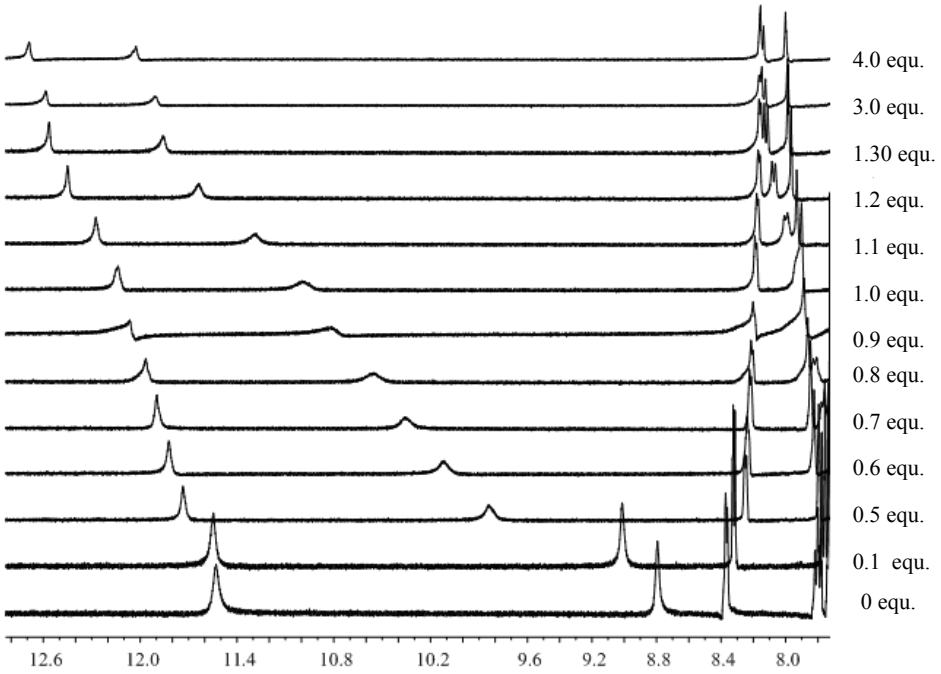

Figure 4.11 Stack plot of 3.3 with $TBA^{+}OAc^{-}$ in acetone-d_6

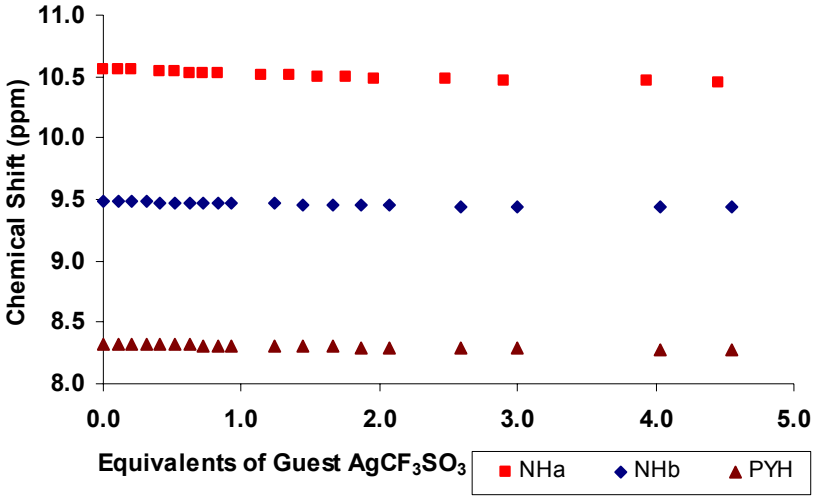

Figure 4.12 Titration of ligand 3.3 with $AgCF_3SO_3$ in DMSO solution

^{1}H-NMR spectroscopic titration was performed with ligand **3.3** and $NBu_4^+MeCO_2^-$ in the presence of 0.5, 1 and 2 equivalents of $AgCF_3SO_3$, relative to ligand **3.3**. In the presence of 0.5 equivalents of Ag(I) (a 2:1 **3.3**: Ag ratio), no change in the chemical shift of NH_a proton was observed until 0.5 equivalent of anion has been added, but NH_b proton underwent a downfield chemical shift change of *ca.* 0.4 ppm in the same range. In the presence of one equivalent of Ag(I) similar behaviour is observed except that the chemical shift of NH_a remains unchanged until one equivalent of acetate is added. Interestingly the titration isotherm in the presence of two equivalents of Ag(I) looks very similar to the plot obtained in the presence of one equivalent of silver, *i.e.* the chemical shift of NH_a begins to change after addition of one equivalent of acetate. We interpret this data by postulating anion binding by a 1:1 complex of silver(I) and **3.3**. Thus in the presence of 0.5 equivalents of Ag(I) the first 0.5 equivalents of acetate are bound by the silver complex, affecting NH_b but not NH_a. After this process is complete additional acetate is bound by the excess free ligand (as demonstrated by Fig. **4.10**(b), and/or by the "Ag **3.3**$^+$" complex in a different binding mode. In the presence of one equivalent of Ag(I) it requires one equivalent of acetate to bind to the "Ag**3.3**$^+$" complex. Additional acetate is then bound in a different binding mode to give an "Ag**3.3**·2$MeCO_2^-$" species. There is precedent for this binding of more than one anion by these kinds of complexes.[5] In the presence of two equivalents of silver(I) half of the silver is in excess and makes no difference to the shape of the isotherm. This latter experiment establishes that acetate is not being bound by Ag(I) in the absence of **3.3**. The fact that it is NH_b and not NH_a that is most affected by acetate anion binding by "Ag**3.3**$^+$" is surprising. Examination of the crystal structure data shown in Fig. **4.2** suggests that both NH resonances should be affected. It is possible that a different binding mode occurs in solution along the lines of those shown in Fig. **4.15**.

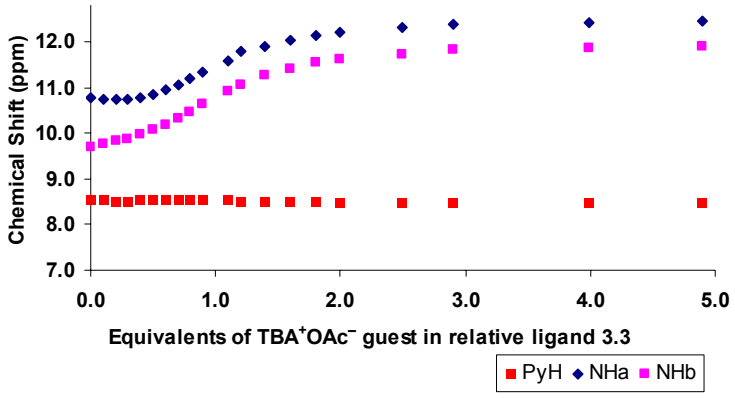

a)

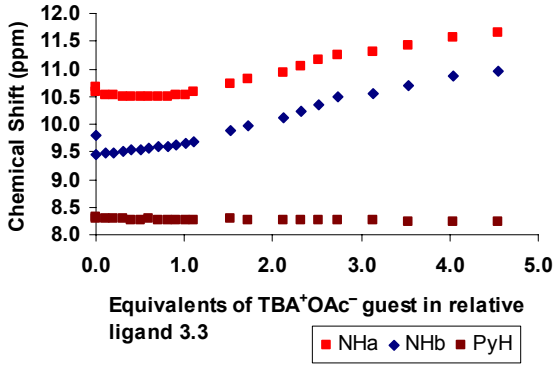

(b)

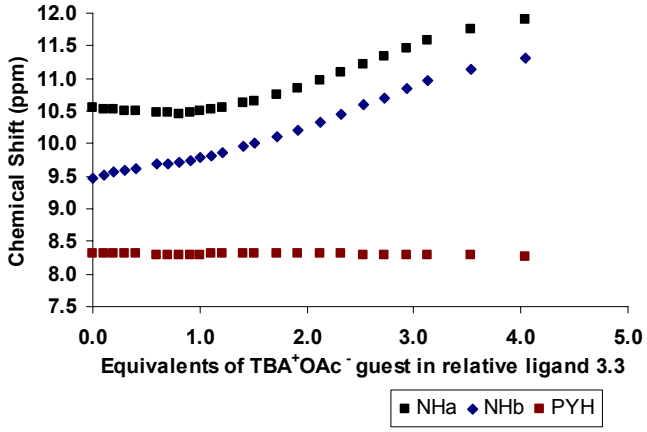

(c)

Figure 4.13: ^{1}H-NMR spectroscopic titration of 3.3 with $NBu_4^+OAc^-$ in the presence of (a) 0.5, (b) 1.0 and (c) 2.0 equivalents of $AgCF_3SO_3$.

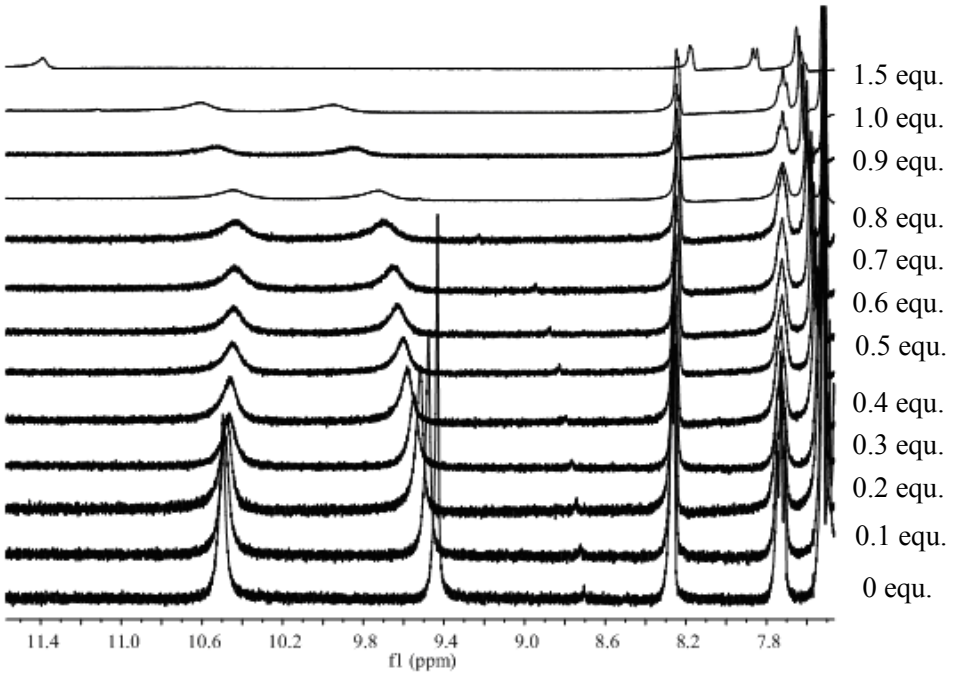

Figure 4.14 Plot of ^{1}H-NMR spectroscopic titration of ligand 3.3 with NBu_4^+ OAc^- in the acetone solvent.

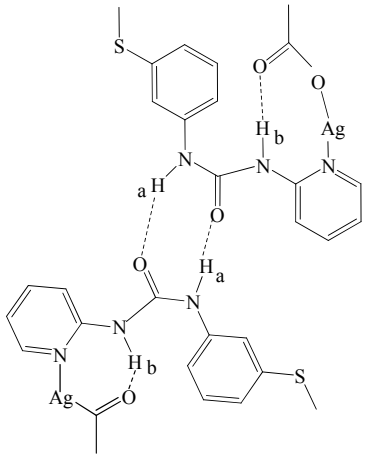

Figure 4.15 Speculative acetate binding mode involving1:1 Ag: 3.3 complexes giving rise to a chemical shift change in NH_b but not in NH_a upon acetate binding

Table 4.1: Crystal data and structure refinement for compounds 4.1 (forms A and B), and 4.2 – 4.4.

Compound	4.1 A	4.1 B	4.2	4.4	4.3
Formula	$(C_{13}H_{13}N_3OS)Ag(CH_3CO_2)$		$(C_{13}H_{13}N_3OS)Ag(NO_3)$	$(C_{13}H_{13}N_3OS)Ag(PF_6)$	$(C_{13}H_{13}N_3OS)_4Ag(BF_4)(C_4H_8O)$
Formula weight	426.24		429.20	512.16	1304.08
Crystal system	Monoclinic	Triclinic	Triclinic	Orthorhombic	Orthorhombic
space group	$P\ 2_1/c$	P-1	P-1	$P\ 2_1\ 2_1\ 2_1$	$P\ c\ a\ 2_1$
a, Å	4.3552(1)	7.6567(4)	7.9094(2)	8.7396(2)	11.034(2)
b, Å	19.5739(6)	9.7852(4)	9.6883(3)	12.2836(2)	32.057(6)
c, Å	18.4288(6)	11.5435(5)	10.6752(3)	15.3536(3)	16.422(3)
α, °	90	73.77(1)	89.97(1)	90	90
β, °	95.12(2)	77.40(1)	69.83(1)	90	90
γ, °	90	75.77(1)	75.89(1)	90	90
Volume	1564.75(8)	794.47(6)	741.53(4)	1648.27(6)	5809(2)
Z	4	2	2	4	4
ρ (calc.), mg/m^3	1.809	1.782	1.922	2.064	1.491
μ, mm^{-1}	1.439	1.417	1.526	1.519	0.563
F(000)	856	428	428	1008	2688
Reflections collected	14537	8976	9809	21967	36273
Independent refl., R_{int}	4130, 0.062	4591, 0.018	4302, 0.0182	4817,0.026	11378, 0.116
N of parameters	272	272	260	243	684
Final R_1 [I>2σ(I)]	0.0359	0.0282	0.0278	0.0255	0.0941
wR_2 (all data)	0.1035	0.0789	0.0758	0.0615	0.2317
GOF on F^2	1.085	1.020	1.018	0.979	1.023

4.4 Experimental

4.4.1 X-Ray crystallography

Suitable single crystals were grown by slow evaporation in the dark and mounted using silicon grease on a thin glass fibre. Crystallographic measurements were carried out on a Bruker SMART CCD 6000 (**4.1A**, **4.1B**, **4.2**, **4.3**) and Rigaku R-AXIS Spider IP (**4.4**) diffractometer using graphite monochromated Mo-Kα radiation (λ = 0.71073 Å). The standard data collection temperature was 120 K, maintained using an open flow N_2 Cryostream (OxfordCryosystems) device. Integration was carried out using the Bruker SAINT and Rigaku FSProcess packages. Data sets were corrected for Lorentz and polarisation effects and for the effects of absorption. Structures were solved using direct methods and refined by full-matrix least squares on F^2 for all data using SHELXTL software. All non-hydrogen atoms were refined with anisotropic displacement parameters; H-atoms were located on the difference map and refined isotropically. Molecular graphics were produced using the programs X-Seed[34] and POV-Ray.[35] Crystal data for the structures studied are listed in Table **4.1**

4.4.2 Syntheses

[Ag(3.3)](CH_3CO_2) 4.1 (form A). Ligand **3.3** (0.30 g, 0.115 x 10^{-3} mol) in THF (2 ml) was mixed with silver acetate (0.19 g, 0.115 x 10^{-3} mol) in methanol: H_2O (1:1 v/v, 2 ml) and the mixture allowed to evaporate slowly resulting in a formation of colourless single crystals suitable for x-ray diffraction analysis. IR (ν /cm-1) 1200, 1441, 1548, 1576, 1765 (s, νa(CO2)), 3323(m, ν(NH)). M.p. 185 ^{0}C (decomp.); Anal. Calcd (%) for $C_{15}H_{16}N_3O_3SAg$: C, 42.27; H, 3.78; N, 9.86. Found (%) C, 42.02; H, 3.73; N, 9.66.

[Ag(3.3)](CH_3CO_2) 4.1 (form B). The second polymorph of **4.1** was obtained by dissolving **3.3** (0.30 g, 0.115 x 10^{-3} mol) in THF (2 ml) and mixing with silver acetate (0.19 g, 0.115 x 10^{-3} mol) in methanol : acetonitrile (1 : 1 v/v, 2 ml) and leaving the mixture to evaporate slowly. This resulted in the formation of colourless single crystal suitable for X-ray diffraction analysis. IR (ν /cm-1) 1411, 1467, 1531, 1579, 1612, 1718 (s, νa(CO_2)), 3199 (m, ν(NH)), 3279 (m, ν(NH)). M.p. 180 ^{o}C (decomp.). Anal. Calcd (%) for $C_{15}H_{16}N_3O_3SAg$: C, 42.27; H, 3.78; N, 9.86. Found (%) C, 42.03; H, 3.75; N, 9.91.

[Ag(3.3)](NO$_3$) 4.2. Ligand 3.3 (0.30 g, 0.115 x 10^{-3} mol) was dissolved in THF (2 ml) and added to a solution of silver nitrate (0.20, 0.118 x 10^{-3} mol) in H_2O (2 ml). The mixture was left to slowly evaporate for five days resulting in a formation of colourless single crystals. IR (ν /cm-1) 681, 760, 1304, 1387, 1535, 1578, 1608, 1709, 3129, 3278. M.p. 180 ^{o}C (decomp.). Anal. Calcd; (%) for $C_{13}H_{13}N_4O_4SAg$: C, 36.40; H, 3.01; N, 13.10. Found (%) C, 36.30; H, 3.07; N, 13.07.

[Ag(3.3)$_4$](BF$_4$)·thf 4.3. Ligand **3.3** (0.30 g, 0.115 x 10^{-3} mol) in THF (2 ml) was mixed with a solution of silver tetrafluoroborate (0.23 g, 115 x 10^{-3} mol) in THF : H_2O (1 : 1 v/v, 2 ml) and the mixture allowed to evaporate resulting in a formation of colourless single crystals. IR (ν /cm-1) 1037 (s, BF_4), 1597, 1554, 1657, 3307 (m, NH), 3368 (m, NH). Anal. Calcd; (%) for $C_{52}H_{52}N_{12}O_4S_4AgBF_4$: C, 52.75; H, 4.43; N, 14.20 Found (%) C, 51.50; H, 4.43; N, 14.10.

[Ag(3.3)](PF$_6$) 4.4. Ligand **3.3** (0.30 g, 0.115 x 10^{-3} mol) was dissolved in THF (2 ml) and added to a solution of silver hexafluorophosphate (0.20 g, 0.079 x 10^{-3} mol) in H_2O (2 ml). The mixture was left to slowly evaporate for five days resulting in a formation of colourless single crystals. IR (ν /cm^{-1}) 987 (br, PF_6), 1649 (s, C=O), 3308 (br, NH), 3477 (br, H_2O) Anal. Calcd (%) for $C_{13}H_{12}N_3OSAgPF_6$: C, 30.42; H, 2.56; N, 8.11. Found (%) C, 30.50; H, 2.56; N, 8.22. Mass 511.16 (M + H)

4.5 Conclusions

2-Ureidopyridine **3.3** is a versatile ligand that not only exhibits significant polymorphism in its own right, but also shows simultaneous binding of silver metal and a series of anions to form contact ion pair complexes in the case of coordinating anions (OAc^- and NO_3^-). In the case of the acetate complex polymorphism is also observed. The structures of the contact ion pair complexes are influenced by the stronger basicity of acetate and its lower symmetry. In each case the silver ion is coordinated with the nitrogen atom of the pyridyl group, the sulphur atom of the thioether and the oxygen atoms of the nitrate or acetate anions forming $R_2^1(6)$ and $R_2^2(8)$ type hydrogen bonding with acetate and nitrate anion in solid state structures. The complexes are thus both coordination polymeric in the solid state. There are two different polymorphic forms formed with silver acetate one of them is monoclinic and other is triclinic in structure, however both polymorphs have $R_2^1(6)$ type hydrogen bonding to the coordinated anion. In contrast the complex of the non-coordinating anion PF_6^- results in the formation of a separated ion pair in the solid state and the system reverts to a distorted urea tape type of hydrogen bonding. The reaction of $AgBF_4$ with **3.3** forms 1: 4 complex that is distorted tetrahedral in structure. The stoichiometry arises from the decomposition of silver(I) and the saturation of the metal centre by the ligands means there is not metal-anion interaction.

^{1}H NMR spectroscopic titration experiments on both free **3.3** and its silver complexes were performed in DMSO solution due to the poor solubility of the complexes. The data suggest that the ion pair motif is retained in solution.

4.6 References

1. C. R. Rice, *Coord. Chem. Rev.*, 2006, **250**, 3190-3199.
2. C. R. Bondy, P. A. Gale and S. J. Loeb, *Chem. Commun.*, 2001, 729-730.
3. C. R. Bondy and S. J. Loeb, *Coord. Chem. Rev.*, 2003, **240**, 77-99.
4. C. R. Bondy, P. A. Gale and S. J. Loeb, *J. Am. Chem. Soc.*, 2004, **126**, 5030-5031.
5. D. R. Turner, B. Smith, E. C. Spencer, A. E. Goeta, I. R. Evans, D. A. Tocher, J. A. K. Howard and J. W. Steed, *New J. Chem.*, 2005, **29**, 90-98.
6. J. M. Russell, A. D. M. Parker, I. Radosavljevic-Evans, J. A. K. Howard and J. W. Steed, *Chem. Commun.*, 2006, **8**, 269-271.
7. J. M. Russell, A. D. M. Parker, I. Radosavljevic-Evans, J. A. K. Howard and J. W. Steed, *Crystengcomm*, 2006, **8**, 119-122.
8. P. Blondeau, A. van der Lee and M. Barboiu, *Inorg. Chem.*, 2005, **44**, 5649-5653.
9. J. M. Russell, A. D. M. Parker, I. Radosavljevie-Evans, J. A. K. Howard and J. W. Steed, *Chem. Commun.*, 2006, 269-271.
10. A. V. Koulov, J. M. Mahoney and B. D. Smith, *Org. Biomol. Chem.*, 2003, **1**, 27-29.
11. J. M. Mahoney, J. P. Davis, A. M. Beatty and B. D. Smith, *J. Org. Chem.*, 2003, **68**, 9819-9820.
12. J. M. Mahoney, A. M. Beatty and B. D. Smith, *J. Am. Chem. Soc.*, 2001, **123**, 5847-5848.
13. J. M. Mahoney, R. A. Marshall, A. M. Beatty, B. D. Smith, S. Camiolo and P. A. Gale, *J. Supramol. Chem.*, 2001, **1**, 289.
14. J. M. Mahoney, A. M. Beatty and B. D. Smith, *Inorg. Chem.*, 2004, **43**, 7617-7621.
15. J. M. Mahoney, G. U. Nawaratna, A. M. Beatty, P. J. Duggan and B. D. Smith, *Inorg. Chem.*, 2004, **43**, 5902-5907.
16. P. J. Smith, M. V. Reddington and C.S. Wilcox, Craig S., *Tetrahedron Letters*, 1992, **33**, 6085-6088.
17. D. N. Reinhoudt, J. Scheerder, R. H. Vreekamp, J. F. J. Engbersen, W. Verboom and J. P. M. van Duynhoven, *J. Org. Chem.*, 1996, **61**, 3476-3481.
18. S. M. Bromidge, S. Dabbs, D. T. Davies, S. Davies, D. M. Duckworth, I. T. Forbes, A. Gadre, P. Ham, G. E. Jones, F. D. King, D. V. Saunders, K. M.

Thewlis, D. Vyas, T. P. Blackburn, V. Holland, G. A. Kennett, G. J. Riley and M. D. Wood, *Bioorg. Med. Chem.*, 1999, **7**, 2767-2773.

19. P. A. Gale, M. E. Light, B. McNally, K. Navakhun, K. E. Sliwinski and B. D. Smith, *Chem. Commun.*, 2005, 3773-3775.
20. J. L. Seganish and J. T. Davis, *Chem. Commun.*, 2005, **7**, 5781 - 5783.
21. P. A. Gale, *Coord. Chem. Rev.*, 2001, **213**, 79-128.
22. J. W. Steed and K. J. Wallace, in *Ad. Supramolecular Chemistry*, Ed., 2003, vol. 5.
23. J. van Esch, F. Schoonbeek, M. de Loos, H. Kooijman, A. L. Spek, R. M. Kellogg and B. L. Feringa, *Chem.-Eur. J.*, 1999, **5**, 937-950.
24. V. Sidorov, F. W. Kotch, J. L. Kuebler, Y. F. Lam and J. T. Davis, *J. Am. Chem. Soc.*, 2003, **125**, 2840-2841.
25. D. R. Turner, E. C. Spencer, J. A. K. Howard, D. A. Tocher and J. W. Steed, *Chem. Commun.*, 2004, **7**, 1352-1353.
26. M. Jansen, Ang. Chemie-Int. Ed.,1987, **26**, 1098-1110.
27. N. N. Greenwood and A. Earnshaw, *Chemistry of the Elements*, 1st Edn., Pergamon, Oxford, 1984.
28. V. J. Catalano and A. O. Etogo, *J. Organometallic Chemistry*, 2005, **690**, 6041-6050.
29. M. C. Etter, *Acc. Chem. Res*, 1990, **23**, 120-126.
30. M. C. Etter, Z. Urbanczyk-Lipkowska, M. Zia-Ebrahimi and T. W. Panunto, *J. Am. Chem. Soc*, 1990, **112**, 8415-8426.
31. L. S. Reddy, N. J. Babu and A. Nangia, *Chem. Commun.*, 2006, **7**, 1369-1371.
32. L. S. Reddy, S. Basavoju, V. R. Vangala and A. Nangia, *Cryst. Growth. Des.*, 2006, **6**, 161-173.
34. L. J. Barbour, *J. Supramol. Chem.*, 2001, **1**, 189-191.
35. C. J. Cason, in POV-Ray', 2002.

Chapter 5: Anion binding by copper(II) complexes of 2-Ureidopyridine derivative.

5.1 Aim and Targets

The element copper is very widely distributed as salts and complexes in plants, invertebrates, animals and common minerals.[1] The known oxidation states are I, II, III and IV.[2] Of course, the copper (II) or cupric form is by far the most common. Copper(II) displays a wide variety of coordination geometries in its many salts and complexes. Its most common coordination numbers are four, five and six.[2] The aim of this part of the project is to synthesise simple artificial ligands that can selectively bind with metals such as copper through contact ion pair in solid state and solution chemistry. Copper metal and others are increasingly being used in the construction of hosts for anion and neutral molecules. Metals act as a Lewis acidic binding sites or as sensing units, carry positive charge and can increase the strength of non–covalent interactions such as hydrogen bonds.[2, 3] As discussed in section **1.4** recent work by the groups of Gale,[4] Loeb,[5, 6] and Steed[7-9] have elegantly shown that simple coordination compounds containing a combination of a cationic metal centre and monodendate ligands featuring hydrogen bond donor groups can be used as hosts for selective binding of particular counter anions. Simple compounds based on 3-aminopyridine,[7] 3-(aminomethyl)pyridine and 3-ureidopyridine[10, 11] type ligands have shown a range of separated ion pair binding behaviour. Steed's group has reported ureidopyridyl ligands and the solid state structures of their copper and silver complexes.[7, 12] In the previous chapter we described contact-ion pair binding of a 2-ureidopyridine ligand with silver(I) and their solution anion binding properties.[13] In this chapter we now describe the extension of this work to copper(II) complexes.

5.2 Results and Discussion

5.2.1 2-Ureidopyridine with copper chloride complex [Cu(3.1)Cl_2] 5.1

The reaction of 2-ureidopyridine ligand **3.1** with $CuCl_2$ in an equimolar ratio resulted in a formation of single crystals of a complex of formula [Cu(**3.1**)Cl_2] (**5.1**) that was characterized by X-ray crystallography. The material crystallizes in triclinic space group P-1 with two formula units in the unit cell and all the atoms are located in general positions. In an asymmetric unit, the copper(II) ion is attached to the nitrogen atom of the pyridyl ring (N3-Cu1 = 2.004 Å) and the oxygen atom of the carbonyl group, Cu1-O1 = 1.957Å in a bidendate fashion forming a 6-membered chelate ring ∟N3-Cu1-O1 = 89.32˚. The CuCl2 distances are almost same Cu1-Cl1 = 2.269 Å and Cu-Cl2 = 2.254 Å forming an angle at the metal that slightly larger than a right angle, ∟Cl2 -Cu1-Cl1 = 95.48˚ suggesting strong binding as proposed by Orpen and Brammer14-16 Figure **5.1**.

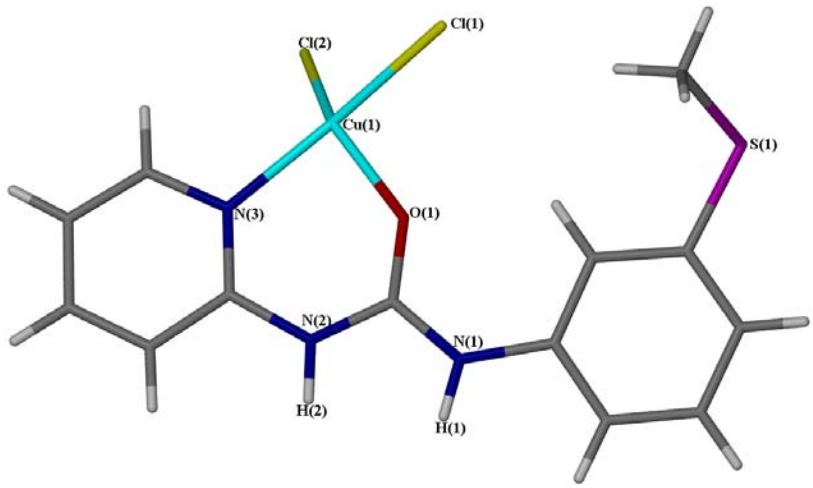

Figure 5.1 Asymmetric unit of ligand 3.1 with $CuCl_2$

Hydrogen bonding is an important property that helps in most of the biological processes and crystal engineering to make supramolecular synthons.[17] The halogen atoms attached to carbon are regarded as weak hydrogen bond acceptors as reported by Taylor.[18] Hydrogen bonding is stronger to metal halides, however.[15, 16, 19] The coordination mode in **5.1** makes the urea unit available as a hydrogen bond donor pointing away from the metal centre, in contrast to the silver(I) compounds discussed in chapter 4. In the crystal structure of **5.1** two copper-bound chloride ligands form

hydrogen bonds with urea NH protons in a $R_2^2(8)$ type fashion, in which N2-Cl2 = 3.371 Å is greater than N1-Cl1 = 3.156 Å as shown in Figure **5.2**. In the crystal the compound exists in a chloride-bridged dimer structure situated on an inversion centre, with two short and two long Cu–Cl bonds to the bridging chloride, Cl1. This result in urea groups of the dimmer arranged in opposite directions, Figure **5.3**.

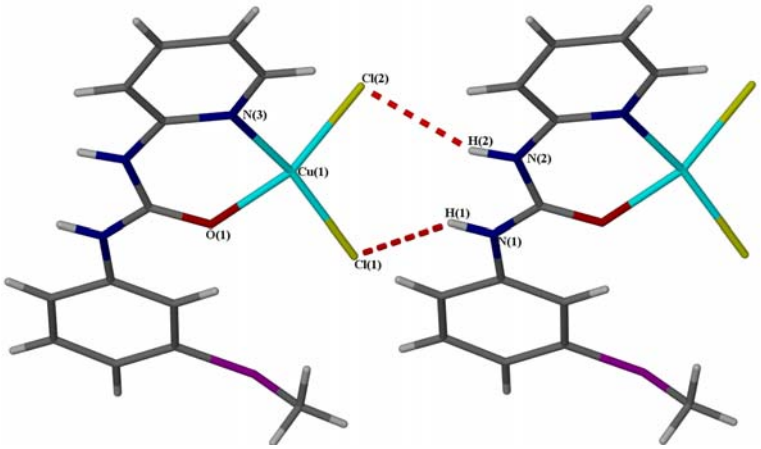

Figure 5.2 Hydrogen bonding between urea NH and Cl atoms. Selected distances are in Å N2-Cl2 = 3.371 and N1-Cl1 = 3.156.

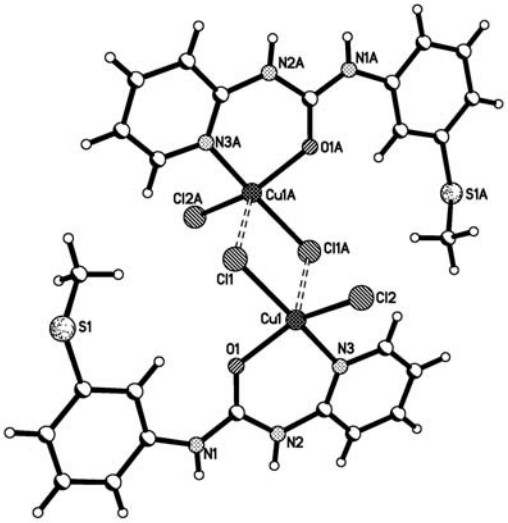

Figure 5.3 Dimerisation of 5.1 in the solid state via bridging chloride ligands, Cu–Cl1 2.269, Cu1–Cl1A 2.787 Å.

The crystal structure along the a-axis forms perpendicular tilted sheet like structures in which thiomethyl substituents are arranged in trans in orientations as shown in figure **5.4**.

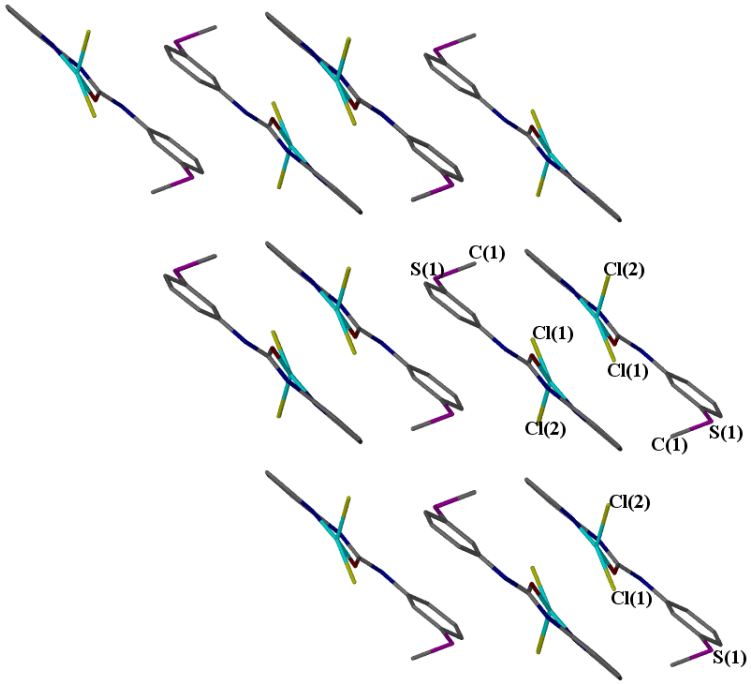

Figure 5.4 Crystal structures packing in 5.1 viewed along the a-axis forming sheet like structures (hydrogen bonds are omitted for clarity).

5.2.2 2- Ureidopyridine with copper bromide complex [Cu(3.1)$_2$Br$_2$]5.2

The reaction of 2-ureidopyridine ligand 3.1 with $CuBr_2$ in an equimolar ratio resulted in the formation of a complex of formula [Cu(3.1)2Br_2] crystallizing in triclinic space group P-1 with half of one formula unit in the unit cell, with the copper(II) ion located on an inversion centre. The 2:1 L: M stoichiometry is surprising given that equimolar amounts of the metal and ligand were added and contrasts to the 1:1 formulation of 5.1, however the structure is related to copper(II) complexes of dipyridyl-diurea ligands recently reported by our group.[20] The copper(II) ion is attached to the nitrogen atom of the pyridyl ring (N3-Cu1 = 2.001 Å) and oxygen of carbonyl Cu1-O1 = 1.984 Å ring in a bidendate fashion forming hexagonal chelate ∟N3-Cu1-O1 = 88.88˚ as shown in Figure **5.6**. The one symmetry-unique bromide ligand forms a very long axial with the distorted octahedral copper centre Cu-Br = 2.935 Å21 and forms almost

a right angle with nitrogen atom of the pyridyl ligand ∟N3-Cu1-Br1 = 90.22 Å and oxygen atom of the carbonyl group ∟O1- Cu- Br1 = 89.75 Å as shown in Figure **5.6.** Because axial bonding interactions to copper (II) ion are reported up to 3.3 Å and the angle between Cu-Br vector and normal to the equatorial plane, which is the measure of the metal-ligand orbitals, is close 0°[22] The structure can be regarded as being six-coordinate distorted octahedral with a typical of Jahn-Teller distortions because of the d^9 electron configuration of copper(II),[22] Figure **5.7**. As in **5.1** the urea groups are situated on the periphery of the molecule and form hydrogen bonds between the urea NH protons and the bromide anion in an $R_2^1(6)$ type fashion as shown in Figure **5.8**.

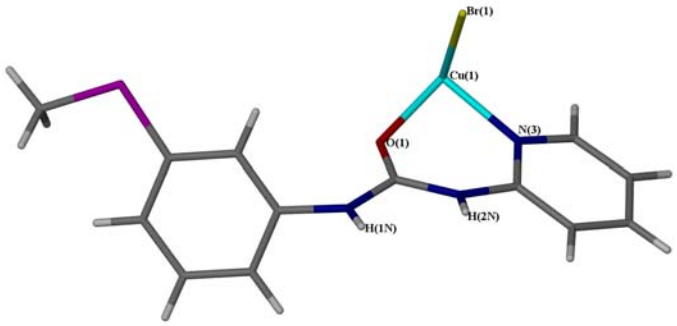

Figure 5.5 Asymmetric unit formed by complex 5.2.

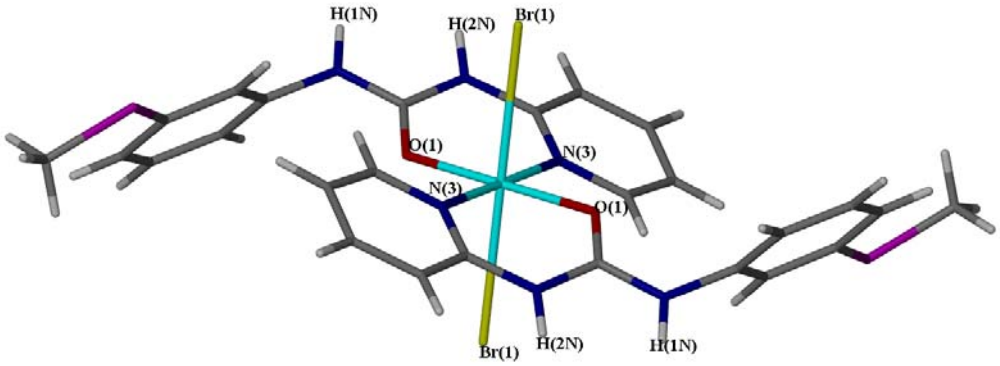

Figure 5.6 Crystal structure showing octahedral geometry of complex 5.2

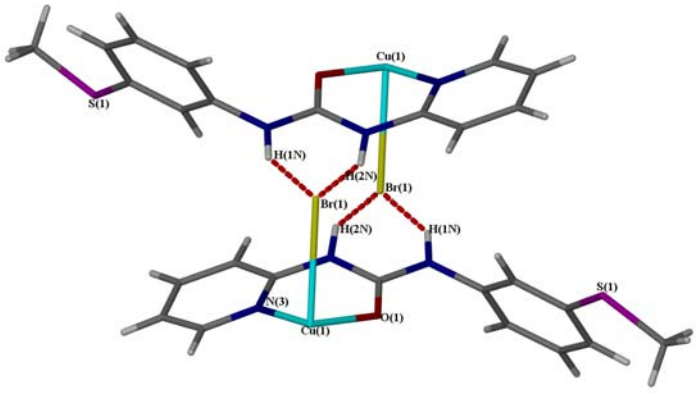

Figure 5.7 Hydrogen bonding to bromide in complex 5.2.

The crystal packing along the *b*-axis shows that the bromide anion forms hydrogen bonds with NH ureas in $R_2^1(6)$ type bifurcated hydrogen bonds.[12] These hydrogen bonds are extended axially to give a hydrogen bonded polymer. The NH groups of the urea moieties and thiomethyl substituents are arranged in opposite direction in the packing as shown in Figure **5.9**.

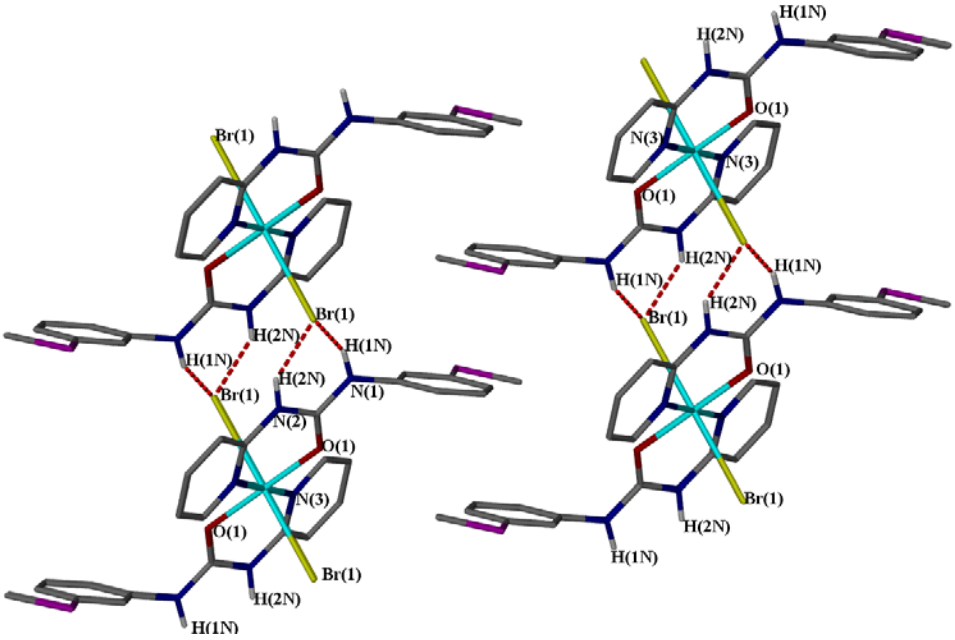

Figure 5.8 Crystal structure packing along b-axis of complex 5.2

5.2.3 2-Ureidopyridine with copper nitrato complex [Cu(3.1)$_2$(NO$_3$)$_2$] 5.3

Copper nitrate is of interest, because of low basicity of the nitrate anion compared to acetate even though they have a somewhat similar structure.[23] The reaction of the 2-ureidopyridine ligand with copper nitrate in an equimolar ratio resulted in a formation of a crystalline product of formula [Cu(**3.1**)$_2$(NO$_3$)$_2$] (**5.3**).[24] The complex was characterized by X-ray crystallography which revealed an asymmetric unit comprised of one symmetry-independent ligand, one copper(II) ion situated on an inversion centre and one nitrate anion. The copper ion is centrosymmetrically bonded with the pyridyl nitrogen atom (Cu-N = 2.030 Å) and the oxygen atom of the carbonyl group (Cu-O = 1.959 Å) in a bidentate fashion forming a six-membered chelate ring in a similar fashion to **5.2**. The oxygen atom of the nitrato ion also bonds to the copper centre (Cu1-O2 = 2.404 Å) with angle ∟O1-Cu1-O2 = 93.22^o as shown in Figure **5.10**. The crystal structure is stabilized through formation of axial hydrogen bond chains and two oxygen atoms of the nitrato anion form hydrogen bonds with the urea NH protons in a $R_2^2(8)$ type fashion as shown in Figure **5.11,** (O2-N2 = O4-N1 = 2.817 Å).[13] The coordination geometry is distorted octahedral due to typical Jahn-Teller effects,[23, 25] as shown in Figure **5.12**. As in **5.2** and in contrast to the compounds reported in Chapter 4, there is no contact ion pair binding by the ligand in this case.

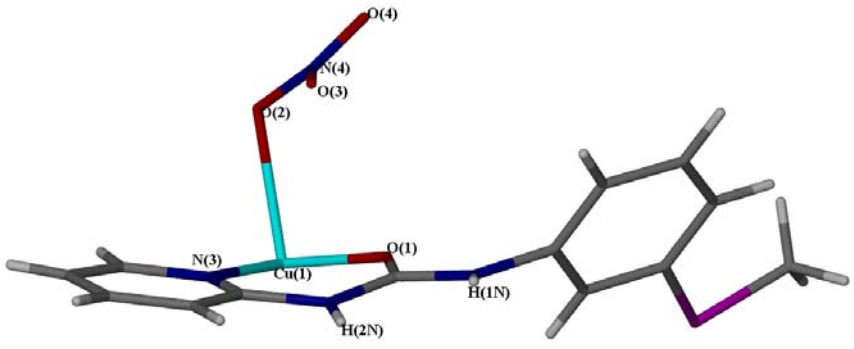

Figure 5.9 Asymmetric unit of complex 5.3

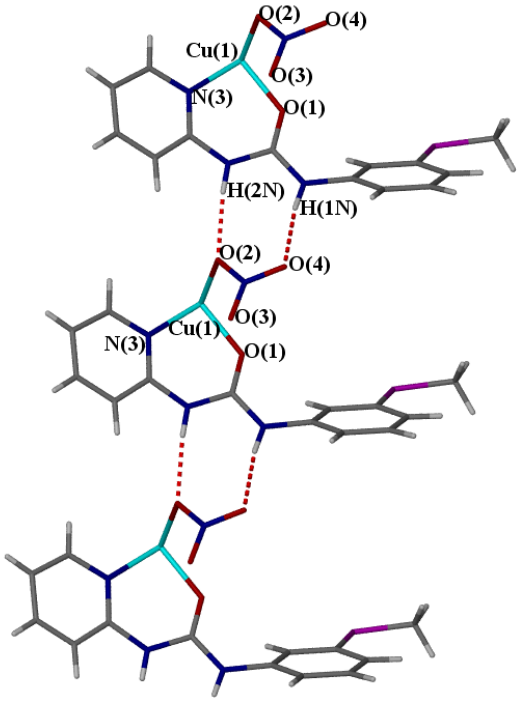

Figure 5.10 Hydrogen bonds formed between complex 5.3 and the nitrate anion.

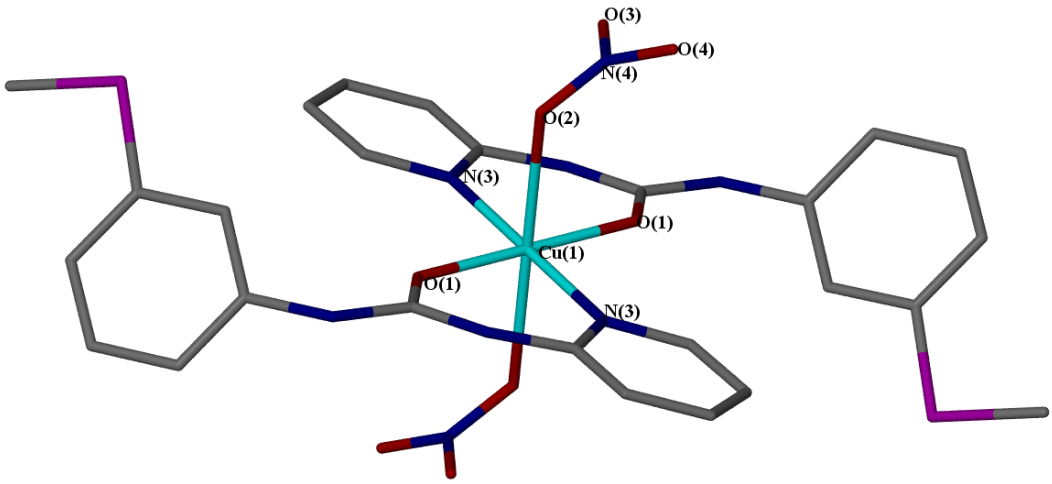

Figure 5.11 Distorted octahedral geometry of complex 5.3

Table 5.1 Crystallographic data for compound 5.1 – 5.3

Compound	**5.1**	**5.2**	**5.3**
Formula	$C_{13}H_{13}N_3OCuCl_2S$	$C_{26}H_{26}N_6O_2CuBr_2S_2$	$C_{26}H_{26}N_8CuS_2O_8$
Formula weight	393.76	742.01	706.21
Crystal system	Triclinic	Triclinic	Monoclinic
Space group	P -1	P -1	$P2_1/c$
a, Å	7.7680(16)	7.8394(16)	8.9556(3)
b, Å	9.1578(18)	8.1920(16)	21.6859(9)
c, Å	10.466(2)	12.372(3)	7.1433(4)
α, °	90.77(3)	104.40(3)	90.00
β, °	98.75(3)	92.42(3)	98.90(1)
γ, °	95.52(3)	116.28(3)	90.00
Volume	732.1(3)	679.3(2)	1370.60(11)
Z	2	1	2
ρ (calc.), g/cm^3	1.786	1.814	1.711
μ, mm^{-1}	1.999	3.937	1.018
F(000)	398	371	726
Reflections collected	9240	17441	13846
Independent refl., R_{int}	2846, 0.0990	4319, 0.0336	3301, 0.0534
N of parameters	192	179	253
Final R_1 [I>2σ(I)]	0.0864	0.0268	0.0405
wR_2 (all data)	0.2365	0.0627	0.1069
GOF on F^2	1.036	1.021	1.063

5.2.4 2-Ureidopyridine with HBF_4 [H(3.1)BF_4] 5.4

Attempts were also made to prepare a 1:1 complex with ligand **3.1** and $Cu(BF_4)_2$, however, the final isolated product proved to be an interesting protonated BF_4 salt that has been characterized through X-ray crystallography. The asymmetric unit is comprised of protonated ligand **3.1** with tetrafluorobarate anion in which the protonated pyridyl group interacts with the oxygen atom of the carbonyl group O1-N3 = 2.645 Å in an S(6) type intramolecular hydrogen bonded arrangement.[13] The tetrafluoroborate anion interacts with the urea NH protons N1-F2 = 2.870 Å and N2-F4 = 2.823 Å in $R_2^2(8)$ type arrangement which contrasts to the non-interacting, poor hydrogen bonded nature of the silver tetrafluoroborate complex[13] as shown in figure **5.13**. The crystal structure packing along a-axis suggest that an alternating arrangement of discrete cation-anion pairs has been formed, figure **5.14**. The metal $Cu(BF_4)_2$ was hexahydrated which we used for ligand metal complex formation; single crystal was also hygroscopic, absorbing water when it was subjected for microanalysis, because of these resons our microanalysis is far out.

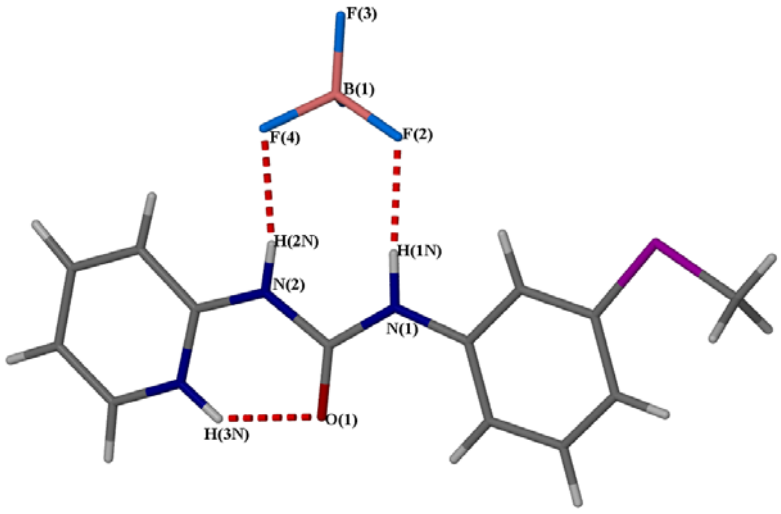

Figure 5.12 Asymmetric unit complexes of 5.4

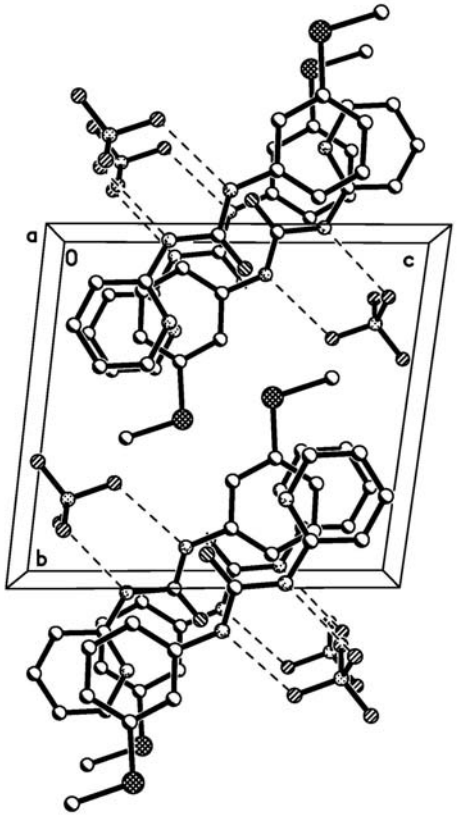

Figure 5.13 Crystal structures packing along a-axis of complex 5.4

5.2.5 2-Ureidopyridine with copper trifluromethanesulphonate [Cu(3.1)$_2$(CF$_3$SO$_3$)$_2$] 5.5 forms A & B

The reaction of 2-ureidopyridine ligand **3.1** with $Cu(CF_3SO_3)_2$ in an equimolar ratio resulted in a formation of a complex of formula [Cu(**3.1**)$_2$(CF_3SO_3)$_2$] (**5.5**) related to **5.2** and **5.3**. The complex was characterized by X-ray crystallography and found to exist in two polymorphic modifications, termed A and B. The molecular structures of these two polymorphs are very similar and comprise a Jahn-Teller distorted octahedral complex with the anions axially coordinated in a similar way to **5.2** and **5.3**. The asymmetric unit comprises one symmetry-independent ligand **3.1,** half of a copper(II) centre and one triflate anion. The copper(II) ion is centrosymmetrically bonded with the nitrogen atom of the pyridyl group N3-Cu1 = 1.998 Å and the oxygen atom of the urea carbonyl group O1-Cu1 = 1.930 Å forming a six-membered chelate ring. The bite angle is slightly less than a right angle ∟N3-Cu1-O1 = 88.22^o. The Cu is axially coordinated to the oxygen atom of the trifluromethane-sulphonate anion Cu1–O2 = 2.447 Å. The only difference between the two polymorphs that in polymorph A the thiomethyl substituents point away from one another in the crystal structure whereas they point towards one another in polymorph B as shown in Figure **5.15**. This difference is reminiscent of the conformational polymorphism of the free ligand discussed in Chapter 3.

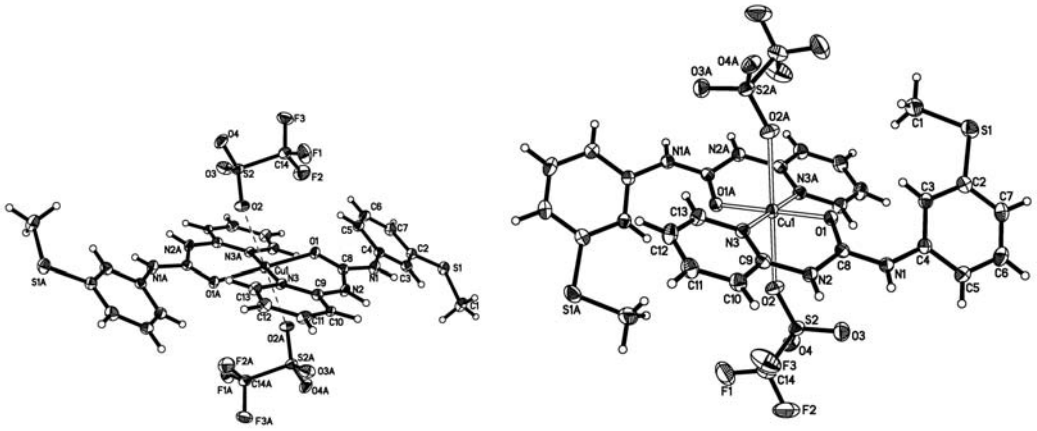

(A) (B)

Figure 5.14 Crystal structures of complex 5.5

Table 5.2 Crystallographic data for compound 5.4 and 5.5 (form A and B).

Compound	**5.4**	**5.5** A	**5.5** B
Formula	$C_{13}H_{14}SON_3\ BF_4$	$(C_{13}H_{13}N_3OS)_2$ Cu $(CF_3SO_3)_2$	
Formula weight	347.14	880.3	880.33
Crystal system	Triclinic	Triclinic	Monoclinic
Space group	P -1	P -1	$P2_1/c$
a, Å	6.6282(3)	8.2365(3)	12.6428(3)
b, Å	10.3741(5)	9.6360(3)	9.0531(2)
c, Å	10.466(2)	11.5943(4)	15.2733(4)
α, °	96.700(10)	110.59(2)	90.00
β, °	92.305(10)	97.00(2)	99.138(10)
γ, °	99.927(10)	103.85(2)	90.00
Volume	746.47(6)	814.57(5)	1725.94(7)
Z	2	1	2
ρ (calc.), g/cm^3	1.544	1.795	1.694
μ, mm^{-1}	0.266	1.023	0.966
F(000)	356	447	894
Reflections collected	9369	10725	23373
Independent refl., R_{int}	3948, 0.0420	4645, 0.0374	5028, 0.0524
N of parameters	264	242	293
Final R_1 [$I>2\sigma(I)$]	0.0479	0.0641	0.0594
wR_2 (all data)	0.1324	0.1662	0.1084
GOF on F^2	1.099	0.874	1.020

5.3 Experimental

5.3.1 X-ray Crystallography

Suitable single crystals were grown by slow evaporation and mounted using silicon grease on a thin glass fibre. Crystallographic measurements were carried out on a Bruker SMART CCD 6000 diffractometer using graphite monochromated Mo-Kα radiation (λ = 0.71073 Å). The standard data collection temperature was 120 K, maintained using an open flow N_2 Cryostream (OxfordCryosystems) device. Integration was carried out using the Bruker SAINT and Rigaku FSProcess packages. Data sets were corrected for Lorentz and polarisation effects and for the effects of absorption. Structures were solved using direct methods and refined by full-matrix least squares on F^2 for all data using SHELXTL[26] software. All non-hydrogen atoms were refined with anisotropic displacement parameters; H-atoms were located on the difference map and refined isotropically. Molecular graphics were produced using the programs X-Seed[27, 28] and POV-Ray.[29]

5.3.2 2-Ureidopyridine with copper chloride complex [Cu (3.1)Cl_2] 5.1 ***:*** Ligand **3.1** (0.30 g, 0.115 x 10^{-3} mol) was dissolved in THF (2 ml) and added to a solution of copper chloride (0.20 g, 0.118 x 10^{-3}) in MeOH (2 ml). The mixture was left to slowly evaporate for few days resulting in a formation of green coloured single crystals. IR (ν /cm-1) 1387, 1535, 1578. 1608, 1709, 3129, 3278. Anal. Calcd; (%) for $C_{13}H_{13}N_3OCuCl_2S$: C, 39.6; H, 3.56; N, 10.66. Found (%) C, 39.10; H, 3.07; N, 10.24.

5.3.3 2-Ureidopyridine with copper bromide complex [Cu(3.1)Br_2] 5.2*:* Ligand **3.1** (0.30 g, 0.115 x 10^{-3} mol) was dissolved in THF (2 ml) and added to a solution of copper bromide (0.19 g, 0.116 x 10^{-3} mol) in H_2O (1 ml). The mixture was left to slowly evaporate resulting in a formation of green coloured single crystals. IR (ν /cm-1) 1478, 1535, 1612.97 (NH bend.), 1660.90 (s, C=O), 3026.19 (w, CH str.) and 3325(vw, NH str.). Anal. Calcd; (%) for $C_{26}H_{26}N_6O_2CuBr_2S_2$: C, 42.09; H, 3.53; N, 11.33. Found (%) C, 41.96; H, 3.63; N, 10.93.

5.3.4 2-Ureidopyridine with copper nitrato complex [Cu(3.1) NO_3] 5.3: Ligand **3.1** (0.30 g, 0.115 x 10^{-3} mol) was dissolved in THF (2 ml) and added to a solution of

copper nitrate (22 g, 0.116 x 10^{-3} mol) in THF: H_2O (2 ml). The mixture was left to slowly evaporate resulting in a formation of green coloured single crystals. IR (ν /cm-1) 1529.4 (NH str), 1668 (vs, C=O), 3027.19 (vbr, NH str.). Anal. Calcd; (%) for $C_{26}H_{26}N_8O_8CuS_2$: C, 44.22; H, 3.71; N, 15.87. Found (%) C, 40.28; H, 5.25; N,19.23.

5.3.5 2-Ureidopyridine with copper boron-tetrafluoride [H (3.1) BF_4] 5.4: Ligand **3.1** (0.30 g, 0.115 x 10^{-3} mol) was dissolved in THF (4 ml) and added to a solution of copper boron-tetraflouride hexahydrate (0.40 g, 0.155 x 10^{-3} mol) in THF (4 ml). The mixture was refluxed under nitrogen for 19 h, filtered and left for slow evaporation resulted in a formation of single green crystal for X-ray crystallography. IR (ν /cm-1) 711.2 (br, BF_4), 1054.54 (br, BF_4), 1673.03 (s, C=O), 2925.1(w, Ar CH str), 3206.7 (wbr, NH). Anal. Calcd; (%) for $C_{13}H_{14}BF_4$: C, 44.98; H, 4.06; N, 12.10. Found (%) C, 27.22; H, 4.04; N,10.94.

5.3.5 2-Ureidopyridine with copper trifluromethanesulphonate complex [Cu (3.1) CF_3SO_3] 5.5 A & B

[Cu(3.1)](CF_3SO_3) 5.5 (form A)*:* Ligand **3.1** (0.120 g, 0.463 x 10^{-3} mol) in THF (2 ml) was mixed with copper trifluromethanesulphonate (0.168 g, 0.464 x 10^{-3} mol) in methanol : H_2O (1:1 v/v, 2 ml) and the mixture allowed to evaporate slowly resulting in a formation of green colour single crystals suitable for X-ray diffraction analysis. IR (ν /cm^{-1}) 1227, 1438, 1548, 1585, 1651, 3282 (vbr, NH). Anal. Calcd (%) for $C_{26}H_{26}N_6O_2S_2$ $Cu(CF_3SO_3)_2$: C, 38..20; H, 2.98; N, 9.55.. Found (%) C, 34.96; H, 2.75; N, 12.28.

[Cu(3.1)](CF_3SO_3) 5.5 (form B)*:* The second polymorph of **5.5** was obtained by dissolving **L** (0.30mg, 0.115 x 10^{-3} mol) in THF (2 ml) and mixing with silver acetate (0.19 g, 0.115 x 10^{-3} mol) in methanol : acetonitrile (1 : 1 v/v, 2 ml) and leaving the mixture to evaporate slowly. This resulted in the formation of colourless single crystal suitable for X-ray diffraction analysis. IR (ν /cm^{-1}) 1411, 1467, 1531, 1579, 1612, 1718 (s, $\nu_a(CO_2)$), 3199 (m, ν(NH)), 3279 (m, ν(NH)). M.p. 180 ^oC (decomp.). Anal. Calcd (%) for $C_{26}H_{26}N_6O_2S_2$ $Cu(CF_3SO_3)_2$: C, 38..20; H, 2.98; N, 9.55.Found (%) C, 42.03; H, 3.75; N, 9.91.

5.4 Conclusions

In conclusion we have obtained solid state structures of a series of copper complexes CuX_2 (X = Cl, NO_3, CF_3SO_3, Br) and one of a salt of ligand **3.1** with BF_4 anion. We have not been successful in designing simple solid state structures showing contact ion pair binding. All the copper complexes apart from copper chloride and boron-tetraflouride show a six-coordinate complex with a Jahn-Teller distorted octahedral geometry. The $Cu(CF_3SO_3)_2$ complex exists in two polymorphs differing in the orientation of the thiomethyl substituents in a similar way to the free ligand. The copper chloride structure is forming hydrogen bonds in a typical forming $R_2^2(8)$ fashion, which supports concept that metal coordinated halides can form stronger hydrogen bonds than organohalides. Copper tetrafluoroborate did not produce any copper-containing product, but formed a salt of ligand **3.1** in which the BF_4^- anion interacts with the urea NH protons in an $R_2^2(8)$ fashion. In conclusion, the copper systems were less successful than the silver-based complexes in forming ion pair binding systems and their solution chemistry was not pursued.

5.5 Overall conclusion of the project

We have made simple calixarene based urea and amide based receptors that can specifically bind chloride anion in a 1:1 stoichiometry exclusively through hydrogen bonding. The thiomethyl urea calixarene **2.15** binds chloride anion stronger than other receptors reported above. The crystal structures of intermediate products **2.3**, **2.4**, **2.5** and **2.6** provide better understanding of partial cone, pinched cone and cone conformations respectively. We failed to understand and control the reactions of higher butyronitrile **2.3**, **2.4** and calix[8]arene due to poor solubility and selectivity. The reaction with series of bis –isocyanates also failed to provide any well characterised product . Reactions of amine **2.7** with substituted aryl isocyanate, naphthyl isocyanate, dansyl and octadecyl isocyanate resulted in a formation of clean urea-based products. The solid state structures of these complexes can be compared on the basis of differences between the urea hydrogen bonding. The solid state structure of thiomethyl urea calixarene **2.15** form a bifurcated hydrogen bonding interaction of the $R_2^1(6)$ 'urea tape' type; while crystal packing of **2.16** exhibits intermolecular $R_2^2(8)$ type hydrogen bonding between α–NH proton and β–oxygen atom. The remaining naphthyl moiety trans to each other in crystal structure packing. However in thiourea calixarene **2.20**, the γ– NH proton with respect to meta methyl phenyl (lower rim substituent) forms hydrogen bonds with the phenolic oxygen atom, that in turn bonds to an adjacent oxygen atom of the calixarene lower rim.

2-Ureidopyridine **3.3** is a versatile ligand that not only exhibits significant polymorphism in its own right, but also shows simultaneous binding of silver metal and a series of anions to form contact ion pair complexes in the case of coordinating anions (OAc^- and NO_3^-). In the case of the acetate complex polymorphism is also observed. The structures of the contact ion pair complexes are influenced by the stronger basicity of acetate and its lower symmetry. In each case the silver ion is coordinated with the nitrogen atom of the pyridyl group, the sulphur atom of the thioether and the oxygen atoms of the nitrate or acetate anions forming $R_2^1(6)$ and $R_2^2(8)$ type hydrogen bonding with acetate and nitrate anion in solid state structures. The complexes are thus both coordination polymeric in the solid state. There are two different polymorphic forms formed with silver acetate one of them is monoclinic and other is triclinic in structure, however both polymorphs have $R_2^1(6)$ type hydrogen bonding to the coordinated anion. In contrast the complex of the non-coordinating anion PF_6^- results in the formation of a separated ion pair in the solid

state and the system reverts to a distorted urea tape type of hydrogen bonding. The reaction of $AgBF_4$ with **3.3** forms 1: 4 complex that is distorted tetrahedral in structure. The stoichiometry arises from the decomposition of silver(I) and the saturation of the metal centre by the ligands means there is not metal-anion interaction.

^1H NMR spectroscopic titration experiments on both free **3.3** and its silver complexes were performed in DMSO solution due to the poor solubility of the complexes. The data suggest that the ion pair motif is retained in solution.

Not only this, but we have also obtained solid state structures of a series of copper complexes CuX_2 (X = Cl, NO_3, CF_3SO_3, Br) and one of a salt of ligand **3.1** with BF_4 anion. We have not been successful in designing simple solid state structures showing contact ion pair binding. All the copper complexes apart from copper chloride and boron-tetraflouride show a six-coordinate complex with a Jahn-Teller distorted octahedral geometry. The $Cu(CF_3SO_3)_2$ complex exists in two polymorphs differing in the orientation of the thiomethyl substituents in a similar way to the free ligand. The copper chloride structure is forming hydrogen bonds in a typical forming $R_2^2(8)$ fashion, which supports concept that metal coordinated halides can form stronger hydrogen bonds than organohalides. Copper tetrafluoroborate did not produce any copper-containing product, but formed a salt of ligand **3.1** in which the BF_4^- anion interacts with the urea NH protons in an $R_2^2(8)$ fashion. In conclusion, the copper systems were less successful than the silver-based complexes in forming ion pair binding systems and their solution chemistry was not pursued.

5.6 References:

1. K. G. Caulton, G. Davies and E. M. Holt, *Polyhedron*, 1990, **9**, 2319-2351.
2. N. N. Greenwood and A. Earnshaw, *Chemistry of the Elements*, 1st Ed., Pergamon, Oxford, 1984.
3. M. T. Reetz, C. M. Niemeyer and K. Harms, *Ang. Chem. Int.,* 1991, **30**, 1472-1474.
4. C. R. Bondy, P. A. Gale and S. J. Loeb, *Chem. Commun.*, 2001, **7,** 729-730.
5. C. R. Bondy and S. J. Loeb, *Coord. Chem. Rev.,* 2003, **240**, 77-99.
6. C. R. Bondy, P. A. Gale and S. J. Loeb, *J. Am. Chem. Soc.,* 2004, **126**, 5030-5031.
7. D. R. Turner, B. Smith, E. C. Spencer, A. E. Goeta, I. R. Evans, D. A. Tocher, J. A. K. Howard and J. W. Steed, *New J. Chem.*, 2005, **29**, 90-98.
8. J. M. Russell, A. D. M. Parker, I. Radosavljevic-Evans, J. A. K. Howard and J. W. Steed, *Chem. Commun.*, 2006, **8,** 269-271.
9. J. M. Russell, A. D. M. Parker, I. Radosavljevic-Evans, J. A. K. Howard and J. W. Steed, *Cryst. Eng. Comm.,* 2006, **8**, 119-122.
10. P. Blondeau, A. van der Lee and M. Barboiu, *Inorg. Chem.*, 2005, **44**, 5649-5653.
11. J. M. Russell, A. D. M. Parker, I. Radosavljevie-Evans, J. A. K. Howard and J. W. Steed, *Chem. Commun.,* 2006, 269-271.
12. D. R. Turner, B. Smith, A. E. Goeta, I. R. Evans, D. A. Tocher, J. A. K. Howard and J. W. Steed, *Cryst. Eng. Comm.*, 2004, **6**, 633-641.
13. N. Qureshi, D. S. Yufit, J. A. K. Howard and J. W. Steed, *Dalton Trans.,*2009, **29**, 5708 - 5714.
14. G. Aullon, D. Bellamy, L. Brammer, E. A. Bruton and A. G. Orpen, *Chem. Commun.*, 1998, **5**, 653-654.
15. L. Brammer, *Dalton Transactions*, 2003, **13**, 3145-3157.
16. L. Brammer, E. A. Bruton and P. Sherwood, *Cryst. Growth. Des.*, 2001, **1**, 277-290.
17. G. R. Desiraju and T. Steiner, *The Weak Hydrogen Bond*, OUP/IUPAC, Oxford, 1999.
18. J. D. Dunitz and R. Taylor, *Chem. Eur. J.,* 1997, **3**, 89-98.
19. G. Aullón, D. Bellamy, L. Brammer, E. A. Bruton and A. G. Orpen, *Chem. Commun.*, 1998, 653-654.

20. M. O. M. Piepenbrock, K. M. Anderson, B. C. R. Sansam, N. Clarke and J. W. Steed, *Cryst Eng. Comm.*, 2009, **11**, 118-121.
21. S. Myllyviita, R. Sillanpaa, J. J. A. Kolnaar and J. Reedijk, *J. Chem. Soc., Dalton Trans.,* 1995, 2209-2213.
22. F. A. Mautner, M. A. S. Goher and A. E. H. Abdou, *Polyhedron*, 1993, **12**, 2815-2821.
23. L. Gou, X. W. Qu, B. Zheng, D. Y. Wang and H. M. Hu, *Acta Crystallogr. Sect. E.,*2005, **61**, M441-M442.
24. B. H. Qian, W. X. Ma, L. D. Lu, X. J. Yang and X. Wang, *Acta Crystallogr. Sect. E.,* 2006, **62**, M2818-M2819.
25. B. Zheng, G. Liu, L. Gou, D. Y. Wang and H. M. Hu, *Acta Crystallogr. Sect. A.,* 2005, **61**, M499-M501.
26. G. M. Sheldrick, *Acta Crystallogr. Sect. A*, 2008, **64**, 112-122.
27. L. J. Barbour, *J. Supramol. Chem.*, 2001, **1**, 189-191.
28. J. L. Atwood and L. J. Barbour, *Cryst. Growth Des.*, 2003, **3**, 3-8.
29. C. J. Cason, in POV-Ray', 2002.

5.7 List of Publications

1- Ion-Pair Binding by Mixed N,S-Donor 2-ureidopyridine Ligands Qureshi, N., Yufit, D. S., Howard, J. A. K., Steed, J. W (Dalton Trans., 2009, 5708 – 5714.

2- Hydrogen Bonding is not Everything: Extensive Polymorphism in a System with Conserved Hydrogen Bonded Synthons K.Fucke, N. Qureshi, D. S. Yufit, J.A. K. Howard and J. W. Steed (accepted in Crystal Growth and Design).

3- Urea- derivatized p-tert- butylcalix [4]arenes: Neutral Ligands for selective anion complexation (in preparation).

4- Anion binding by cooper (II) complexes of a 2- ureidopyridine derivative (in preparation).